

QUANTITATIVE EVALUATION OF A THRUST VECTOR CONTROLLED TRANSPORT AT  
THE CONCEPTUAL DESIGN PHASE

by

VINCENT PATRICK RICKETTS

Presented to the Faculty of the Graduate School of  
The University of Texas at Arlington in Partial Fulfillment  
of the Requirements  
for the Degree of

MASTER OF SCIENCE IN AEROSPACE ENGINEERING

THE UNIVERSITY OF TEXAS AT ARLINGTON

December 2015

Copyright © by Vincent Patrick Ricketts 2015

All Rights Reserved



## ACKNOWLEDGEMENTS

Over the course of this research, I have been supported by many people. I would like take this chance to acknowledge a number of the most influential that contributed to the success of this research.

First, I cannot begin to express my gratitude to the one whom without, my life and this research would be possible. I thank and give all glory to my heavenly Father, and his Son Jesus Christ, my savior.

Second, I give thanks to my advisor, Dr. Bernd Chudoba for is direction, encouragement, suggestions, and his high standard of quality, of which have all greatly influenced my life. Without his advice I would surely not be where I am today.

Third, I want to thank my AVD Lab colleagues, most notably Thomas McCall, Amen Omoragbon, Lex Gonzalez, Amit Oza, Doug Coley, and Loveneesh Rana. Without their assistance, criticism, constant pressure, and friendship, this research undertaking would not have been possible.

Forth, I would like to thank Dr. Gary Coleman for his advice, direction, and inspiration to always strive for the perceived unattainable.

Finally, I would like to give thanks to my family and friends for their love and support throughout my life and educational career. I would also like to dedicate this work to my late Father, Johnny Ricketts. Without his love and support I would not be the man I am today

December 9, 2015

## ABSTRACT

### QUANTITATIVE EVALUATION OF A THRUST VECTOR CONTROLLED TRANSPORT AT THE CONCEPTUAL DESIGN PHASE

Vincent Patrick Ricketts, M.S.

The University of Texas at Arlington, 2014

Supervising Professor: Bernd Chudoba

The impetus to innovate, to push the bounds and break the molds of evolutionary design trends, often comes from competition but sometimes requires catalytic political legislature. For this research study, the 'catalyzing legislation' comes in response to the rise in cost of fossil fuels and the request put forth by NASA on aircraft manufacturers to show reduced aircraft fuel consumption of +60% within 30 years. This necessitates that novel technologies be considered to achieve these values of improved performance. One such novel technology to commercial aviation is thrust vector control (TVC). The beneficial characteristic of TVC technology applied to the traditional tail-aft configuration (TAC) commercial transport is its ability to retain the operational advantage of this highly evolved aircraft type like cabin evacuation, ground operation, safety, and certification. This study explores if the TVC transport concept offers improved flight performance due to synergistically reducing the traditional empennage size, overall resulting in reduced weight and drag, and therefore reduced aircraft fuel consumption. In particular, this study explores if the TVC technology in combination with the reduced empennage method enables the TAC aircraft to evolve synergistically while complying with current safety and certification regulation. For the category of commercial transports, the overall TVC performance benefit has to be measured in the context of the objective function: Direct Operating Cost (DOC). To assess the potential reduction of DOC through the utilization of

TVC commercial transports, the discipline stability & control must be addressed in the total system context during the early conceptual design phase.

The research methodology utilizes two tools: 1) the multi-disciplinary parametric sizing software, AVD Sizing, developed by the Aerospace Vehicle Design (AVD) Laboratory, and 2) a unique TVC-TAC S&C tool, developed by the author. The sizing software is responsible for visualizing the total system solution space via parametric trades. The S&C tool is responsible for assessing the controllability of the total system solution space. Together, these tools make up the methods utilized by the research methodology, which is capable of determining if the TVC technology can enable the TAC aircraft to evolve synergistically, showing marked improvements in performance and cost whilst retaining safe and certifiable.

This study indicates that the TVC plus reduced empennage method shows marked improvements in performance and cost.

## TABLE OF CONTENTS

ACKNOWLEDGEMENTS .....	iii
ABSTRACT .....	iv
LIST OF ILLUSTRATIONS.....	viii
LIST OF TABLES .....	x
NOMENCLATURE .....	xi
Chapter 1 INTRODUCTION .....	1
1.1 Research Motivation .....	1
1.2 Product Development Life Cycle (PDLC) .....	3
1.3 Aircraft Design Phase .....	4
1.4 Conceptual Design Selection Logic .....	7
1.5 Research Objective.....	12
Chapter 2 LITERATURE RESEARCH.....	14
2.1 TVC Literature Survey .....	14
2.2 Novel Technology within Commercial Aviation.....	18
Chapter 3 SOLUTION CONCEPT ARCHITECTURE .....	41
3.1 Solution Concept Methodology .....	41
3.2 Methodology Methods – CD Synthesis System .....	44
3.3 Case Study .....	65
Chapter 4 RESULTS AND DISCUSSION.....	79
4.1 Results of Solution Concept Methodology.....	79
Chapter 5 CONCLUSIONS AND RECOMMENDATIONS.....	93
APPENDIX A.....	97
BIBLIOGRAPHY.....	128

BIOGRAPHICAL INFORMATION ..... 145

## LIST OF ILLUSTRATIONS

Figure 1.1: NASA Subsonic Transport System Level Metrics [3].....	2
Figure 1.2: Evolutionary Benefit Plateau of Aircraft Passenger Number [1].....	3
Figure 1.3 The Three Phases or Levels of Aircraft Design [11].....	5
Figure 1.4 Product Life Cycle [10].....	7
Figure 1.5. Product Development Life-Cycle Breakdown .....	9
Figure 1.6 AVD Standard to Design [15].....	9
Figure 1.7 Cost of Change and Design Freedom versus Product Life Cycle .....	11
Figure 2.1 Thrust Vectoring Aircraft Example .....	20
Figure 2.2 Thrust Vectoring Spectrum .....	21
Figure 2.3 Thrust Vectoring Principle Methods: Full Engine Movement (left), Exhaust Manipulation (center), and Separate/Augmented Propulsion (right) [17].....	24
Figure 2.4 Numerically Holistic View of TVC Enabled Aircraft.....	29
Figure 2.5 Evolution of Multi-Role Propulsion System Technology .....	31
Figure 2.6 Synthesized Commercial TVC System.....	40
Figure 3.1 Solution Space Visualization.....	42
Figure 3.2 Solution Concept Methodology .....	43
Figure 3.3 AVDS Input File Design Variables .....	49
Figure 3.4 Fundamental AVD Sizing Logic [15].....	51
Figure 3.5 Expanded Fundamental AVD Sizing Logic [15].....	56
Figure 3.6 Mission Critical Corners of the Flight Profile for Control Power Assessment of a TVC Enabled Aircraft.....	58
Figure 3.7 Directional Control Free-Body Diagram.....	60
Figure 3.8 Control Effector Effectiveness Comparison among Thin Airfoil Theory, the Vortex Panel Method, and Experimental Data [31] .....	62
Figure 3.9 Longitudinal Control Free-Body Diagram (Specifically Take-off Rotation) .....	63

Figure 3.10 Case Study Modification Overview .....	70
Figure 3.11 Solution Space Visualization of TOGW vs. <i>Spln</i> (Top Left), Fuel Weight vs. <i>Spln</i> (Top Right), Total DOC vs. <i>Spln</i> (Bottom Center) .....	72
Figure 4.1 Fuel Weight vs. Empennage-Reduction Factor .....	80
Figure 4.2 Normalized Total DOC vs. Empennage-Reduction Factor .....	81
Figure 4.3 Thrust vs. Empennage-Reduction Factor .....	82
Figure 4.4 Unit Cost vs. Empennage-Reduction Factor .....	82
Figure 4.5 Percent Change of Empennage <i>Spln</i> .....	83
Figure 4.6 S&C Output Visualization of Solution Concept Methodology .....	86
Figure 4.7 LoCE Sizing with TVC off on the 60% Reduced Empennage Trade Study .....	87
Figure 4.8 DiCE Sizing with TVC off, OEI, and indicated CW on the 60% Reduced Empennage Trade Study .....	88
Figure 4.9 LoCE Sizing with TVC off on the 50% Reduced Empennage Trade Study .....	88
Figure 4.10 DiCE Sizing with TVC off, OEI, and indicated CW on the 50% Reduced Empennage Trade Study .....	89

## LIST OF TABLES

Table 2.1 References on the Topic of Mechanical TVC .....	16
Table 2.2 References on the Topic of Fluidic TVC .....	17
Table 2.3 References on the Topic of Generic TVC .....	18
Table 2.4 Methodology of TVC Literature Research.....	19
Table 2.5 Thrust Vectoring Fundamentals .....	23
Table 2.6 Advantages of a TVC Enabled Commercial Air Transport .....	37
Table 2.7 Disadvantages of a TVC Enabled Commercial Air Transport.....	38
Table 3.1 Primary Methodology Methods of the TVC Feasibility Assessment .....	42
Table 3.2 Conceptual Design Synthesis System Breakdown .....	45
Table 3.3 Selected 'By-Hand' Conceptual Design Texts and Course Material [14].....	46
Table 3.4 Selected Computer-Integrated Conceptual Design Synthesis Systems [15].....	46
Table 3.5 AVDS Methods for TAC Aircraft [15] .....	52
Table 3.6 Design Constraining Flight Condition (DCFC) Test Matrix .....	59
Table 3.7 Case Study Breakdown.....	66
Table 3.8 AVDS Mission Requirements.....	67
Table 3.9 B777-300ER Mission Profile .....	69
Table 3.10 Comparison of B777-300ER Reference vs. Reverse Engineered Baseline.....	74
Table 3.11 TVC Receptive Baseline Modification Summary .....	77
Table 3.12 TVC Enabled Aircraft Modification Summary.....	78
Table 4.1 Data Presentation Format .....	80
Table 4.2 DCFC Test Matrix of 60% and 50% Reduced Empennage .....	90
Table 5.1 Innovative Technology Savings Comparison.....	94

## NOMENCLATURE

Symbol	DESCRIPTION
Alt	Altitude
b	Wing Span
$C_L$	Coefficient of Lift
$C_{L\alpha T}$	Coefficient of Lift versus Angle of Attack for the HTP
$D_{fus}$	Diameter of Fuselage
ETW	Engine Thrust to Weight Ratio
$f_{sys}$	Ratio of Systems Weight to OEW
$K_{ve}$	Engine Volume Coefficient
$K_{vs}$	Systems Volume Coefficient
$K_{vv}$	Void Volume Coefficient
$l_{fus}$	Length of Fuselage
L/D	Lift versus Drag Ratio
$S_{pln}$	Wing Planform Area
T/W	Thrust Loading
$V_{crew}$	Crew Volume
$\bar{V}_{HTP}$	Tail Volume Quotient for the HTP
$V_{pay}$	Payload Volume
$\bar{V}_{VTP}$	Tail Volume Quotient for the VTP
W	Weight
W/S	Wing Loading
$W_{crew}$	Crew Weight
$W_{pay}$	Payload Weight
WR	Weight Ratio

$W_{str}$	Wing Structural Weight
$W_{sys}$	Systems Weight
$X_{cg_g}, Z_{cg_g}$	CG X, Z Location from Nose of A/C
$X_{mg_g}, Z_{mg_g}$	X, Z Location of Main Gear
$Z_{T_g}$	Z Location of Thrust from the Nose of A/C
$X_{ac_{wfg}}$	X Location of Aerodynamic Center of the Wing Fuselage from the Nose of A/C
$X_{ac_{Hg}}$	X Location of Aerodynamic Center of the HTP from the Nose of A/C
$Z_{D_g}$	Z Location of the Drag of the Wing Fuselage from the Nose of A/C

Acronym	DESCRIPTION
AEI	All Engines Inoperative
AR	Aspect Ratio
ARw	wing Aspect Ratio
AVD	Aerospace Vehicle Design
AVDS	Aerospace Vehicle Design Sizing
CD	Conceptual Design
CE	Configuration Evaluation
CE	Control Effector
CL	Configuration Layout
CONOPS	Concept of Operations
CW	Crosswind
DCFC	Design Constraining Flight Condition

DD	Detailed Design
DICE	Directional Control Effector
DOC	Direct Operating Cost
ERF	Empennage-Reduction Factor
FAA	Federal Aviation Administration
FAR	Federal Aviation Regulation
HTP	Horizontal Tail Plane
LoCE	Longitudinal Control Effector
MESPET	Market, Economic, Societal, Political, Environmental, and Technological
MLW	Maximum Landing Weight
MR	Mission Requirements
NASA	National Aeronautics and Space Administration
NIA	National Institute of Aeronautics
OEI	One Engine Inoperative
OEW	Operating Empty Weight
PAX	Passengers
PCA	Propulsion-Controlled Aircraft
PD	Preliminary Design
PDLC	Product Development Life-Cycle
PS	Parametric Sizing
RT&D	Research, Technology, and Demonstration
SAS	Stability Augmentation System
SFC	Specific Fuel Consumption
STOL	Short Takeoff and Landing
STOVL	Short Takeoff Vertical Landing

TAC	Tail-Aft Configuration
TOGW	Take-Off Gross Weight
Total DOC	Total Direct Operating Cost
TVC	Thrust Vectoring Control
V/STOL	Vertical or Short Takeoff and Landing
VTP	Vertical Tail Plane

Greek Symbol	DESCRIPTION
$\alpha$	Angle of Attack
$\beta$	Crosswind angle (Sideslip)
$\epsilon_f$	LoCE Effectiveness (S&C)
$\mu_a$	OEW Margin
$\mu_g$	Wheel-Ground Friction Coefficient
$\tau$	Kucheman's Slenderness Parameter (AVDS)
$\tau_f$	DiCE Effectiveness (S&C)
$\ddot{\theta}_{mg}$	Angular Acceleration about the Main Gear Rotation Point

## Chapter 1

### INTRODUCTION

The significance and feasibility of novel technology applied to a system is best visualized during the phase that the act of design parameter variation can have the greatest impact on the total system. Potential for knowledge growth is the highest during the phase that knowledge growth from design parameter variation is at its greatest. The conceptual design phase embodies these aspects. To determine if a novel technology is truly an innovative technology in commercial air transportation, it must be analyzed first during the earliest conceptual design phase in order to appreciate its effect on the total system.

The following sub-sections of the introduction chapter expound upon the research motivation and provide background information on the **Product Development Life-Cycle (PDLC)**. From the PDLC discussion, and its components, it will be made abundantly clear why it was necessary to select the conceptual design phase (which occurs at the beginning of the PDLC) for the research environment.

#### 1.1 Research Motivation

The requirements that have varying degrees of influence on the aircraft design are typically categorized by the following impact disciplines: **Market, Economic, Societal, Political, Environmental, and Technological (MESPET)** [1]. The trend of the commercial industry to continue down the derivative design path, making improvements to already established and proven airframes, based on the aircraft MESPET requirements, does not always give sufficient motivation for the company to risk pursuing innovative technology and unconventional designs. Sterk and Torenbeek similarly express that:

*“... It is unlikely that the design trends are set merely by the conservatism, for example a desire to continue a proven concept in order to avoid the large financial risks of totally new development programs. The sharp competition always sets incentives to new and*

*innovative concepts since new designs must be considerably improved to be competitive to (derivative of) already established and proven types. ...” [2]*

The impetus to innovate, to push the bounds and break the molds of evolutionary design trends, often comes from competition but sometimes requires catalytic political legislature. For this research endeavor, the ‘catalyzing legislation’ comes in response to the rise in cost of fossil fuels and the request put forth by the **National Aeronautics and Space Administration (NASA)** on aircraft manufacturers to show a performance gain of +60% within 30 years (N+3) [3]. Figure 1.1 represents a portion of the MESPET requirements that influence the drive to innovate.

TECHNOLOGY BENEFITS*	TECHNOLOGY GENERATIONS (Technology Readiness Level = 4-6)		
	N+1 (2015)	N+2 (2020**)	N+3 (2025)
Noise (cum margin rel. to Stage 4)	-32 dB	-42 dB	-71 dB
LTO NOx Emissions (rel. to CAEP 6)	-60%	-75%	-80%
Cruise NOx Emissions (rel. to 2005 best in class)	-55%	-70%	-80%
Aircraft Fuel/Energy Consumption† (rel. to 2005 best in class)	-33%	-50%	-60%

\* Projected benefits once technologies are matured and implemented by industry. Benefits vary by vehicle size and mission. N+1 and N+3 values are referenced to a 737-800 with CFM56-7B engines, N+2 values are referenced to a 777-200 with GE90 engines

\*\* ERA's time-phased approach includes advancing "long-pole" technologies to TRL 6 by 2015

† CO<sub>2</sub> emission benefits dependent on life-cycle CO<sub>2e</sub> per MJ for fuel and/or energy source used

Figure 1.1: NASA Subsonic Transport System Level Metrics [3]

Since derivative designs trend asymptotically towards a benefit plateau of their respective evolution, they will never reach this level of performance put forth by NASA. Figure 1.2 represents the benefit plateau seen in passenger capacity of aircraft, and demonstrates the evolutionary jumps due to the application of game changing developments in science and technology.

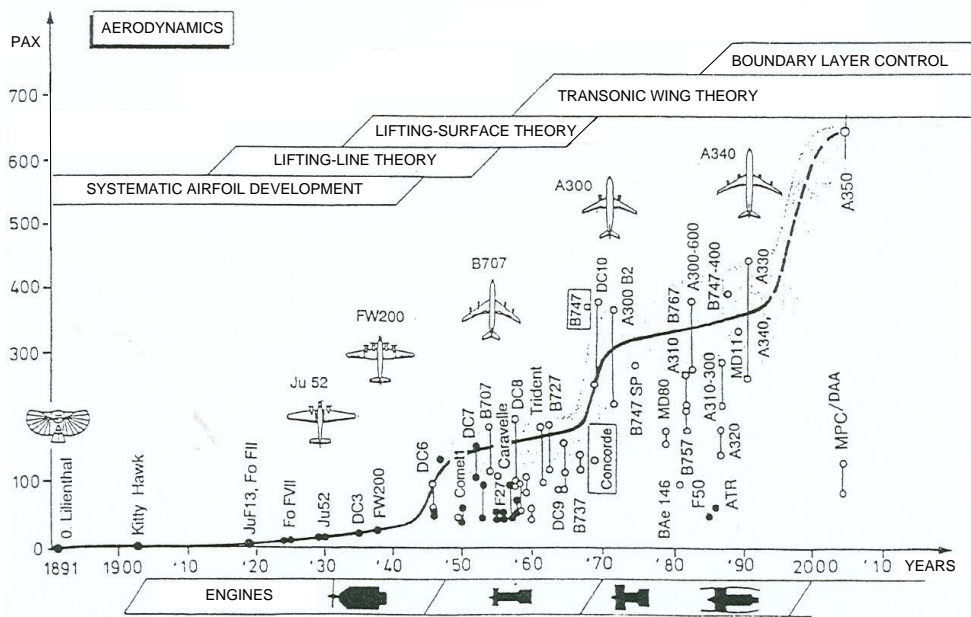


Figure 1.2: Evolutionary Benefit Plateau of Aircraft Passenger Number [1]

The usage of innovative technologies is necessary in order to achieve the aforementioned goals. This research study assesses the hypothesis that the characteristics of **Thrust Vectoring Control (TVC)** technology applied to the traditional **Tail-Aft Configuration (TAC)** commercial transport is its ability to improve performance through reduced weight, reduced drag, and therefore reduced aircraft fuel consumption. Additionally, it is maintained that the highly evolved and practical adopted characteristics of the TAC (cabin evacuation, ground operation, safety and certification, etc.) are retained. In order to evaluate this hypothesis, the significance and feasibility of this novel technology must be determined through capturing (understanding, modeling, assessing) of the first order multi-disciplinary effects. However, in order to determine the best development phase for the said analysis, an overview of the PDLC is presented.

## 1.2 Product Development Life Cycle (PDLC)

From the prospective of product development programs, the development of revolutionary or evolutionary aircraft requires significant financial resources. This translates into

typical characteristics of development programs: considerably high success expectations, time pressure, and financial commitments. Consequently, the aerospace industry has evolved a structured development process. [4] The PDLC serves as the framework that describes the path a product takes from 'cradle to grave.' In general, the phases of the PDLC are as follows: Design, Manufacturing, Testing, Certification, Supportive Operations, and Accident Investigation. For commercial aircraft programs, this path begins at the foundation, where the design group determines the **Mission Requirements (MR)**. Classically, the airline industry would set the MR alone, manufacturing products with little to no input from the customer. [5] Modern airline industries have since moved away from this approach, adapting a collaborative style. As an example, the Boeing Company's development of the 777 aircraft established an industry practice where the "Gang of Eight"—the eight major airlines—were directly involved in the development process. [6] This translated into one of Boeing's most extensive research and development programs, costing an estimated 5 Billion United States Dollars. Fortunately, this substantial commitment succeeded by producing one of the most profitable commercial transportation aircraft to date. [5]

After the establishment of the MR, the PDLC progresses further into the design phase, transitioning to testing, certification, and manufacturing, closing with supportive operations and finally incident/accident investigation. The following sub-sections provide high-level support to enhance the readers understanding of the activities design groups tackle over the course of the design phase alone. From this, it will become clear why the conceptual phase of the design phase is pre-determined for the present research investigation.

### 1.3 Aircraft Design Phase

The aircraft design process starts with the establishment of the MR and begins to conclude with the initiation of manufacturing. The MR phase should not be viewed as a separate phase as it is part of the iterative design process. As stated by Shute, "*A beautiful*

aircraft is the expression of the genius of a great engineer who is also a great artist.” [7] The design process is an intellectual activity based in the multi-disciplinary sciences, but to some degree tempered by good intuition and judgement developed via experience of the individual designer. The opportunity of the engineer to make design decisions based on experience and wisdom provide the artistic freedom in the aircraft design process. The design activities are conveniently broken down into the following three design sub-phases:

- 1) **Conceptual Design (CD)** – Development and evaluation of design alternatives
- 2) **Preliminary Design (PD)** – Development of baseline specification for manufacturing
- 3) **Detailed Design (DD)** – Development, Testing, and Certification of physical structure [4]

The list above describes the major results of each design sub-phase. Figure 1.3 illustrates the activities of each sub-phase of the design phase.

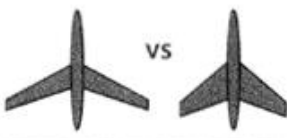
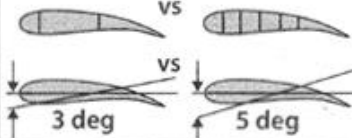
	<b>Phase 1 Conceptual Design</b>	<b>Phase 2 Preliminary Design</b>	<b>Phase 3 Detail Design</b>				
							
<b>Known</b>	Basic Mission Requirements Range, Altitude, & Speed Basic Material Properties $\sigma/\rho$ $E/\rho$ $S/lb$	Aeroelastic Requirements Fatigue Requirements Flutter Requirements Overall Strength Requirements	Local Strength Requirements Producibility Functional Requirements				
<b>Results</b>	<table border="1" style="width: 100%;"> <tr> <th style="width: 50%;">Geometry</th> <th style="width: 50%;">Design Objectives</th> </tr> <tr> <td>Airfoil Type R t/c <math>\lambda</math> <math>\Delta</math></td> <td>Drag Level Weight Goals Cost Goals</td> </tr> </table>	Geometry	Design Objectives	Airfoil Type R t/c $\lambda$ $\Delta$	Drag Level Weight Goals Cost Goals	Basic Internal Arrangement Complete External Configuration <i>Camber &amp; Twist Distribution</i> <i>Local Flow Problems Solved</i> Major Loads, Stresses, Deflections	Detail Design <i>Mechanisms</i> <i>Joint Fittings and Attachments</i> Design Refinements as Result of Testing
Geometry	Design Objectives						
Airfoil Type R t/c $\lambda$ $\Delta$	Drag Level Weight Goals Cost Goals						
<b>Output</b>	Feasible Design	Mature Design	Shop Designs				
<b>TRL</b>	2 – 3	4 – 5	6 – 7				

Figure 1.3 The Three Phases or Levels of Aircraft Design [11]

As stated earlier and visualized in Figure 1.3, the CD phase starts with the establishment of the MR, the 'Known' row, and concludes with the selection of major design aspects such as airframe configuration layout and global design parameters. Correctness is stressed over accuracy during the CD phase.

The PD phase further matures the design, making only minor changes to the configuration layout. The implementation of higher fidelity tools such as computational fluid dynamics code and finite element methods are incorporated to further develop the accuracy of the design. The end of the PD phase ends with the freezing of the configuration, and the decision to commit to the manufacturing of the aircraft.

The DD phase begins the process of designing everything under the skin. The DD phase "*... is literally the nuts and bolts phase of airplane design. ...*" [8] This phase follows strict established guidelines, regulations, and structural tolerances in the design of detail parts and assemblies. Near the end of this phase, many aspects of the aircraft are ready for fabrication. It is common to begin fabrication of detail parts and assemblies while the airframe is still in the late design phase. This allows the beneficial effect of bilateral communication between the shop floor and the design engineers. The DD phase can even continue past initial flight test where results of these test can influence the design.

Although the three design sub-phases occur chronologically as listed above in Figure 1.3, the design sub-phases do not have clearly defined boundaries. In practice, there exists some overlap between the design sub-phases. Figure 1.4 visualizes this overlap.

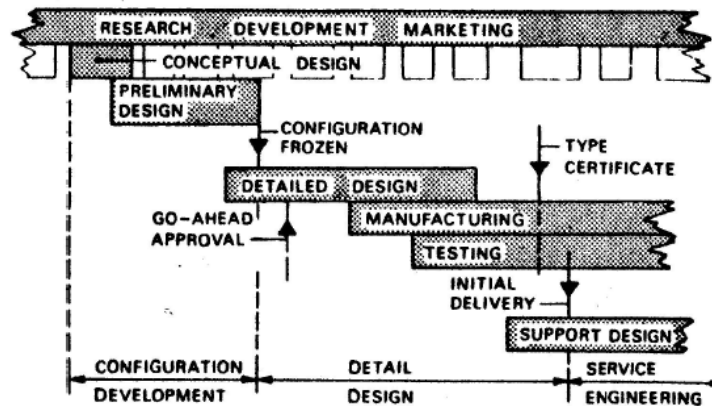


Figure 1.4 Product Life Cycle [10]

For more detailed descriptions on the inner workings of each sub-phase, one should refer to mainline airplane design texts by Anderson [8], Raymer [9], Torenbeek [10], Nicolai [11], and Roskam [12]. Of the three sub-phases of the aircraft design phase—CD, PD, and DD—the logic for selecting the CD phase for technology trades is discussed next.

#### 1.4 Conceptual Design Selection Logic

Of the three design sub-phases, the CD phase is the least understood phase of the entire PDLC. [4] It is the goal of the CD phase to develop the competence of the designer to advise the decision makers through a systematic industry-best-practice approach to forecasting. This competence is measured by the ability of the designer to visualize and explain the design solution space. As expressed by Corning, the early CD phase *“...is the area where there is little known or established data at the time the design is being initiated. ...”* [13] This results in many design decisions being based, to a certain degree, on the judgement and experience of the individual designer. As is typical of many organizations, their *“...conceptual design teams are usually organized into highly multi-disciplinary entities of small size ... directly reporting to top management. ...”* [4] The highly complex task of aircraft design constitutes a multidisciplinary approach, where no part is designed in total vacuum unrelated to the other parts. [8] The major

vehicle parameters come to fruition during the CD phase. As stated by Chudoba, it is during the CD phase that “... *primary design decisions are made like selection, evaluation, and predefinition of configuration type and election of global design parameters. ...*” [14] It is during this phase that many configuration and concept trades are performed. Chudoba defines the aircraft configuration as “... *the arrangement of the lift generating surfaces relative to the positioning, and/or number, and/or integration of the longitudinal control effector(s) (e.g., Tail-Aft Configuration (TAC), Three-Surface Configuration (TSC), Flying-Wing Configuration (FWC), etc.). ...*” [1] The aircraft concept is defined, per configuration, as “... *possible permutations of either lift-, volume-, control-, and propulsion-generating contributors (i.e., possible wing concepts for a specific TAC are: high-aspect ratio wing, delta wing, variable sweep wing, etc.). ...*” [1]

In order to address the logic behind selecting the CD phase of the PDLIC for a feasibility assessment, one must ask: What is the fundamental objective of the CD phase? As postulated by Coleman, “... *The fundamental objective of this conceptual design phase is to satisfy the designer and decision maker that the selected concept is worthy of preliminary design continuation. ...*” [15] This satisfaction is normally established by a comprehensive investigation of the viability of the conceptual design to satisfy the MR. The CD phase itself is broken down into the following three fundamental steps:

- 1) **Parametric Sizing (PS)** – Definition of the gross vehicle design solution space
- 2) **Configuration Layout (CL)** – Brainstorming and initial sizing of the possible configuration concepts
- 3) **Configuration Evaluation (CE)** – Evaluation of initial configuration concepts and trade-studies [4]

As expressed in the text thus far, the PDLC has been broken-down as visualized by Figure 1.5.

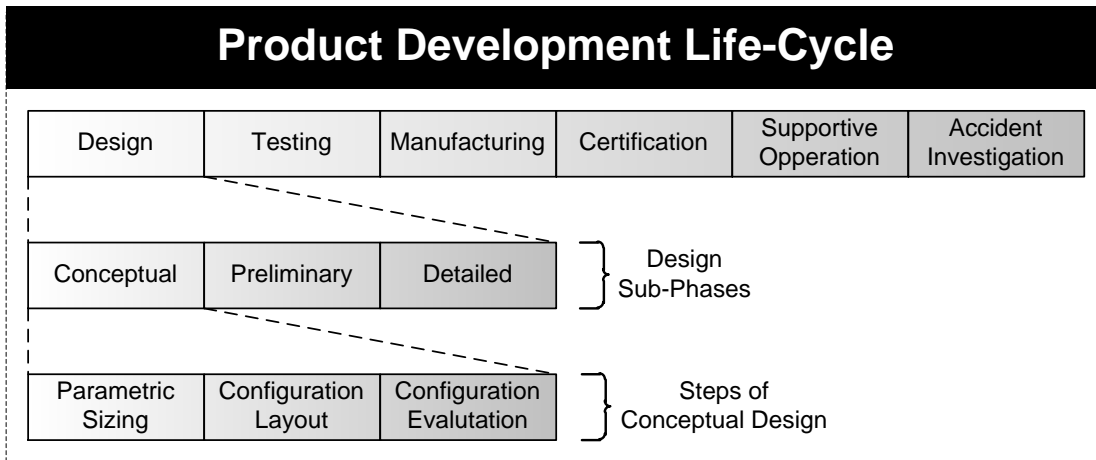


Figure 1.5. Product Development Life-Cycle Breakdown

The objective of the PS step is to identify and visualize the design solution space by applying the steps of the ‘Standard to Design (Ladder).’ Figure 1.6 is a representation of the steps of a closed-loop design process.

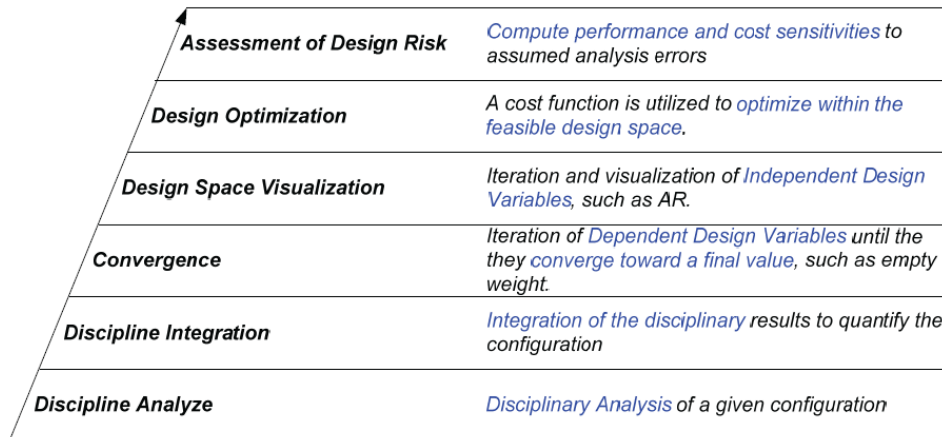


Figure 1.6 AVD Standard to Design [15]

The goal of the PS step is to answer the following design questions:

- 1) Is satisfying the MR feasible with current industrial capability and what, if any, new industrial capability is required?

2) What scale (weight, size, energy solution space) of vehicle is required to satisfy the MR? [15]

The objective of the CL step is to identify alternative design solutions through brainstorming and unstructured creativity. As Torenbeek restates, “... *the expression configuration ... refers to the general layout, the external shape, dimensions and other relevant characteristics. ...*” [10] This step requires the designer to utilize experience, aircraft design knowledge base systems, and statistics to complement the PS step. These qualitative and quantitative lessons learned are applied to provide the layout of specific systems not required during the PS step. The addition of these systems may require the design to return to the PS step, iterating until both steps agree.

Having identified the solution space and relevant aircraft geometries with the PS and CL steps respectively, the CE step compares the solution space permutations of aircraft configurations and concepts for overall suitability. The main objective of the CE step is to identify the baseline aircraft, which resides in the design solution space. This step includes a multi-disciplinary evaluation of integrated aircraft concepts, and provides an answer to the question: Which aircraft concept satisfies the MR?

As the design transitions further into the realm of reality, the cost of change in the design increases while the design freedom decreases. This increase in costs is due to many reasons such as retooling, manufacturing stops, increased employment, etc... As emphasized by Nicolai, “... *the cost of making a design change is small during conceptual design but is extremely large during detail design. ...*” [11] As the design moves further along the design phase, the more ‘rigid’ the design becomes. This design rigidity, reducing the freedom the designers have in making changes, causes configuration and concept design trades to have an overall reduced impact on the design. This can lead to incorrect design decisions. The necessity to implement configuration & concept trades during the CD phase is in an effort to reduce the design opportunity cost. For example, a concept trade performed during the DD phase may

yield a smaller overall benefit compared to the same concept trade performed during the CD phase. The difference between the measured benefits (e.g. performance improvements) is the design opportunity cost. Thus, when the designer desires to perform configuration and concept trades, it has to occur during the phase in which major design changes are the cheapest and most effective. Figure 1.7 below, adapted from Chudoba and Heinze [16], visualizes the cost of change and design freedom over the course of the PDLC.

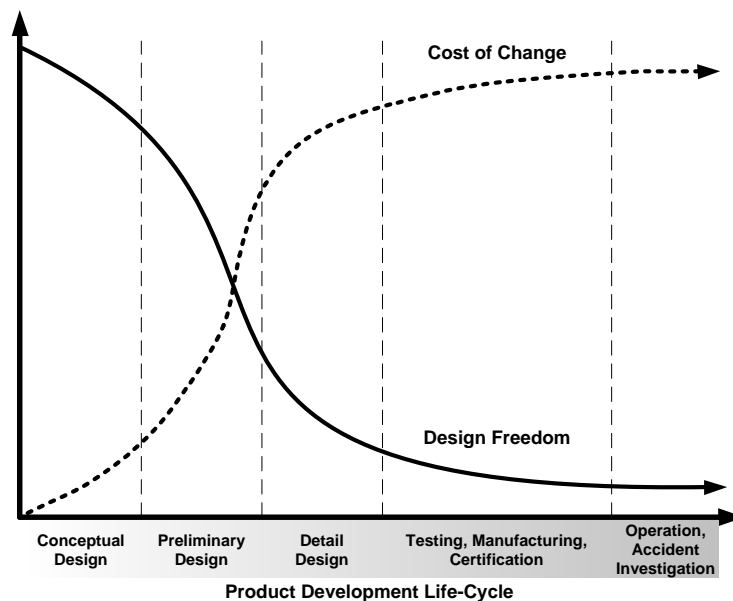


Figure 1.7 Cost of Change and Design Freedom versus Product Life Cycle

It is postulated by Chudoba and Heinze that “... around 80% of the flight vehicle configuration and mission ... is determined during the CD phase. ...” [16] With many major design decisions being established under strict time constraints during the CD phase, Coleman comments that the CD phase “... is crucial to explore new ... technologies under existing and new objectives ...” [15] Having key aspects locked-in too early in the life cycle lowers the potential design impact of introducing novel technology. As Torenbeek reflects, “... the object of this conceptual design phase is to investigate the viability of the project and to obtain a first impression of its most important characteristics. ...” [10] Within the reference frame of the

current research, “... *project* ...” is taken to mean ‘feasibility of a novel technology’ and “... *most important characteristics* ...” is taken to mean, ‘first order multi-disciplinary design drivers.’ As the goal of this research is to analyze the effect a novel technology has in the total system context, it is essential to study the prospective technology as early into the design process as possible. This ensures the most significant ‘field of view’ of the technology onto the overall conceptual design. It is only logical to conclude that the early CD phase is the most opportune environment for measuring primary multi-disciplinary design drivers since this phase serves as the forecasting ‘test bed’ for evaluating concept trades such as the novel technology considered here, Thrust Vector Control.

#### 1.5 Research Objective

The goal of this research is to produce a conceptual design (CD) phase feasibility assessment of TVC technology applied to commercial transportation aircraft. This approach is dissimilar to legacy studies where the TVC technology has been analyzed as ‘add-on’ hardware. Within the realm of commercial air transportation, numerous studies have been performed analyzing controllability of TVC technology applied to existing configurations (adding TVC to an existing, manufactured aircraft). The conclusion of many of these studies is that stability and controllability of ‘add-on’ TVC technology to the commercial transport class aircraft is sufficiently capable control effector while engines are operating. Additionally, these studies show little to no reduction in total aircraft fuel consumption (performance improvement metric). The approach of these legacy studies represents a saturated field of study where little to no one is examining the technology (TVC) early into the conceptual design phase of the aircraft. It is postulated by Van Der Veen that “... *a net benefit may result for future aircraft by integrating thrust vectoring technology into the design process from the outset. ...*” [17] The beneficial characteristic of TVC technology applied to the TAC commercial transport is its ability to retain the operational advantage of this highly evolved aircraft type like cabin evacuation, ground

operation, safety, and certification. Thus, this research performs a feasibility analysis during the aircraft CD phase utilizing a multi-disciplinary parametric sizing tool capable of determining if the TVC technology can enable the TAC aircraft to synergistically evolve, showing marked improvements in performance and cost.

## Chapter 2

### LITERATURE RESEARCH

As with all research projects, one of the most important phases is the building of a strong foundation on which everything stands. This is normally accomplished by performing an extensive literature survey of the material related to the topic. Beautifully stated, literature research is the process where you have to “... *self-examine and educate yourself about everything that has been done related to the problem. ...*” [14] Furthermore, Yin describes literature research as a function used to “... *develop sharper and more insightful questions about the topic. ...*” [18] Thus, literature research is the process of gaining an understanding of the fundamentals, history, and the latest methods and theories related to the research topic; expanding their base of knowledge beyond the bounds of their respective specialty. This enables the researcher to ask the correct questions and properly address the research objective.

Literature research is the act of standing on the shoulders of giants; In this case, thrust vectoring giants. As such, the following sections will cover the research topic of the novel technology within commercial aviation (TVC). The next section begins this discussion by addressing the literature surveyed (not the specific details of the literature), summarizing the literature research in the form of a knowledge storage matrix.

#### 2.1 TVC Literature Survey

This research endeavor highlights the categories of the reviewed available TVC literature and discusses the data richness of each category. The references are categorized according to the *area of application* and *research strategy*. The *areas of application* are educational, military, and non-military. These categories are defined as follows:

- 1) Education - Institutional research origination (University ABC)

- 2) Military - Military Research (DARPA, AFRL, etc.)
- 3) Non-Military - Government funded and administered research (NASA)

The category, *areas of application*, provides the reader knowledge of what organizational body performed such research. The category, *research strategy*, provides insight into the overall goal of the associated research and the way the research is carried out. The research strategies are categorized as, historical, experimental, and case studies. It must be noted that the boundaries between the strategies are not clear and distinct; there exist areas of overlap amongst them.

[18] Each particular research strategy provides the reader with an idea of what to expect from reviewing the associated references. The research strategy categories are defined as follows:

- 1) Historical - Research organized in a historic overview to uncover knowledge of a particular topic or phenomenon that lacks any definitive analysis or opinions.
- 2) Experimental - Research focused on understanding a distinct phenomenon by demonstration to extract empirical data, often to determine the validity of the hypothesis.
- 3) Case Study - Research focused on understanding the behavior of phenomenon when the boundaries between the phenomenon, context and catalysts are not clearly evident.

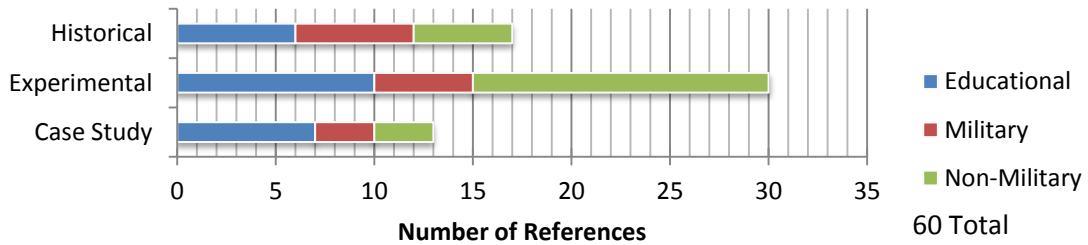
The following tables--Table 2.1, Table 2.2, and Table 2.3--illustrate the reviewed references arranged in matrix format. This format identifies the combinations of *research strategies* and *areas of application* to which each associated references belong. These tables serve as a knowledge storage matrix. The reviewed literature is sorted into three tables: 1) Mechanical TVC, 2) Fluidic TVC, and 3) Generic TVC. This sorting methodology is based, in part, on the primary method utilized by the TVC system to manipulate the medium: mechanical and fluidic. Also used as a sorting filter is generic TVC literature. These types of literature are not related to any specific manipulation medium. These references tend to address the utilization of the technology as opposed to the physics and mechanics of the technology itself.

Table 2.1 References on the Topic of Mechanical TVC

	Educational	Military	Non-Military
<b>Historical</b>	[17] [26] [109] [106] [38] [19]	[34] [50] [53] [51] [35] [43]	[146] [110] [63] [36] [145]**
<b>Experimental</b>	[131] [107] [71] [44] [96] [119] [66] [142] [149] [123]	[61] [138] [137] [97] [37]	[85] [94] [117] [70] [95] [64] [79] [116] [73] [143] [55] [121] [140] [69] [22]*
<b>Case Study</b>	[144] [99] [103] [49] [57] [98] [129]	[108] [134] [100]	[62] [148] [90]

[x]\*: Reference classified as Hybrid manipulation method

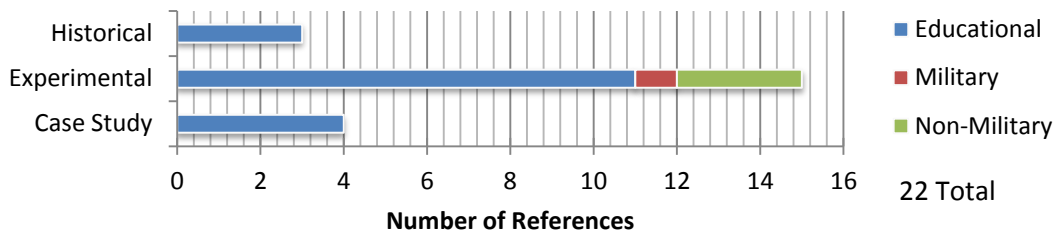
[x]\*\*: Reference classified as both *mechanical* and *fluidic* manipulation method



As seen in the reviewed literature with respect to the mechanical manipulation medium, the majority of the research is experimental, with the greater amount being performed by Non-Military organizations. Also highlighted by Table 2.1 is that the majority of case study research is performed by educational institutions.

Table 2.2 References on the Topic of Fluidic TVC

	<b>Educational</b>	<b>Military</b>	<b>Non-Military</b>
<b>Historical</b>	[102] [41] [105]	N/A	N/A
<b>Experimental</b>	[84] [21] [87] [86] [91] [118] [111] [141] [60] [112] [127]	[136]	[128] [120] [130]
<b>Case Study</b>	[133] [92] [93] [113]	N/A	N/A

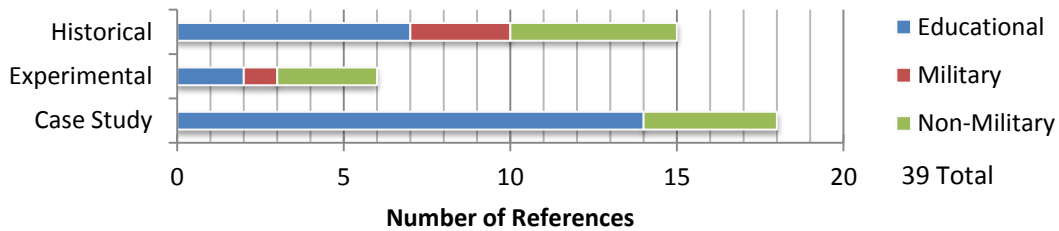


The reviewed literature in Table 2.2 shows a strong tendency to follow the experimental research strategy. Investment into experimental research is needed to understand the distinct phenomenon; this investment provides empirical data for testing the validity of the associated analytical methods, models, and simulations. As this method of TVC manipulation has yet to leave the lab (not evaluated on full scale aircraft), the educational environment is conducive for pure research focused on the pursuit of knowledge.

Table 2.3 References on the Topic of Generic TVC

	Educational	Military	Non-Military
<b>Historical</b>	[33] [76] [58] [56] [54] [52] [77]*	[135] [74] [59]	[126]* [101]* [83]* [65]* [42]*
<b>Experimental</b>	[125] [67]	[68]	[25]* [48] [40]*
<b>Case Study</b>	[132] [124] [122] [114] [104] [89] [88] [80] [78] [75] [47] [46] [45] [39]	N/A	[147] [139] [81] [72]

[x]\*: Reference classified as Propulsion Controlled Aircraft Systems



The majority of references in Table 2.3 follow the case study approach, which is centered on the simulation, prediction, and discussion of how the application and utilization of the TVC technology affects the airframe. Many of these case studies are geared towards studying the stability and control aspects of TVC enabled airframes.

## 2.2 Novel Technology within Commercial Aviation

This section presents the knowledge gained by examining the literature in detail. To begin with, a discussion of the literature research methodology is presented from a top-level perspective. This perspective provides the reader with an outline of the literature research presented.

As lessons are learned and new knowledge has been gained, new research filters are applied to focus the research endeavor. The application of new filters creates an adaptive

holistic approach to the literature research. The process begins with the complete thrust vectoring propulsion domain, then passes through a sequence of various filtering levels until sufficient TVC relevant knowledge is assembled. This process ends when the knowledge gained is able to satisfy and support the research objective. As stated in Chapter 1.5, the research objective is to produce a feasibility analysis of the TVC technology applied to commercial transportation aircraft designed with TVC during the CD phase. The methodology of the current literature research endeavor is described in Table 2.4 providing the research layer titles and major outcomes of each layer.

Table 2.4 Methodology of TVC Literature Research

	<b>Research Layer</b>	<b>Section</b>	<b>Major Outcomes</b>
1	Thrust Vectoring Propulsion Technology	2.2.1	Thrust Vectoring Spectrum, Generic Definition
2	Thrust Vectoring Propulsion within Aeronautics	2.2.2	Technology Fundamentals, Historic Application
3	Thrust Vectoring Propulsion within Commercial Aviation	2.2.3	Military / Commercial TVC Propulsion System Distinction, Commercial TVC Advantage-Disadvantage

In Table 2.4, each successive research layer is supported and deduced by the knowledge gained by the layer above. This table serves as the ‘organizational scaffolding’ that supports the TVC literature research.

### 2.2.1 TVC Fundamentals

In order to address the feasibility of the novel technology, TVC, as applied to a commercial transport aircraft, a primary literature research of this technology has been performed. The general definition of TVC is the manipulation of an object’s propulsive force to provide control over the attitude or velocity of the object. For aircraft, this force is typically generated using one or a combination of jet engines, propellers, ramjets, or rocket engines. To further narrow the generic definition applicable to aircraft, vectoring the propulsive force of an

aircraft is the technique of directing the primary thrust generated by a propulsion system in a direction away from the main flight direction. Thrust vectoring represents a control effector aimed at inducing longitudinal, directional, and/or lateral moments with the objective of beneficially affecting trim, stability, control, and overall flight performance. This enables the aircraft's propulsion systems to be used for more than just providing forward force. A TVC equipped aircraft can directly modify its attitude and flight path, augmenting or even exceeding the limitations of conventional aerodynamic control effectors. Figure 2.1 below visualizes this technique.

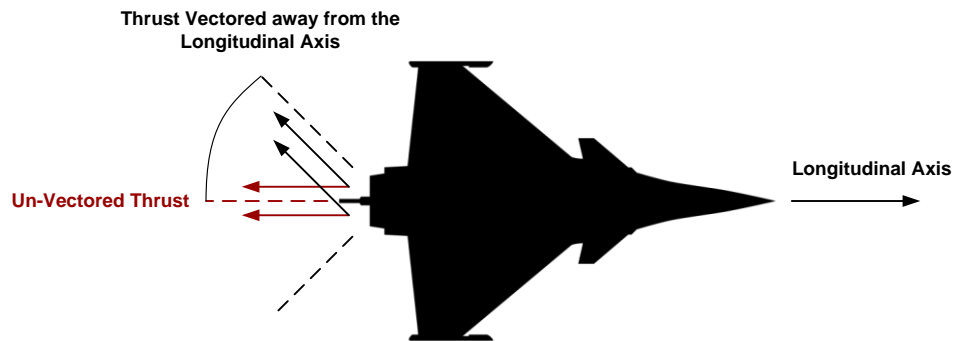


Figure 2.1 Thrust Vectoring Aircraft Example

The act of synergistically coupling the propulsion mechanism with the control mechanism can be seen across the spectrum of vehicular locomotion from water, land, air, and space. As one looks back into the history of humanity's adaptation of their natural resources to better suit their situation, nature is often a major source of inspiration in tool development. When inspecting nature under the lens of locomotion, many forms of life couple the acts of movement with control, utilizing one mechanism for both. This evolutionary-optimized approach to locomotion is found ranging from the smallest forms of life, microorganisms, to the largest lifeforms, blue whales. The next logical step for humanity would be to take advantage of the untapped potential of the propulsive force within commercial aviation, and direct it for means of control and movement. Figure 2.2 visualizes the thrust vectoring spectrum through two

categories: systems seen in nature and systems created through human ingenuity. Also listed in Figure 2.2 is an example user and mechanism for each category.

		Operational Medium			
		Water	Land	Air	Space
Nature	User	Dolphin / Fish	Humans / Dogs	Birds / Bees	?
	Mechanism	 Tail Fins	 Legs	 Wings	
Humanity	User	Boats / Submarines	Automotive / Tracked Vehicle	Rockets / Military Aircraft	Rockets / Spacecraft
	Mechanism	 Gimbaling / Nozzle Deflection	 Powered-Wheels For Directional Control	 Gimbaling / Nozzle Deflection	 Gimbaling / Nozzle Deflection

Figure 2.2 Thrust Vectoring Spectrum

As one can see, TVC, in its generic definition, is utilized quite extensively across the spectrum in nature with the exception of the space medium.

However, having one synergistic system responsible for multiple functions creates the opportunity of catastrophic failure. Risk mitigation has influenced the design of aircraft propulsion and control systems down separate paths. The TVC technology is most often used in water, land, and space mediums. Beginning in the middle of the last century, TVC technology has started to mature in the air medium for highly maneuverable fighter configurations.

Aircraft control is normally accomplished with aerodynamic control surfaces, which are movable structural surfaces that are used to generate aerodynamic forces and moments. This method of control is highly mature and effective. As stated by Sutton, "... *Even though aerodynamic control surfaces provide some additional drag, their effectiveness in terms of vehicle weight, turning moment and actuating power consumption is difficult to surpass with any other flight control method. ...*" [19]

Rockets and space access vehicles frequently operate in flight regimes where aerodynamic control surfaces do not provide sufficient control authority to remain effective. These vehicles typically incorporate TVC systems for use in both low speed and high altitude operation due to low atmospheric density conditions. There are many different mechanisms to achieve TVC from either gimbaling the engine or nozzle, or by internal/external manipulation of the propulsive medium [19]. For more information about successfully tested TVC mechanisms in the rocket industry, see Sutton [19]. The next section discusses the mechanisms of TVC related to aircraft.

As Jane expresses, “... about 50 years ago a few visionaries realized that it is possible to design a nozzle that can vector. ...” [20] Since that point in history, there have been numerous TVC methods researched, developed, and manufactured. Many thrust vectoring techniques are utilized across the aircraft thrust vectoring spectrum. For example, engine gimbaling or nozzle deflection in rockets and watercraft.

The field of TVC research involves complex technology with various implementations that accomplish the same fundamental goal. In order to realize the synthesis of a TVC system for commercial aircraft, the fundamental TVC mechanisms utilized in aircraft are identified. When cross-referencing the related TVC literature, one sees clear categories and types. Primarily, the TVC system can be broken down into seven fundamental categories and each category sub-divided into multiple types. Table 2.5 presents the fundamental thrust vectoring categories and lists the types associated with each category.

Table 2.5 Thrust Vectoring Fundamentals

Fundamental Categories	Types		
Thrust Generation Scheme	Separate Propulsion Systems	Coupled Propulsion Systems	
Vector Method	Engine Orientation Manipulation	Exhaust Gas Manipulation	Separate/Augmented Propulsion
Manipulation Medium	Mechanical	Fluidic	Hybrid
Nozzle Dimension	Two-Dimensional	Three-Dimensional	
Thrust Vector Axis Capability	Single Axis	Multiple Axis	
Exhaust Gas Manipulation Location	Up-Stream	At Nozzle	Down-Stream
Nozzle Geometry	Convergent	Convergent-Divergent	

The fundamental categories of manipulation medium, nozzle dimension, thrust vector axis capability, exhaust gas manipulation location, and nozzle geometry are thrust vector fundamental categories associated to exhaust gas manipulation.

The following subsections (titled by the fundamental categories) explain the types listed in Table 2.5. These subsections provide a summary of the thrust vectoring fundamentals and concepts that have been researched, developed, and manufactured in aircraft. The reader is encouraged to examine the details of the technology in the designated references.

#### 2.2.1.1 Thrust Generation Scheme

The thrust generation scheme can be separated into two major types: separate propulsion systems and coupled propulsion systems. Separate propulsion systems are characterized by independently powered systems for both propulsion and control. The coupled

propulsion system is a single system responsible for both propulsion and control. Of the two types, the more common is the coupled propulsion system.

#### 2.2.1.2 Vector Method

Full engine movement, exhaust manipulation, and separate/augmented propulsion are the three vector method types used to achieve TVC. Figure 2.3 visualizes the three main vector methods utilized in TVC.

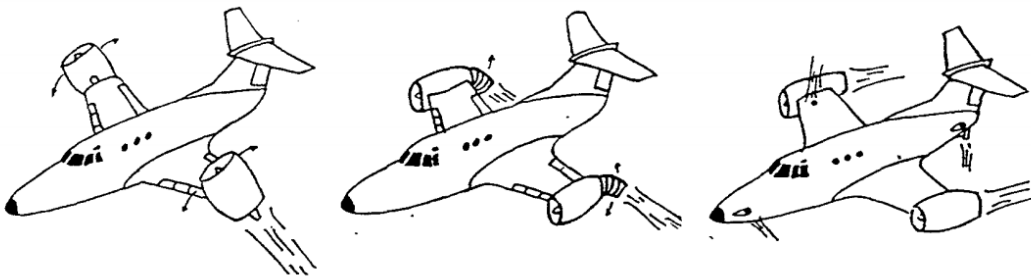


Figure 2.3 Thrust Vectoring Principle Methods: Full Engine Movement (left), Exhaust Manipulation (center), and Separate/Augmented Propulsion (right) [17]

Full engine thrust vectoring involves the mechanical manipulation of the engines' orientation to alter the thrust line. Detrimental inlet performance can be experienced when the full engine movement technique is applied to gas turbine engines. Additionally, the full engine movement technique “... involves high penalties with respect to weight and complexity. ...” [17] The V-22 Osprey is an example production-class vehicle utilizing this TVC vector method type.

Exhaust manipulation is the second vector method type. Frequently referred to as nozzle vectoring, the exhaust manipulation type is the most “... efficient and versatile system...” [17]. This system can alter the exhaust vector of the primary propulsion system without affecting the principal position or orientation of the engine components ahead of the nozzle. The F-22 Raptor is an example production vehicle that employs the exhaust manipulation vectoring method for TVC.

The separate/augmented propulsion vector method consist of a set of subsystems that work together to achieve total aircraft TVC. This type includes propulsion systems that achieve TVC by augmenting the primary propulsion system or implementing separate/secondary propulsion systems. For example, a portion of the total TVC system of the F-35B Lighting II is accomplished by augmenting the primary propulsion system to mechanically withdraw power to operate a lift-fan. The Yakovlev Yak-38 is an example of using the secondary propulsion systems to provide a portion of the TVC requirements. Another form of propulsion system augmentation is using engine exhaust bleed off redirected to provide control. In comparison to the other two methods, exhaust bleeding typically “... *produces very low vectorable thrust levels. ...*” [17] The Harrier “Jump Jet” is a production level example of this type of system.

#### 2.2.1.3 Manipulation Medium

Within or around the nozzle of the propulsion system, there are three types for actuating TVC — mechanical, fluidic, or a combination of both. Each approach has its respective advantages and disadvantages. As described by Deere, “... *Mechanical thrust vectoring nozzles use actuated hardware to manipulate the primary exhaust flow. ...*” [21] Mechanical systems can be complex and expensive in comparison to fluidic but are more reliable and predictable. [21] Mechanical TVC systems are a proven technology being implemented on several military aircraft over the years.

The fluidic type of the manipulation medium category gained popularity in the 1990's. [21] Research shifted from mechanical thrust vectoring techniques in favor of the light-weight, fixed-geometry and fewer parts typically associated with fluidic thrust vectoring systems. The three primary methods within the fluidic thrust vectoring technique are: shock vector control, throat shifting, and counter flow. Each method accomplishes TVC differently but “... *all three methods are simply the creation of an asymmetric pressure distribution on the nozzle surfaces. ...*” [21] Although fluidic thrust vectoring techniques shows promise in weight reduction, they are

mostly experimental and have not made their way onto production vehicles like the mechanical methods.

The hybrid mechanical/fluidic thrust vectoring technique is a combination of many features associated with each manipulation method. For more information regarding this technique, the reader is encouraged to examine the appropriate reference material [22].

#### 2.2.1.4 Nozzle Dimension

Nozzle dimension category is a description of the flow geometry within the nozzle. There are two nozzle types — the two-dimensional and the three-dimensional type. The design of the propulsion system's nozzle is a balance between competing MESPET requirements. Two-dimensional nozzles are often found on aircraft where signature-stealth and economical propulsion-performance prediction analyses are primary driving functions of engine design. Three-dimensional nozzles, used on cylindrical-axial-jet engines, are used to lower performance loss from altering the direction of the flow, post turbine. Of the two types, the two-dimensional nozzle offers the advantage of mechanical simplicity in TVC implementation.

#### 2.2.1.5 Thrust Vector Axis Capability

The thrust vector axis capability is the description of the thrust vectoring system's ability to impart a force about a single axis or multiple axes. The design choice between single axis and multiple axes is a function of the aircraft configuration and desired operational capabilities. For example, propulsion systems placed near the tail and close to the centerline can effectively contribute control moments in the yaw and pitch axes. This allows the propulsion system to provide multiple axes TVC. This in turn would influence the decision to implement three-dimensional nozzles. Likewise, propulsion systems located away from the centerline of the aircraft, e.g. on the wing, could effectively influence roll control. Aircraft designs that desire only pitch control would lean towards implementing a single axis design.

#### 2.2.1.6 Exhaust Gas Manipulation Location

The Exhaust Gas Manipulation Location category identifies the geometric position within the nozzle that the exhaust gas manipulation occurs. Three terms have been coined to describe the manipulation location: 'up-stream', 'at nozzle', or 'down-stream'. The 'up-stream' term refers to actuation of the exhaust gas after it leaves the turbines and before it enters the convergent section of the nozzle. The 'at nozzle' term refers to the actuation of the exhaust gas at the exit plane of the nozzle. The 'down-stream' term refers to manipulation of the exhaust gas after it has exited the nozzle.

#### 2.2.1.7 Nozzle Geometry

A nozzle's geometry is either convergent-divergent or convergent. The nozzle type is dictated by the desired exit flow conditions. The convergent-divergent nozzle is associated with exhaust flow velocities exceeding the speed of sound. Convergent-divergent nozzles are normally found on supersonic vehicles. The convergent nozzle geometry is associated with exhaust flow velocities below the speed of sound. For civilian applications, the convergent nozzle is normally used.

The next section covers the various historical applications of TVC applied to aircraft, addressing the what, when and where TVC systems are utilized in the aircraft industry.

### 2.2.2 *Historic Application*

As with any novel technology, it is important to understand the what, when, and where of the particular technology. This is accomplished with a holistic approach of TVC's utilization within the aeronautical community. The following subsections establish an aircraft-TVC technology utilization foundation.

#### 2.2.2.1 Early TVC Technology Catalyst

Beginning in the 1950's, a few visionaries realized the need to enable aircraft to takeoff from damaged thus shortened airfields. This drove the need to develop aircraft that could takeoff similar to rotorcraft but retain the speed, range, and payload capabilities associated with fixed-wing aircraft. This demand required the development of technology that could enable aircraft the ability to operate in non-traditional flight modes such as **Short Takeoff and Landing (STOL)**, **Short Takeoff Vertical Landing (STOVL)**, and **Vertical or Short Takeoff and Landing (V/STOL)**. Traditionally, the propulsion system of an aircraft was designed to provide unidirectional forward force. To meet the new design challenges, a paradigm shift in propulsion system utilization and integration was required. This new design challenge would establish a new category of aircraft utilizing a multi-role propulsion system.

#### 2.2.2.2 Development of TVC Technology

Aircraft that reach the flight test phase are of interest as they provide insight to the capabilities of the TVC technology. As new aircraft technology matures, moving from theory, lab, and eventually flight-test; the aircraft technology that makes it to production is of utmost significance. Reaching this status shows a readiness level of the technology, demonstrating its viability and strength. Many TVC concepts remain low on the technology readiness scale, with few making it to flight test. Even fewer designs satisfy enough requirements to become worthy of production class aircraft. Figure 2.4 is a numerical holistic collection of all known aircraft incorporating TVC technology that made it out of the lab and into flight test.

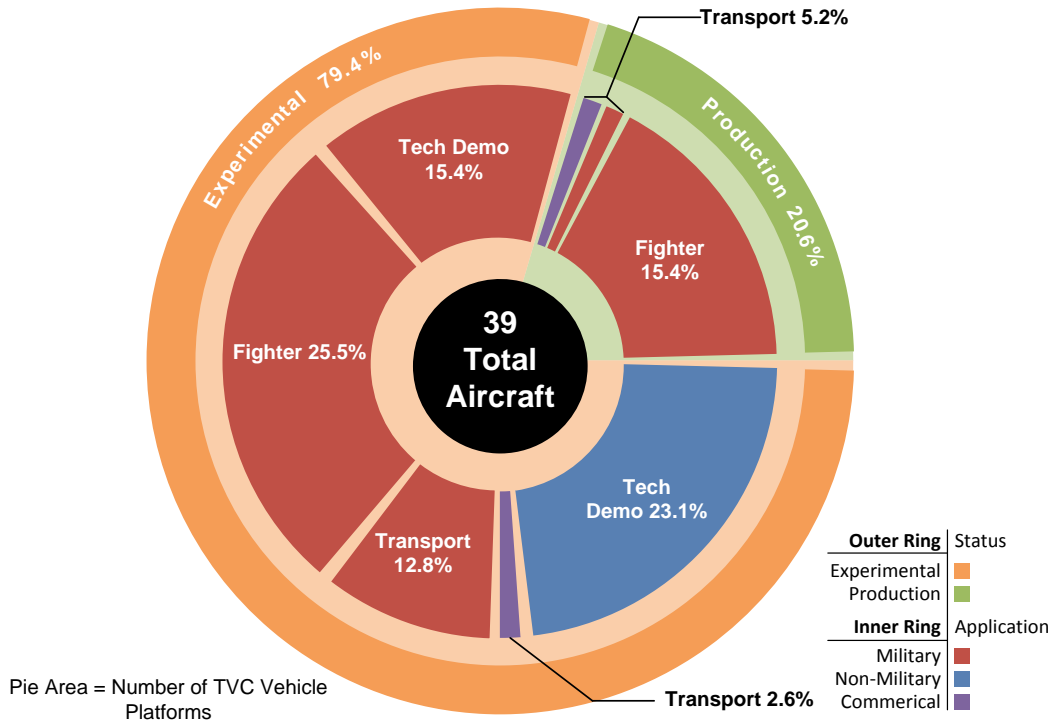


Figure 2.4 Numerically Holistic View of TVC Enabled Aircraft

As shown in Figure 2.4, the traditional operator of TVC enabled aircraft has been the military, with an overwhelming percentage of approximately 71.7 percent. The next largest demand of 23.1 percent comes from non-military government funded entities such as NASA. The goal of the non-military funded application category is normally associated with pure experimental research, with no aircraft continuing into production. The smallest application category is the commercial aviation industry. This low turnout is indicative of the high-perceived risk associated with novel technology and its integration into new designs. This is an example that illustrates the trend of the commercial industry to prefer continuing down the evolutionary design path.

With so few examples of the TVC technology being applied in the commercial industry, this research capitalizes on the efforts of military funded programs. When applying technology developed for aircraft with different **concept of operations (CONOPS)**, one must consider the different requirements and regulations that govern the design and operation of the vehicle.

Expanding upon Figure 2.4, the next section provides an evolutionary perspective of the technology, showing how each method of TVC has advanced.

### 2.2.2.3 Multi-Role Propulsion System Technology

Based on the generic definition of thrust vectoring control expressed in Chapter 2.2.1, any vehicle that utilizes the propulsion system to provide some measure of control outside the propulsion system's normal function, broadens the scope of the research. As described in Table 2.5, the TVC Technology is traditionally classified into three different methods of vectoring the thrust: Engine Orientation Manipulation, Exhaust Gas Manipulation, and Separate/Augmented Propulsion. Opening up the research to include all multi-role propulsion system technology expands the research scope to include thrust reversers and flight control systems designed to vary the thrust of the conventional propulsion system to establish control through fixed-vector variable thrust. This class of aircraft incorporates a flight control system referred to as a **Propulsion-Controlled Aircraft (PCA)** system. [23] All of these thrust vectoring methods provide the aircraft with additional rotational and/or linear momentum effectors.

The purpose of this holistic investigation is to establish a foundation for the novel technology (TVC) that is of interest in this research, providing an understanding of what, when, and where it is or can be used. Figure 2.5 provides an evolution of the TVC technology from the perspective of multi-role propulsion systems.

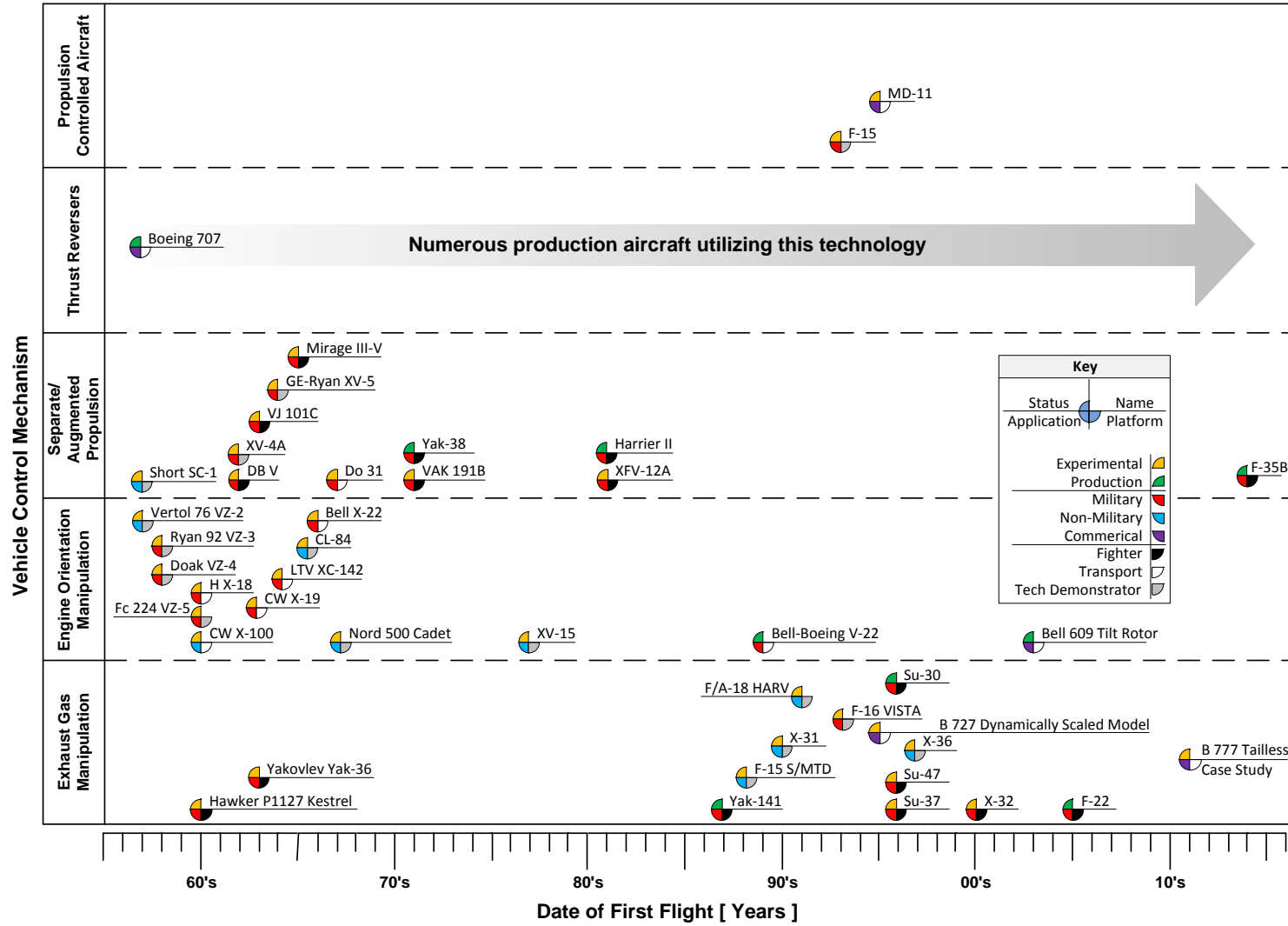


Figure 2.5 Evolution of Multi-Role Propulsion System Technology

As seen in Figure 2.5, in the 60's and 70's the early development of TVC technology was centered on the engine orientation manipulation and separate/augmented propulsion methods. These early methods are much simpler and the physics better understood in comparison to the exhaust gas manipulation method of the 90's and beyond. As such, they represented a natural starting point for TVC research. As discussed in Chapter 1.1, many factors contribute to the success or failure of an aircraft during the design and development phases. These factors include resource availability, political pressure, and design simulation and forecasting capabilities. For a multitude of reasons, many vehicle designs made it to flight test during this era. Many of these vehicles are classified as technology demonstrators, which provide the designers with data to validate and calibrate their respective design tools. This environment contributes to the low number of production aircraft utilizing TVC technology. Beginning in the late 80's, as more advanced design and simulation software became available, the **Research, Technology, and Development (RT&D)** programs of aircraft utilizing the exhaust gas manipulation method began to see the light of day. These systems are mechanically more complex but provide much greater levels of vectorable thrust.

Another category seen in Figure 2.5 is the thrust reverser systems. Thrust reversers use the propulsion system to produce a force to retard forward travel of the aircraft. During the late 1950's, the Boeing 707 became the first production class civilian vehicle outfitted with thrust reversers. Since then, both in the military and commercial arenas, this technology has been successfully adapted to numerous aircraft. Many versions of accomplishing thrust reversal exist.

Although a mature technology with over 50 years since its first implementation in a production commercial vehicle, the use of thrust reversers within the commercial aviation arena has restrictions. According the **Federal Aviation Administration (FAA)**, current **Federal Aviation Regulation (FAR)** concerning the airworthiness standards for transport category airplanes states the following regarding thrust reversing systems: [24]

§25.933 Reversing systems:

(a) *For turbojet reversing systems—*

(1) *Each system intended for ground operation only must be designed so that during any reversal in flight the engine will produce no more than flight idle thrust.*

Thus, within the commercial air transportation industry, this technology can only be used for ground operation. Thrust Reverser technology serves as the only known example of multi-role propulsion systems hardware being implemented into full-scale production class aircraft in the commercial air transportation industry.

The last category, the PCA systems, does not incorporate any additional specialized hardware to the aircraft. The only required alteration to the aircraft is “... *software modifications to existing computers. ...*” [23] This technology was developed to provide flight control during emergencies such as traditional flight control failure. [23] Many simulations using advanced concept flight simulators were used to test this system on various commercial airframes. In 1995, a flight-test concept demonstration of the PCA system was instituted on the MD-11 commercial transport aircraft. As stated by Burcham, “... *In more than 30 hours of flight testing, the PCA system exceeded the objectives, serving as a very acceptable autopilot and performing landings without using any flight control surfaces. ...*” [25] The conclusion of the PCA flight test program proved PCA system’s ability to control a vehicle in the event of aerodynamic control system failure. However, even with the program’s success, no known aircraft have since adopted this system.

Also included in Figure 2.5 is the flight test of an important scale model. In 1995, the flight test of a B-727 dynamically scaled model utilizing exhaust gas manipulation TVC technology was performed at Megiddo Airfield in Haifa, Israel. The U.S. Department of Transportation and the Catastrophic Failure Prevention Department of the FAA funded this ‘proof-of-concept’ flight. The team from the Technion-Israel Institute of Technology successfully demonstrated the capacity of ‘Add-On’ TVC systems to perform flight maneuvers using only

TVC. Additionally, the significance of the test is highlighted due to the scaled nature of the model. A dynamically scaled model implies that the ratio of all forces acting on the fluid and model are equal, thus the results of the test are representative of a full-scale test. This test serves as the only known test of a TVC system in place of conventional aerodynamic control surfaces on a commercial transport class aircraft. Additionally, according to Gal-Or, the goal of this flight test was “... to adapt military TVFC technologies to civil air transport applications by translating combat agility capabilities into unprecedented flight safety standards. ...” [26] This serves as an example of capitalizing on the successes of military funded RT&D programs to advance the commercial air transportation industry.

As expressed in various case studies listed in tables Table 2.1, Table 2.2, and Table 2.3, many researchers have demonstrated the viability of providing flight control through TVC technologies. Additionally, many researchers have studied the performance of ‘Add-On’ TVC systems. As postulated by Van Der Veen “... a net benefit may result for future aircraft by integrating thrust vectoring technology into the design process from the outset. ...” [17] The case study performed by the **Aerospace Vehicle Design (AVD)** laboratory by the team at the University of Texas at Arlington, did just this, designing from the outset, a TVC enhanced commercial transport. The AVD team was tasked by NASA Langley Research Center to investigate the TVC commercial transport as part of the Synergistic Efficiency Technologies for the Truss-Braced Wing Workshop, hosted by the **National Institute of Aeronautics (NIA)** and NASA. [15] The case study conceptually designed a tailless TVC enabled aircraft of the vehicle class and mission similar to the Boeing 777 aircraft. The major results of this study showed marked improvements in performance and cost but “... demonstrated with a generic stability and control tool for conceptual design, that this aircraft would require excessive thrust nozzle deflections for trim and would be uncontrollable during one engine inoperable conditions. ...” [15] This case study serves as the only known example of a commercial transport class aircraft

being designed for TVC from the outset. Completely replacing the aerodynamic effectors of the empennage of the aircraft identifies the extreme of TVC system utilization.

The above activity provides a holistic perspective in which a unique understanding of the maturity of the TVC technology can be established. The level of maturity is illustrated by the identification of successful adaptations of the TVC methods into production class aircraft. This identification is understood by the temporal view of the numerical variance of test aircraft to production aircraft of each category. Also established is an understanding of for what airframes the majority of the technology has been designed, i.e. highly maneuverable fighter aircraft. Identifying and deriving this knowledge of TVC maturity and evolution aids in identifying the type of TVC technology that is most synergistic to its incorporation into military and commercial airframes. This raises the question: what are the differences in TVC methods implemented on military versus commercial airframes? The next section will answer this question and further the literature research of TVC by discussing: 1) the TVC pertinent differences between the military and commercial engines, 2) the advantages, and disadvantages of a TVC system incorporated into the design of a commercial transportation aircraft, and 3) the safety of TVC technology.

### *2.2.3 Commercial Aviation Opportunities of TVC Technology*

Thus far, the literature research has addressed the TVC technology fundamentals, established categories to classify the technology, and determined the holistic characteristics of TVC systems and if they have been utilized in the aircraft industry. Given this historical perspective, the next logical step is to examine the technology's influence on the design of the aircraft.

The major differences between military and commercial propulsion systems are numerous and significant. The following list from Reference [17] summarizes the differences that are pertinent to TVC systems.

- 1) Bypass ratio and core/fan flow mixing

- 2) Nozzle pressure ratios
- 3) Typical presence of afterburners
- 4) Presence of variable throat exhaust nozzles
- 5) Presence of convergent-divergent nozzles
- 6) Presence of thrust reversers

These are the key gross drivers that need to be considered when selecting the type of TVC system. The advantages and disadvantages of TVC technology as it pertains to commercial integration is discussed next.

The application of this technology into commercial air transportation has several operational advantages listed in Table 2.6. The incorporation of TVC technology preserves many beneficial aspects of the commercial airframe such as maintainability, reliability, sustainability, and infrastructure. Due to the low visibility of the technology, public confidence and opinion of the aircraft is not hindered by the incorporation of the TVC technology. Table 2.6 lists expected benefits to commercial air transportation when TVC technology is utilized. For information regarding the opportunities that TVC technology enables in the non-commercial air transportation setting, the reader is encouraged to examine the details of military TVC application from the appropriate references (Table 2.1, Table 2.2, and Table 2.3).

Table 2.6 Advantages of a TVC Enabled Commercial Air Transport

Reference no.	Author/s	Extract
[144]	Matesanz	Enhanced maneuverability
[144], [115], [26]	Matesanz, Omoragbon, Gal-Or	Reduced takeoff and landing speed and field length
[115], [26]	Omoragbon, Gal-Or	Trim drag reduction from elimination of induced drag due to tail lift
[115], [26]	Omoragbon, Gal-Or	Overall drag reduction from reduced tail surface area
[115]	Omoragbon	Weight reduction from reduced empennage and control surface size
[33]	Gal-Or	Improved stall performance and spin recovery due to independence from aerodynamic control effectiveness
[98]	Harefors	Improved safety from utilization of TVC technologies to prevent catastrophic failure when conventional flight controls fail
[99]	Steer	Reduced noise around airfields and improved ability to handle adverse weather and flight conditions
[99]	Steer	Non-Aerodynamic Dependence
[99]	Steer	Control power augmentation for improved low-speed maneuvering
[99]	Steer	Increased control power redundancy
[99]	Steer	Possible reduction in the number of conventional aerodynamic control surfaces and associated actuation
[115]	Omoragbon	The synergistic combination of TVC and Aerodynamic control allows for a more balanced control authority across the flight regime

The major detriments associated with a TVC enabled commercial air transport are listed in Table 2.7.

Table 2.7 Disadvantages of a TVC Enabled Commercial Air Transport

Reference no.	Author/s	Extract
[115]	Omoragbon	Propulsion weight increase from TVC modifications
[115]	Omoragbon	Specific fuel consumption increases from mixed flow turbofan compared to high bypass unmixed turbofan
[99]	Steer	Cost penalty of the nozzle and supporting structure
[99]	Steer	Engine out safety/reduction in control power
[99]	Steer	TVC effectiveness dependent on engine configuration and current thrust setting, i.e. lower thrust at higher altitude
[99]	Steer	Requirement for complex integrated flight and propulsion control
[99]	Steer	Deflection of thrust coupling into forward speed and possibly affecting engine performance
[99]	Steer	Difficulty in obtaining both civil certification and passenger acceptance. Although, nozzle based TVC technology does have low-observability
[99]	Steer	The probability of thrust loss due to engine failure is likely to prohibit the dependence upon TVC for primary aircraft control
[98]	Harefors	Loss in nozzle efficiency due to vectoring

As with all new technology, the safe operation of the system is always paramount. When novel technology is introduced, there is always more attention paid to safety aspects compared to established technology, holding the novel technology under greater scrutiny for establishing appropriate safety standards. Fortunately, this technology is not novel to the military. See the appropriate references regarding the application of the TVC technology with respect to its military application (Table 2.1, Table 2.2, and Table 2.3). TVC technology has been incorporated and matured on several military vehicles and has shown acceptable levels of safety, reliability, and maintainability. Although matured in the military, the reader should consider the major difference in the requirement to prove failure probability analysis between the civil airframes of  $10^{-9}$  versus  $10^{-7}$  for military airframes. Further investigation of the safety aspects of the TVC technology is not the primary objective of this research. The reader is encouraged to examine the details of this technology with respect to its safe operation in the designated references (Table 2.1, Table 2.2, and Table 2.3).

#### 2.2.4 Commercial TVC System Synthesis

A fundamental objective of this research endeavor is to quantitatively evaluate the TVC technology applied to commercial transports aircraft during the conceptual design phase. In order to satisfy the novel technology (TVC) knowledge portion of this research, the above literature review was performed. From this activity, the envisioned TVC system applied within the commercial transportation arena is determined. The type of TVC system that would be best suited for use on a commercial transport airframe and the highlighted activities of the literature review that contributed to this selection are depicted in Figure 2.6. The identified TVC system category types are to be considered for the remainder of this study. The *TVC disciplinary modifications* portion of Figure 2.6 represents the selected requisite modifications that capture the first order multi-disciplinary effects of TVC technology utilized on a commercial transportation aircraft studied during the conceptual design phase. The next chapter begins the discussion of the solution concept architecture.

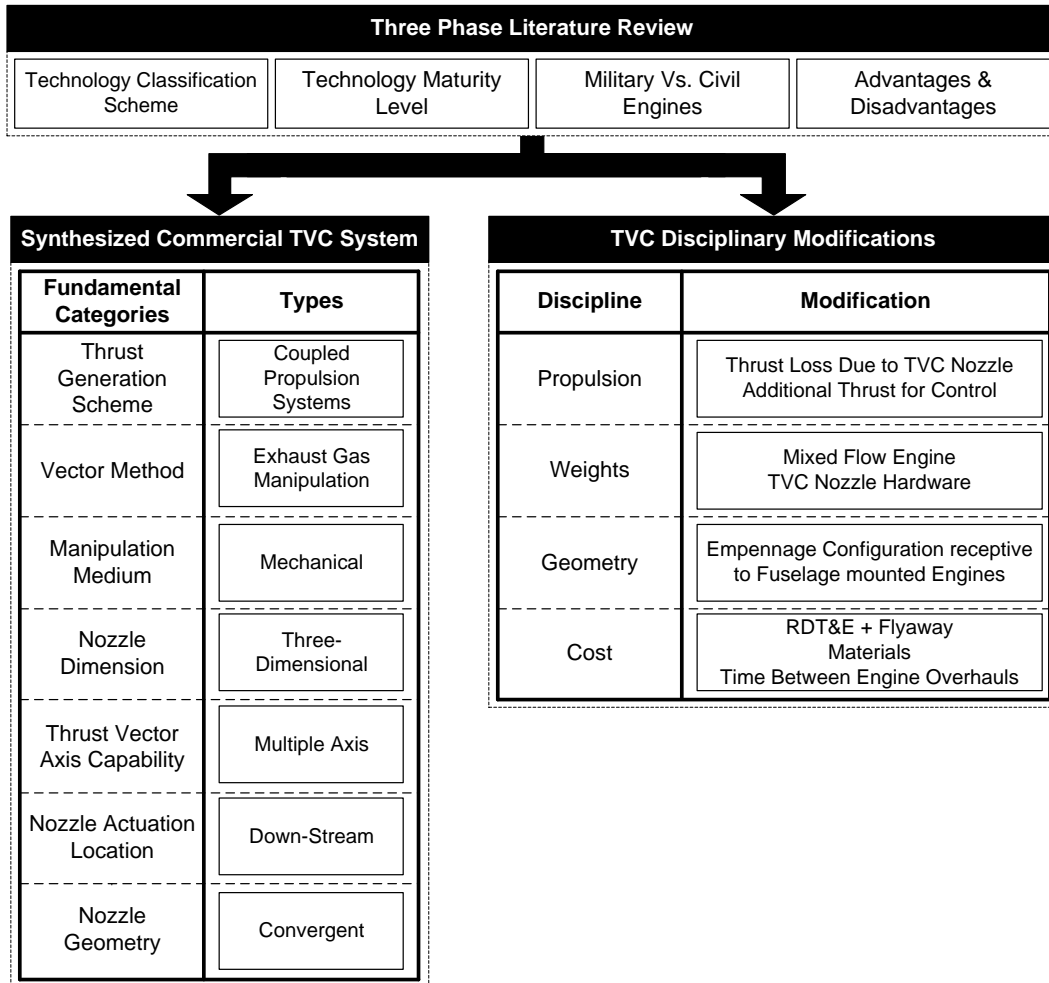


Figure 2.6 Synthesized Commercial TVC System

## Chapter 3

### SOLUTION CONCEPT ARCHITECTURE

This chapter presents the solution concept architecture. The solution concept architecture is the process implemented to identify the solution that satisfies the research objective of the research. As stated in Chapter 1.5, the fundamental objective of this research is to quantitatively evaluate, during the conceptual design phase, TVC technology applied to a commercial transport aircraft. In order to address the research objective, the research approach follows the path blazoned by engineers of the past. During their time, the engineers had to question: how to design a supersonic aircraft, how to design a space launcher, etc. This was their challenge: How do we, for the first time feel, see, taste, and bite on this unknown island, hidden in the fog. This chapter embodies the constructed solution concept architecture that grants access to this unknown island. The solution concept architecture discussion is subdivided into three major sections: 1) Solution Concept Methodology, 2) Methodology Methods – CD Synthesis System, and 3) Case Study. The results and subsequent discussion of the results, presented in Chapter 4 are separated from the explanation of the research methodology and case study.

#### 3.1 Solution Concept Methodology

The research strategy constructed is a systematic, theoretical analysis of the feasibility of a TVC enhanced TAC aircraft, studied at the parametric sizing step of the conceptual design level. In order to address the complete TVC picture, the following flight mechanics aspects must be considered within the solution concept methodology: 1) Performance, 2) **Stability and Control (S&C)**, and 3) Safety / Certification.

The AVD Laboratory TVC case study, discussed in references [15] and [27], has addressed the extremes of the complete TVC picture by analyzing, at a sizing level, the 100% Aerodynamic CE (Reverse engineered B777-300ER) and the 100% TVC CE (complete removal

of the empennage). The result of the 100% empennage removal study demonstrated “... with AeroMech (a generic stability and control tool for conceptual design) in this study that this aircraft would require excessive thrust nozzle deflections for trim and would be uncontrollable during OEI conditions. ...” [15] proving certification was not possible. As visualized in Figure 3.1, the next step is to identify synergistic balance in-between 100% Aerodynamic CE and 100% TVC CE.

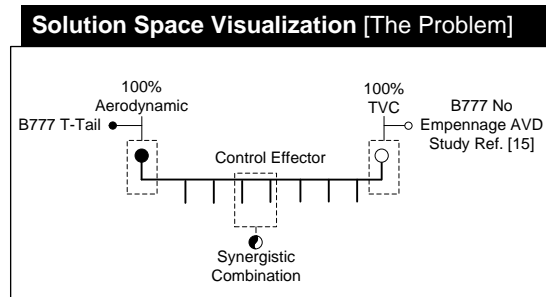


Figure 3.1 Solution Space Visualization

This requires both a performance sizing study and an S&C study; however, there is no sizing study on this topic. As such, this research begins with a performance sizing study and incorporates the S&C study by analyzing the **Design Constraining Flight Conditions (DCFCs)** related to the **Longitudinal Control Effectors (LoCEs)** and **Directional Control Effectors (DiCEs)**.

The primary methods that makeup the solution concept methodology are organized into two major components described in Table 3.1.

Table 3.1 Primary Methodology Methods of the TVC Feasibility Assessment

Primary Methods	Responsibility
1 AVDS Analysis	Size, Performance, and Cost Analysis
2 S&C Analysis	Controllability Assessment

The roadmap of the procedure in which these methods are utilized to achieve the research objective is visualized in the solution concept methodology, Figure 3.2.

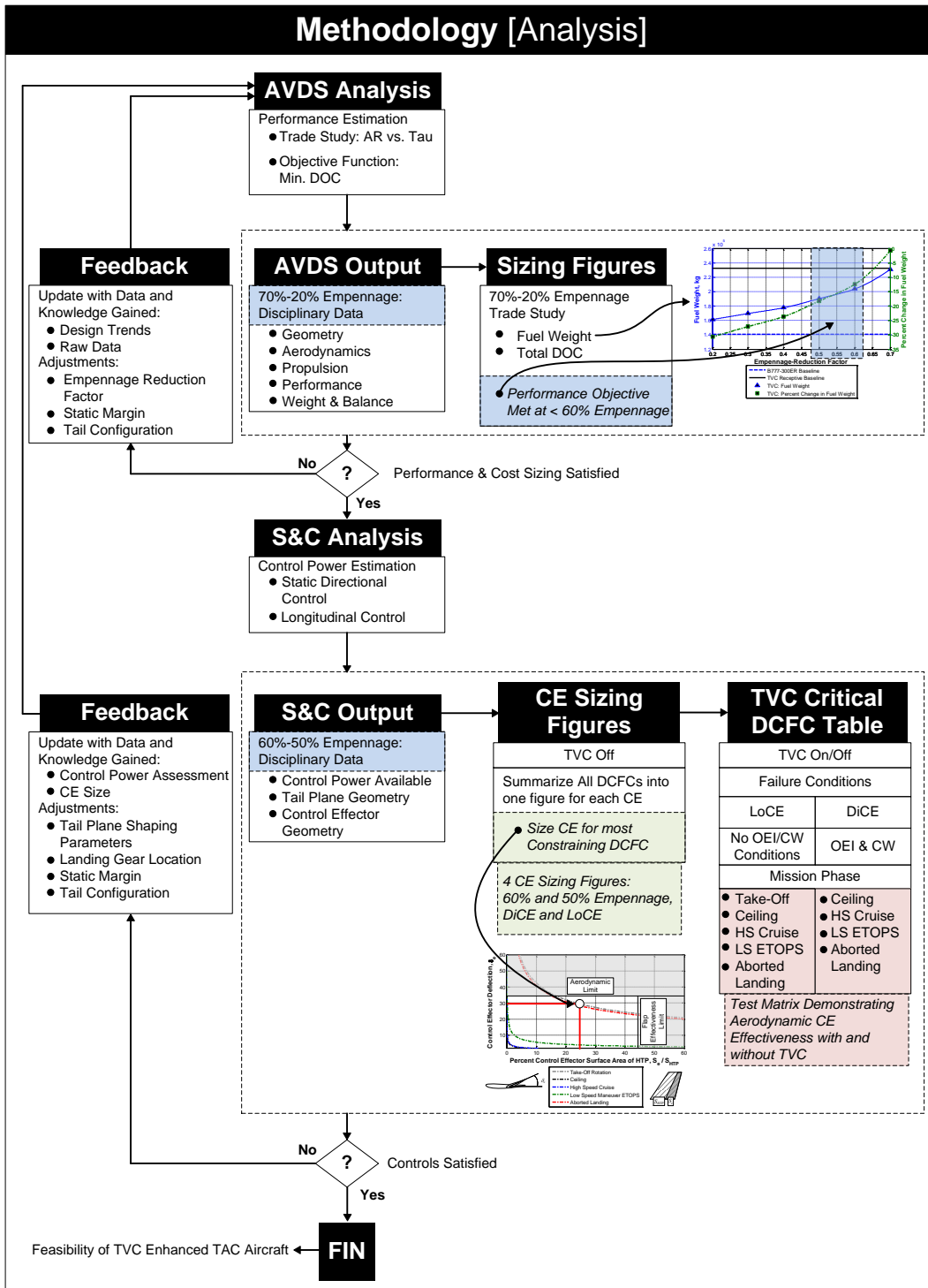


Figure 3.2 Solution Concept Methodology

Put simply, the methodology shown in Figure 3.2 outlines the systematic process in which two input-analysis-output methods are connected, with feedback loops, providing the CD engineer the capacity to properly address the research objective. When interpreting Figure 3.2, the reader should begin from the top most block (AVDS Analysis), and follow the arrows as they represent the flow of data / knowledge from one step to the next. As listed in Table 3.1, there are two primary methods. After each method's analysis, the raw, unfiltered data is collected and stored in a structured database. In order to bring meaning to the raw data, data reduction analysis is performed, visualizing the data in the form of case study independent figures. The engineer is now able to make informed decisions utilizing knowledge gained from the analysis and produced figures. The decision is to utilize the gained knowledge to continue to refine the design (Feedback Loop), or to move forward with the next step in the methodology.

The description of the primary methods and the logic for their respective selection is discussed in Chapter 3.2. After the reader is familiar with the contents of the methodology, the discussion of its application to a case study is presented in Chapter 3.3. As stated previously, the results of this case study are available in Chapter 4.

### 3.2 Methodology Methods – CD Synthesis System

In order to reveal the rationale for selecting the appropriate conceptual design synthesis system, the history of the selected system's conception is presented. The rationale for using the respective software is tied to the reason for its creation. As such, the following chapter sections (3.2.1 and 3.2.2) identify the key points that contributed to the creation of the **Aerospace Vehicle Design Sizing (AVDS)** tool and provide the reader a programmers-level perspective of the AVDS logic and methods. Contained within chapter section 3.2.2 is the description of the associated requisite modification of the method. As the AVDS tool does not directly address conceptual design S&C at an adequate level, a unique TVC-TAC aircraft S&C tool is developed to perform the required S&C analysis. The discussion of the S&C analysis method is discussed

in chapter section 3.2.3. Table 3.2 outlines chapter section 3.2, the CD synthesis system breakdown.

Table 3.2 Conceptual Design Synthesis System Breakdown

	<b>Chapter Title</b>	<b>Section</b>	<b>Major Discussion</b>
1	Conceptual Design Synthesis System Review	3.2.1	Legacy Synthesis Systems, Fundamental Elements of Sizing, State of the Art in Sizing
2	AVDS Parametric Sizing Code	3.2.2	AVDS Programmer-Level Perspective, AVDS Logic, AVDS Methods, Empennage Sizing Method
3	Stability and Control Analysis	3.2.3	Static Directional Control and Longitudinal Control

### 3.2.1 *Conceptual Design Synthesis System Review*

Aerospace companies in the business of conceptual design, develop specific methods of executing conceptual design synthesis. Commonly, companies keep these methods proprietary. [15] Fortunately, many public domain examples exist in the form of textbooks, short course notes, design code user's guides, and published literature. The initial research efforts performed by Chudoba [14], Xiao [28], and later expanded by Coleman [15] culminated in the review of over a hundred public domain, conceptual design synthesis systems. The systems are categorized into two categories:

1. By-hand design processes – The integration task is performed in a manual fashion.
2. Computer-integrated design processes – The integration task is performed in an automated fashion. [15]

Table 3.3 and Table 3.4 are extracts representative of the CD synthesis systems utilized in aerospace development from the past to today. The reader is encouraged to examine the appropriate reference authors for a complete list, including related references, of the material provided in these tables.

Table 3.3 Selected 'By-Hand' Conceptual Design Texts and Course Material [14]

Reference	Original Publication	Latest Publication	Title
Wood	1934	1963	Aerospace Vehicle Design Vol. I, Aircraft Design
Corning	1953	1979	Supersonic and Subsonic, CTOL and VTOL, Airplane Design
Nicolai	1975	1984	Fundamentals of Aircraft Design
Loftin	1980	1980	Subsonic Aircraft: Evolution and the Matching of Size to Performance
Torenbeek	1982	1982	Synthesis of Subsonic Airplane Design
Stinton	1983	1983	The Design of the Aeroplane
Roskam	1985	2003	Airplane Design, Parts I-VIII
Raymer	1989	2006	Aircraft Design: A Conceptual Approach
Jenkinson	1999	1999	Civil Aircraft Design
Howe	2000	2000	Aircraft Conceptual Design Synthesis
Schaufele	2000	2000	The Elements of Aircraft Preliminary Design

Table 3.4 Selected Computer-Integrated Conceptual Design Synthesis Systems [15]

System	Full Name	Developer	Application	Years
AAA	Advanced Airplane Analysis	DARcorporation	Aircraft	1991-
ACES	Aircraft Configuration Expert System	Aeritalia	Aircraft	1989-
ASAP	Aircraft Synthesis and Analysis Program	Vought Aeronautics Company	Fighter Aircraft	Paper 1974
FLOPS	FLight OPTimization System	NASA Langley Research Center	?	1980s-
PrADO	Preliminary Aircraft Design and Optimization	Technical University Braunschweig	Aircraft and Aerospace Vehicle	1986-
VDK/HC	VDK/Hypersonic convergence	MacDonnell Douglas, Hypertec	SAV/Hypersonic Cruise	

The review performed by Coleman [15] determined that six fundamental elements make up the majority of modern, constant mission sizing, processes. The six fundamental elements are listed below:

- 1) **Operating Empty Weight (OEW)** estimation - This represents the vehicle structural, systems, operational items and propulsion system weight.
- 2) Trajectory analysis (fuel weight estimation) - Based on the required range and endurance requirements, the fuel weight is estimated.
- 3) Convergence logic - In its simplest form, convergence is the method of solving the implicit function formed by the OEW estimation and Trajectory analysis.

- 4) Constraint analysis - From the mission and operational requirements such as take-off field length, maximum cruise speed, approach speed, **One Engine Inoperative (OEI)** climb, etc., the required wing loading (W/S) and thrust loading (T/W) are computed.
- 5) Sizing logic - A logic is imposed around the above elements which iterates certain geometry variables (typically wing area) to meet some objective (typically, minimum **Take-Off Gross Weight (TOGW)**).
- 6) Trade studies - By varying the assumed constants and solving the sizing logic for each new set of assumed constants, the designer gains a first-order visualization of the design solution space. These trade-studies can take the form of geometric parameter variation, such as **Aspect Ratio (AR)**, or technology variation, such as composite vs. aluminum materials. In some 'Computer-Based' processes, optimizers are employed to perform trade-studies according to a prescribed objective function (minimum TOGW, minimum **Direct Operating Cost (DOC)**, etc.). [15]

The literature review of 'by-hand' CD synthesis systems brought to light that the majority elected to simplify the convergence logic in an effort to reduce the required number of iterations for convergence. As stated by Coleman, these simplified approaches "... *became too general for even simple trade-studies of the classical aircraft shape. ...*" [15] The short cuts in convergence logic taken by the simplified by-hand approaches serve more as educational tools rather than industry ready, CD synthesis systems.

The review of computer integrated approaches revealed that most did not dramatically advance the state-of-the-art in CD synthesis. The majority of the computer-integrated approaches established their uniqueness with only minor nuances in the order elements are arranged in the convergence logic. Additionally, many processes only incorporated refinement to the disciplinary methods utilized within the general sizing process. These computer-integrated approaches focused on increasing the accuracy and precision of the analysis. One notable exception is the synthesis system developed by Czysz [29]—Hypersonic Convergence.

Hypersonic Convergence is a unique parametric sizing tool. Hypersonic Convergence resets the parametric sizing framework by providing a process in which the sizing logic is independent of the configuration. As stated by Coleman, "... *the design problem posed with hypersonic aircraft requires an advanced sizing logic since the hypersonic aircraft is a fully blended geometry. ...*" [15] As such, the convergence logic within Hypersonic Convergence considers the total aircraft, specifically volume; integrating the volume supply of the fuselage, wing, empennage, and propulsion systems simultaneously. This total system approach leads to the following unique aspects of Hypersonic Convergence:

- 1) Convergence Logic - Two unique elements introduced: 1) simultaneous solution to weight and volume budgets, and 2) the introduction of a unique sizing parameter (Kucheman's Slenderness Parameter,  $\tau$ ) into the convergence logic that links planform area with volume.
- 2) Solution Space - For a given set of assumed constants, a single curve describing the feasible design solution space is visualized. This simplification is not typical of legacy synthesis systems.

An in-depth review of each conceptual design synthesis systems uncovered that the initial step in aircraft conceptual design—parametric sizing—had stagnated and thus presented an opportunity for advancement. The state-of-the-art in CD synthesis, as represented by Hypersonic Convergence, was restricted to the hypersonic flight regime. Realizing the flight regime restriction, Coleman [15] set out to develop the AVDS code. Utilizing the unique techniques and logic used in Hypersonic Convergences, this endeavor resulted in the development of a single conceptual design synthesis system (AVDS) that is independent of vehicle configuration and applicable to subsonic through hypersonic flight regimes. The AVDS code has been validated and calibrated against several studies ranging from subsonic to hypersonic, listed in Coleman [15].

### 3.2.2 AVDS Parametric Sizing Code

Given the above review, AVDS is identified as the state-of-the-art in CD synthesis. As such, AVDS represents the best synthesis tool available. Therefore, this TVC study uses AVDS as the CD synthesis system. As the selected toolset, it is necessary to give a programmers-level perspective presentation on the inner workings of AVDS. For a more in-depth description of the AVDS code, the reader is encouraged to refer to reference [15]. The following presents an introduction to the AVDS code's mathematical relations, methods, and logic.

The AVDS code is a modular CD parametric sizing solution providing a systems-level solution space visualization. AVDS consist of five distinct modules: 1) geometry, 2) constraint analysis, 3) trajectory analysis, 4) weight budget, and 5) volume budget. The modules are executed within an integrated disciplinary analysis environment with constant mission-performance and total system convergence logic that identifies the feasible solution space. The initiation of the AVDS code begins with the development of the input file.

Through the input file, the user selects the appropriate disciplinary methods and identifies all data to define the mission requirements including the basic geometry, propulsion, and configuration assumptions. The contents of the input are categorized into two different sets: independent and dependent variables. These two categories, with summarized inputs, are shown in Figure 3.3.

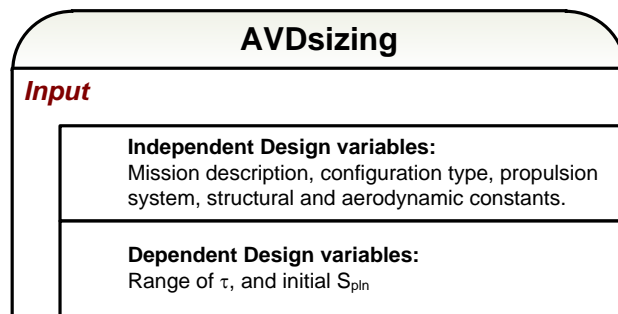


Figure 3.3 AVDS Input File Design Variables

The logic of AVDS follows a strict order of operations as shown in Figure 3.4. For a given  $\tau$  value, the analysis begins with the geometry module and sequentially proceeds through the constraint and trajectory analysis modules. These three modules utilize methods representing the five classical aerospace disciplines: 1) aerodynamics, 2) propulsion, 3) stability and control, 4) structures, and 5) weight and balance. [15] After the execution of these three modules, the outputs are used within the weight budget and volume budget modules to estimate the OEW.

The next step is the application of the convergence logic. The outputs of the weight and volume budget modules are at the heart of the convergence logic. The convergence logic is visualized in Figure 3.4 by the loop immediately surrounding the five modules. The convergence logic iterates the wing planform area ( $S_{pln}$ ), looping through the above order of operations until a specific convergence criterion is satisfied. This specific convergence criterion is satisfied when the two OEW estimations adequately agree. Put simply, convergence is the numerical solution to the algebraic system of two equations and two unknowns. [15] The equations that make up this algebraic system are shown in equations 3.1 and 3.2. [15]

$$\text{Weight Budget} \quad OEW = \frac{W_{str} + W_{sys} + W_{operation\ items} + \frac{T/W}{E_{TW}} WR (W_{pay} + W_{crew})}{\frac{1}{1 + \mu_a} - f_{sys} - \frac{T/W}{E_{TW}} WR} \quad 3.1$$

$$\text{Volume Budget} \quad OEW = \frac{\tau * S_{pln}^{1.5} (1 - K_{vv} - k_{vs}) + V_{pay} + V_{crew}}{\frac{WR - 1}{\rho_{ppl}} - k_{ve} * T/W * WR} \quad 3.2$$

Note:  $OEW = OEW + W_{pay} + W_{crew}$

The remaining step is solution space construction. The single curve representing the solution space is created by executing the above process through a range of  $\tau$ . Lastly, a trade study can be performed by changing any independent design variable and repeating the entire process. Arranged in this manner, “... the fundamental process is applicable to any fixed wing aircraft or launcher with changes in the disciplinary methods and geometry module. ...” [15]

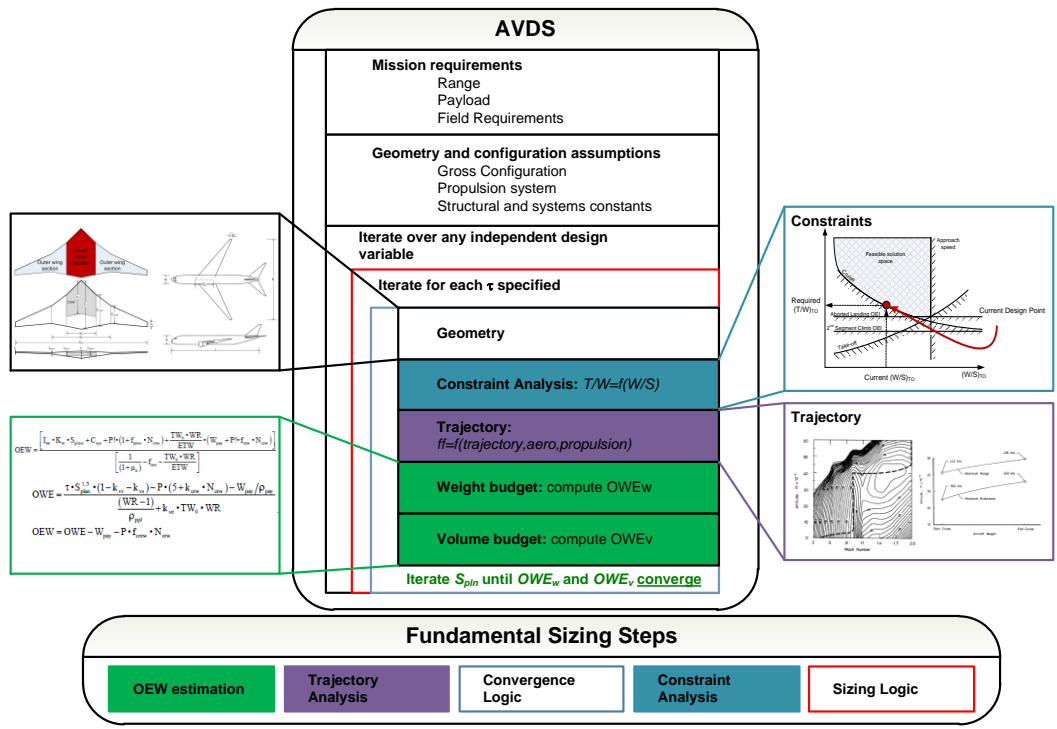


Figure 3.4 Fundamental AVD Sizing Logic [15]

The methods listed in Table 3.5 represent the classical aerospace disciplines, mentioned previously, used by the AVDS code to model a classical TAC commercial transport aircraft mission. The methods listed in Table 3.5 are also the methods selected for this research endeavor.

Table 3.5 AVDS Methods for TAC Aircraft [15]

Use	Method Title	Author	Categorization
<b>Geometry</b>			
Wing & Fuselage Definition	Transonic Tail-Aft Configuration	Coleman	Analytical
Empennage Definition	Modified Tail-Volume Quotient	Hahn, Morris	Empirical
<b>Aerodynamics</b>			
Friction and Form Drag	Subsonic Skin Friction Estimation	Smith	Semi-Empirical
Friction and Form Drag	Subsonic Partial laminar Skin Friction Estimation	Roskam, MACair	Semi-Empirical
Drag Due to Flaps and Landing Gear	Initial Drag Polar Estimation	Roskam	Semi-Empirical
Drag Due to Flaps and Landing Gear	Drag Due to Landing Gear	Roskam	Semi-Empirical
Wave Drag	MAC Wave Drag Approximation	Czysz	Semi-Empirical
Induced Drag	Induced Drag	Wilson	Semi-Empirical
Lift Curve Slope	Lift Curve Slope	Hoak	Semi-Empirical
Maximum Lift Coefficient	Maximum Landing Lift Coefficient	Roskam	Typical Values
Drag Polar Location Specification	Lift to Drag Ratio	Vinh	Analytical
<b>Propulsion</b>			
Specific Fuel Consumption	Turbofans, Turbojet, and Turboprop SFC Variation	Mattingly	Empirical
Thrust Variation	Turbofans, Turbojet, and Turboprop SFC Variation	Mattingly	Empirical
Propulsion System Sizing	Turbofan Engine Preliminary Design	Svoboda	Empirical
<b>Performance</b>			
Stall	Stall Speed Representation	Roskam	Semi-Empirical
Landing Distance	Landing Distance Representation for FAR 25 Aircraft	Roskam	Semi-Empirical
Take-off Distance	Take-off Distance Representation for FAR 25 Aircraft	Roskam	Semi-Empirical
Climb Gradient Requirement	Climb Performance Matching for FAR 25 Aircraft	Loftin	Empirical

Table 3.5—Continued

Take-off and Climb	Take-off and Climb Performance Matching for FAR 25 Aircraft	Coleman	Semi-Empirical
Design Cruise	Cruise Matching	Coleman, Loftin	Analytical
Time to Climb	Climb Requirements for Jet Powered Aircraft	Roskam, Coleman	Semi-Empirical
Descent Performance	Compute the Range and Time to Descent	Roskam	Semi-Empirical
Maximum Velocity	Maximum Velocity Constant for Jet Powered Aircraft	Roskam	Semi-Empirical
Ceiling	Ceiling Requirements for Jet Powered Aircraft	Roskam	Semi-Empirical
Fuel Weight Estimation/Trajectory	Initial Fuel Weight Estimation	Roskam	Semi-Empirical

---

**Stability and Control**

Trim	Approximate Trim Solution	Coleman, Torenbeek	Semi-Empirical
Trim	Approximate Trim Solution	Hoak, Torenbeek	Semi-Empirical

---

**Weight and Balance**

Structural Loads	V-N Diagram and Structural Limits for FAR 25 Aircraft	Roskam	Semi-Empirical
Empty Weight and Volume Formulation	Convergence Empty Weight Estimation	Coleman, Czysz	Empirical
Structural Weight	Wing Structure Group Weight Fraction	Nicolai	Empirical
Structural Weight	Fuselage Mass Estimation	Howe	Empirical
Structural Weight	Tail Structure Group Weight Fraction	Torenbeek	Empirical
Structural Weight	Raymer Cargo/Transport Aircraft nacelle Weight	Roskam	Empirical
Structural Weight	Torenbeek Commercial Transport Landing Gear Weight	Roskam	Empirical
Propulsion System Weight	Power Plant Mass Estimation	Howe	Empirical
Fixed Equipment Weight	Refined Hydraulic and/or Pneumatic Group Weight	Roskam	Empirical
Fixed Equipment Weight	Refined Instrumentation Group Weight	Torenbeek	Empirical
Fixed Equipment Weight	APU Weight	Roskam	Empirical

Table 3.5—Continued

Fixed Equipment Weight	Furnishings Weight	Torenbeek	Empirical
Fixed Equipment Weight	Baggage Handling Equipment Weight	Roskam	Empirical
Operational Items Weight	Operational Items Mass Estimation	Howe	Empirical
<b>Cost</b>			
Life Cycle Cost Formulation	Life Cycle Cost	Roskam	Empirical
RDT&E Estimation	RAND DAPCA IV RDT&E and Production Cost Model	Hess	Empirical
Manufacturing and Acquisition	Method for Estimating Manufacturing and Acquisition	Roskam	Semi-Empirical
Direct Operating Cost	Direct Operating Cost for Commercial Airplanes	Roskam	Semi-Empirical
Block Mission	Block Mission for Commercial Transports	Roskam	Semi-Empirical

### 3.2.2.1 Empennage Sizing Method

The TVC case study, using the AVDS code, addresses empennage sizing using the tail volume quotient method. The tail volume quotient method is a universally accepted—Raymer, Howe, Nicolai, Roskam, Wood, Morris, etc.—method by Hahn and modified by Morris [30], that is well suited for conceptually sizing the empennage and is applicable to conventional TAC transonic transports of fixed cabin cross-section. This method (Equations 3.3 - 3.6) is an empirical “... correlation of tail size against aircraft geometry ...” which connects the position and size of the wing and fuselage to the empennage tail plane surface areas. [29] As such, the case of a 100% aerodynamic control effectors (Full Empennage) sizes the empennage using the relations below:

$$\text{Vertical Tail Volume Quotient} \quad V_V = K_{VT} \left( \frac{d_{max}^2 L_{fus}}{S_{pln} b} M_{VT} + B_{VT} \right) \quad 3.3$$

$$\text{Vertical Tail Surface Area} \quad S_V = \left( \frac{V_V}{l/b} \right) \quad 3.4$$

$$\text{Horizontal Tail Volume Quotient} \quad V_H = \frac{d_{max}^2 L_{fus}}{S_{pln} C} M_{HT} + B_{HT} \quad 3.5$$

$$\text{Horizontal Tail Surface Area} \quad S_H = \left( \frac{V_H}{l/c} \right) \quad 3.6$$

The modifications to the tail volume quotient method for the reduced empennage case so that the TVC aircraft has redundant aerodynamic control surfaces empirically sized to replace the TVC technology are shown below.

$$\text{Vertical Tail Volume Quotient} \quad V_V = K_{VT} \left( \frac{d_{max}^2 L_{fus}}{S_{pln} b} M_{VT} + B_{VT} \right) \quad 3.7$$

$$\text{Vertical Tail Surface Area} \quad S_V = \left( \frac{V_V}{l/b} \right) \quad 3.8$$

$$\text{Horizontal Tail Volume Quotient} \quad V_H = \frac{d_{max}^2 L_{fus}}{S_{pln} \bar{c}} M_{HT} + B_{HT} \quad 3.9$$

$$\text{Horizontal Tail Surface Area} \quad S_H = \left( \frac{ERF}{l/c} \right) V_H \quad 3.10$$

$$\text{Empennage-Reduction Factor} \quad \text{Unmodified: } ERF = 1.0 \quad 3.11$$

This research introduces the **Empennage-Reduction Factor (ERF)** to dictate a reduced empennage. As shown in equation 3.10, the ERF is only applied to the **Horizontal Tail Plane (HTP)** surface area equation. As shown in Figure 3.4 this method lies at the core of the AVDS code within the geometry module. As such, with every change in the independent ERF, the design is completely resized which causes the **Vertical Tail Plane (VTP)** to be empirically sized accordantly. The next section addresses how the empennage is sized and its fundamental link with the static margin method.

As stated in chapter section 3.2.3, according to FAR documentation, the aircraft must remain statically stable. This translates to a static margin convergence constraint that balances the aircraft geometry to achieve a desired margin of longitudinal stability. Static Margin expresses the degree of pitch stability or instability as represented in equation 3.12.

$$\text{Static Margin} \quad S.M. = \frac{X_{np} - X_{cg}}{c} \quad 3.12$$

The static margin is a measurement between the center of gravity and the neutral point of the airframe. Positive static margin means the airframe is longitudinally statically stable. Negative static margin means the airframe is longitudinally statically unstable. The AVDS code

incorporates the static margin formulation within the convergence logic as shown in the expanded visualization of the fundamental AVD sizing logic in Figure 3.5.

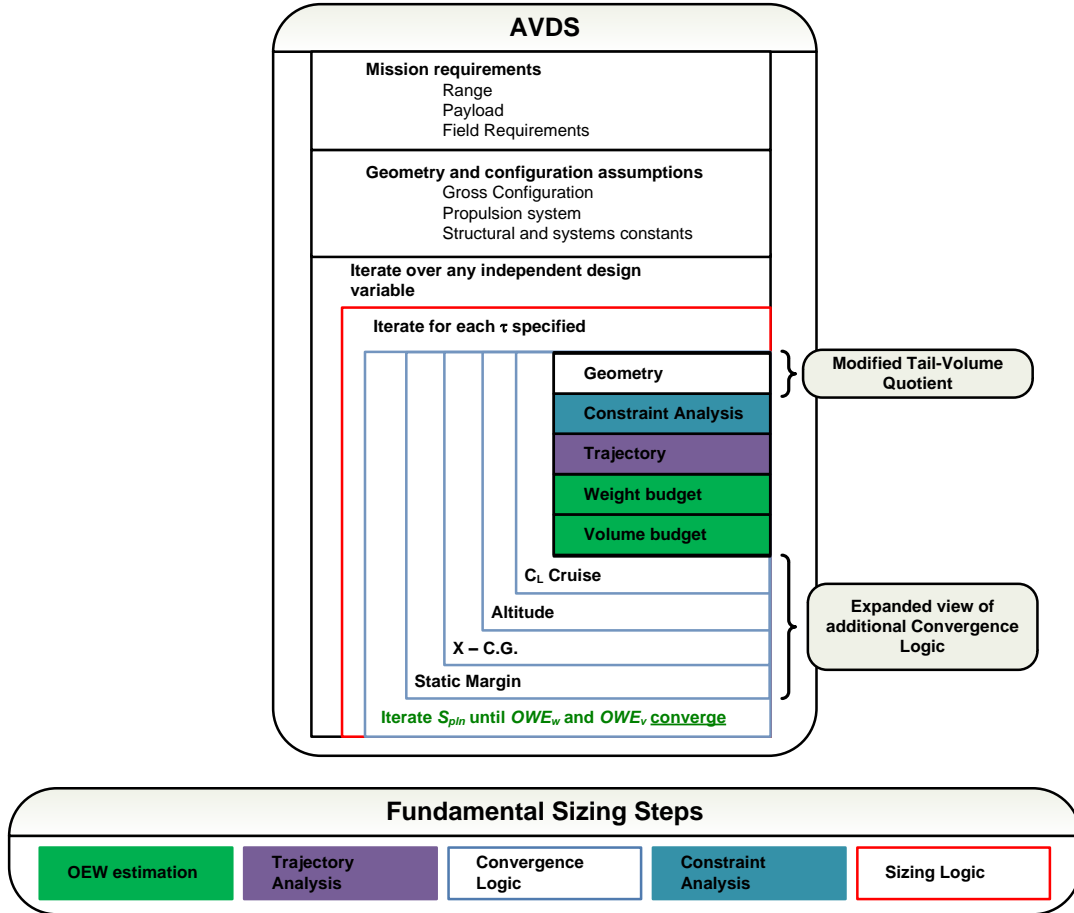


Figure 3.5 Expanded Fundamental AVD Sizing Logic [15]

As seen in Figure 3.5, the static margin method is incorporated at the second outermost shell of the convergence logic. If the static margin criterion is not satisfied, the aircraft geometry is automatically readjusted and resized until the criterion is satisfied. This establishes the link between the tail volume quotient and the static margin methods that allows for the conceptual sizing of the empennage with the converged total aircraft.

The case study is evaluated with a positive static margin of 2.0%. This value is a commonly accepted percentage of static margin associated with commercial transportation airframes. [15], [11]

### 3.2.3 Stability and Control Analysis

When formulating a new methodology—synergistic reduction of empennage size—certain design constraining flight conditions (DCFCs) must be evaluated. This chapter section addresses the stability and controllability aspects of current safety and certification regulation. With the methodology centered on the reduction of the empennage volume, the obvious extreme reduction case would be the configuration with complete removal of the empennage, similar to the study performed by Coleman [15] and Omoragbon [27]. As discussed earlier, the design case study executed by Coleman and Omoragbon would not meet current FAR requirements placed on civilian aircraft. Currently, FAR documentation does not allow for complete deletion of traditional aerodynamic control surfaces due to several safety and certification requirements. These requirements are tied to the safe operation of the aircraft through discussion of stability and control.

FAR 25.171 establishes a general statement of stability. Concerning stability, FAR addresses this issue as follows [24]:

#### § 25.171 General - Stability:

*"The airplane must be longitudinally, directionally, and laterally stable in accordance with the provisions of §§25.173 through 25.177. In addition, suitable stability and control feel (static stability) is required in any condition normally encountered in service, if flight tests show it is necessary for safe operation."*

This statement does not explicitly refer to how stability and control must be achieved. It also does not state that the static stability requirement must be 'naturally' statically stable, achieved without the aid of a **Stability Augmentation System (SAS)**. It only states it must "*feel*" statically stable. Simply stated, Static stability is a state where "... *the resulting forces and moments from the disturbance push the aircraft toward its original equilibrium state...*" without any inputs from pilot. [11] Understanding that if an aircraft can be proven controllable throughout the DCFCs, stability can be achieved with the aid of a SAS system. As restated by Chudoba, "... *the*

availability of sufficient control power is of primary importance, since any stability level can be realized having sufficient control authority available. ...” [14] As such, the next section discusses the controllability assessment performed by the second primary method of Figure 3.2.

FAR documentation addresses the controllability of the aircraft by breaking down the flight profile into the particular mission phases (Takeoff, Climb, Cruise, Approach, and landing), addressing each phase independently. Additionally, the FAR documentation identifies key DCFCs of the flight profile that are applicable to TVC enabled commercial TAC aircraft. These DCFC have been identified and summarized by references [14], [27], [11], [12], and [31]. The following figure visualizes the flight profile and identifies the critical corners that are studied by this S&C analysis.

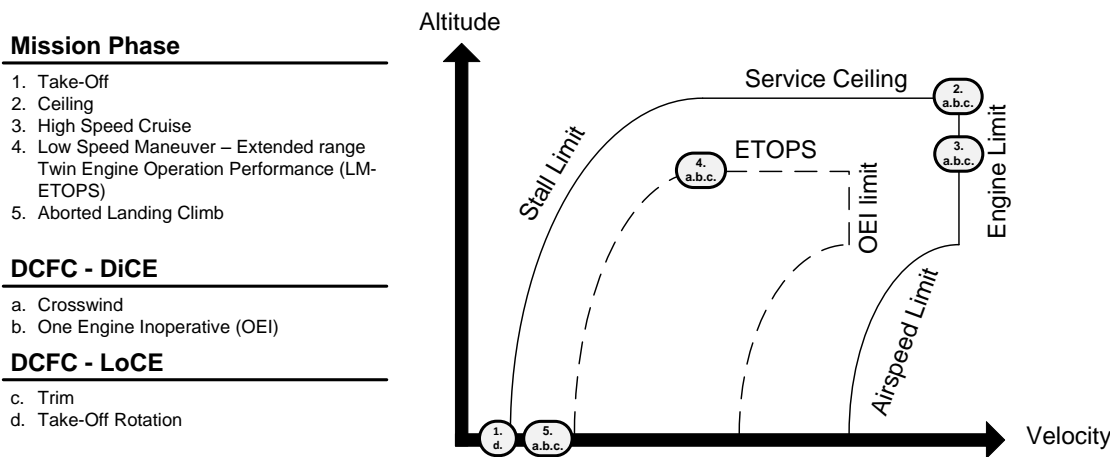


Figure 3.6 Mission Critical Corners of the Flight Profile for Control Power Assessment of a TVC Enabled Aircraft

The DCFC are selected to analyze the available control power at the most critical corners of the flight profile for a TVC enabled TAC aircraft. The goal of this analysis is to determine if the aircraft has adequately sized **Control Effectors (CEs)**. As shown in Figure 3.6, the phases of the mission under investigation are 1) Take-Off, 2) Ceiling, 3) High Speed Cruise, 4) **Low Speed Maneuver – Extended range Twin engine Operation Performance Standards (LM-ETOPS)**, and 5) Aborted Landing Climb. The DCFC scenarios considered are a) asymmetric flight –

Crosswind, b) **One Engine Inoperative (OEI)**, c) Trim, and d) Take-Off Rotation. The high altitude and high-speed conditions, which typically do not size aerodynamic CEs, are investigated because partial control power is supplemented by the TVC system. Under these conditions, the limit of engine thrust is reached. Additionally, under the OEI scenario, the available TVC control power is cut in half. Considering these factors along with the DCFCs detailed in reference [14], a DCFC test-matrix is devised. This matrix is expressed in Table 3.6.

Table 3.6 Design Constraining Flight Condition (DCFC) Test Matrix

Aircraft:		Aircraft Data:						
B777-TVC		Configuration Settings, Flight Condition Variables, Failure Condition						
DCFC Scenario		L.G.	Air Speed	Altitude	Performance Segment	Weight	Engine Status	Crosswind Angle
Mission Phase	Control Effector	(-)	(m/s)	(m)	(-)	(-)	(-)	(deg)
2	DiCE	Up	247.9	12000.0	Ceiling	WR	AEO / OEI	11.5
3	DiCE	Up	255.5	8924.0	Design Cruise	WR	AEO / OEI	11.5
4	DiCE	Up	128.6	3000.0	ETOPS LS Cruise	WR	AEO / OEI	11.5
5	DiCE	Down	71.5	0.0	Aborted Landing	MLW	AEO / OEI	11.5
1	LoCE	Down	66.0	0.0	Take-Off	TOGW	AEO	0
2	LoCE	Up	247.9	12000.0	Ceiling	WR	AEO	0
3	LoCE	Up	255.5	8924.0	Design Cruise	WR	AEO	0
4	LoCE	Up	128.6	3000.0	ETOPS LS Cruise	WR	AEO	0
5	LoCE	Down	71.5	0.0	Aborted Landing	MLW	AEO	0

The applicable methods to analyze the static directional control and longitudinal control are programed, using the MATLAB script language, into a unique TVC-TAC aircraft Stability and Control tool. The S&C tool requires over 220 unique inputs from the traditional aircraft disciplines such as geometry, weights, performance, aerodynamics, propulsion, and stability and control to analyze the DCFCs of Table 3.6. These inputs are provided by the AVDS tool. The output of the S&C tool is a control power assessment, tail plane geometry, and control effector geometry. This data is first visualized by comparing the different DCFC scenarios of a single CE, on a spread of CE deflections versus percent CE tail plane area. The TVC critical DCFCs are identified by investigating the visualizations with and without TVC deflection. This tool and its methods have been check against examples contained within reference [32]. The methods used in the S&C tool are discussed next.

### 3.2.3.1 Static Directional Control Methods

The goal of the following methods is to enable the capability to determine if the DiCE, the rudder, is adequately sized to provide static directional control over the key DCFs discussed in Table 3.6. This is performed by investigating the moment generated by the aircraft under specific scenarios and determining if the CE has sufficient size to produce the required balancing moment. Figure 3.7 represents the free-body diagram of the forces on an aircraft for directional motion.

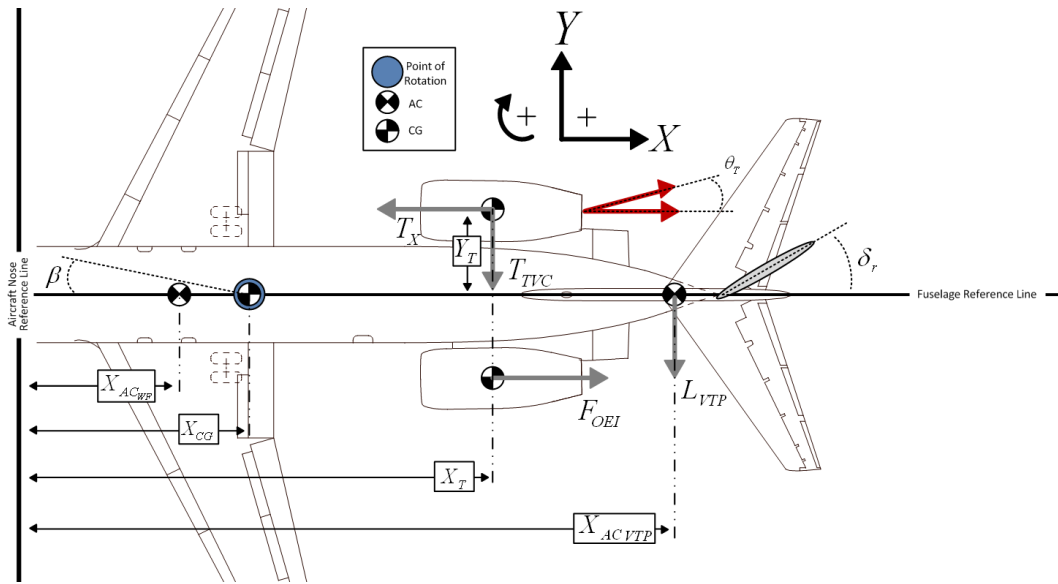


Figure 3.7 Directional Control Free-Body Diagram

The first method to be discussed is the relation that estimates the thrust available for control. Assuming the difference between the geometric thrust angle and the actual thrust angle is negligible; the following trigonometric expression can be used.

$$\begin{array}{l} \text{Thrust Along X-} \\ \text{Axis} \end{array} \quad T_x = T \cos \theta_T \quad 3.13$$

$$\begin{array}{l} \text{Thrust Vected} \\ \text{Away from X-} \\ \text{Axis} \end{array} \quad T_y = T \sin \theta_T \quad 3.14$$

When using the equations 3.13 and 3.14, one must incorporate a check into the code that determines if the requested thrust vector angle reduces the thrust along the X-axis more than

thrust available. This will make sure that there is sufficient thrust available to meet the thrust required by the mission segment.

Considering the moment equilibrium about the Z-axis only, the amount of rudder deflection required to maintain control under the discussed DCFCs is represented by equation 3.15 from references [12], [31], [32] and [11].

$$\text{Required Rudder Deflection } \delta_r = \frac{-C_{n_\beta} \beta - \frac{N_{T_1} + \Delta N_{D_1}}{\bar{q}_1 S b}}{C_{n_{\delta r}}} \quad 3.15$$

From the above relation, rudder control power ( $C_{n_{\delta r}}$ ) can be estimated by the following relation:

$$\text{Rudder Control Power } C_{n_{\delta r}} \approx 0.9 C_{L_{\alpha VT}} \bar{V}_{VT} \tau_f \quad 3.16$$

The directional moment contribution of the engines are modeled by the relation ( $\frac{N_{T_1} + \Delta N_{D_1}}{\bar{q}_1 S b}$ ) in the numerator of equation 3.16. As expressed in reference [12], additional yawing moment is physically caused by drag due to stopped or wind-milling High-Bypass-Ratio Turbofans. In this scenario, the following relation (Equation 3.17) is used to estimate this additional drag.

$$\text{Estimated Wind-milling Drag } N_{T_1} + \Delta N_{D_1} = (F_{OEI}) N_{T_1} \quad \text{where, } F_{OEI} = 1.25 \text{ for High-Bypass Turbofans} \quad 3.17$$

The sideslip or crosswind angle is represented by the term,  $\beta$  in equation 3.15. From equation 3.15, the following are relations that model the contributions from various airplane features as a function of sideslip angle ( $\beta$ ):

$$\text{Yawing Moment Coefficient Versus Sideslip Angle } C_{n_\beta} = C_{n_{\beta fus}} + C_{n_{\beta wing}} + \bar{V}_{VTP} C_{L_{\alpha VT}} \left(1 + \frac{d\sigma}{d\beta}\right) \frac{q_{VT}}{q} \quad 3.18$$

The relation above (Equation 3.18) is comprised of the following equations (3.19, 3.20, and 3.21):

$$\text{Fuselage Component of Yawing Moment } C_{n_{\beta fus}} = -1.3 \frac{Vol h}{S_{ref} W} \quad 3.19$$

Wing Component of Yawing Moment  $C_{n\beta_{wing}} = C_L^2[A B]$  3.20

$$A = \frac{1}{4\pi AR} - \frac{\tan \Lambda_{c/4}}{\pi AR (AR + 4 \cos \Lambda_{c/4})}$$

$$B = \left( \cos \Lambda_{c/4} - \frac{AR}{2} - \frac{AR^2}{8 \cos \Lambda_{c/4}} + \frac{6x \sin \Lambda_{c/4}}{\bar{c} AR} \right)$$

The term  $\left(1 + \frac{d\sigma}{d\beta}\right) \frac{q_{VT}}{q} = A + B$  3.21

$$A = 0.724 + \frac{3.06(\dot{S}_{VT}/S_{ref})}{1 + \cos \Lambda_{c/4}}$$

$$B = 0.4 \frac{Z_w}{d} + 0.009AR$$

Combining and rearranging equations 3.13, 3.14, 3.15, 3.16, and 3.17 allow for the CE effectiveness ( $\tau$ ) to be determined.

Rudder Effectiveness  $\tau_f = \frac{-C_{n\beta} \beta - \frac{(F_{OEI})N_{T_1}}{\bar{q}_1 S b} + \frac{T_y (X_T - X_{cg})}{\bar{q}_1 S b}}{0.9 C_{L_{\alpha VT}} \bar{V}_{VT} \delta_r}$  3.22

Once the rudder effectiveness is determined, the ratio of CE surface area to Tail plane surface area can be determined using the follow figure from reference [31].

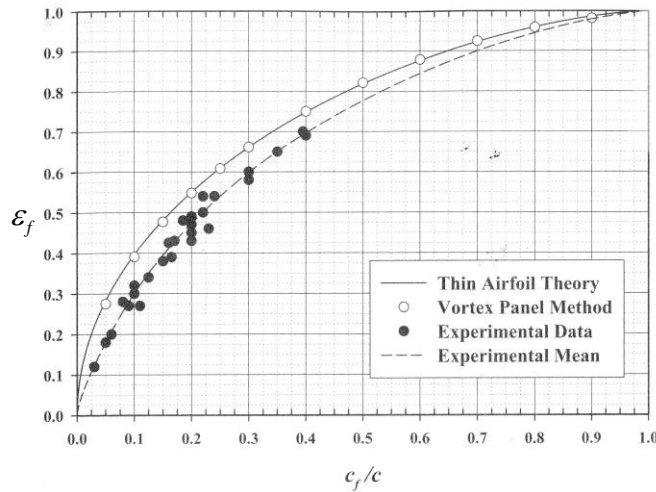


Figure 3.8 Control Effector Effectiveness Comparison among Thin Airfoil Theory, the Vortex Panel Method, and Experimental Data [31]

The next section discusses the longitudinal control methods.

### 3.2.3.2 Longitudinal Control Methods

This section deals with the longitudinal control methods applicable for assessing the longitudinal controllability for trim stability and take-off rotation. The free-body diagram for the static longitudinal control is shown in Figure 3.9 below.

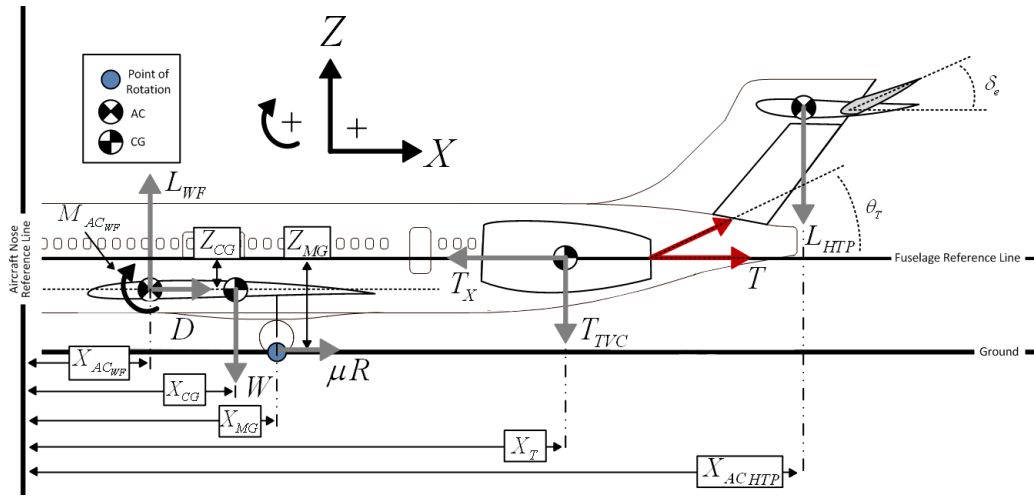


Figure 3.9 Longitudinal Control Free-Body Diagram (Specifically Take-off Rotation)

Figure 3.9 is specific to the take-off rotation maneuver but is applicable to the longitudinal trim stability analysis by neglecting rotation about the main gear and assuming rotation occurs about the **Center of Gravity (CG)**. The method to determine sufficient control power to trim, longitudinally, across the flight profile is given by the follow expressions (3.23-3.25). These relations come from references [31] and [32]. The follow relation gives the expression for required control deflection for trimming the aircraft.

Control Deflection of the Elevator  $\delta_e = \frac{-C_{M_0} + (SM) C_L}{C_{M_\delta}}$  3.23

The components of equation 3.23 are discussed next. The following relation provides the coefficient of moment due to the control deflection.

Coefficient of Horizontal Tail Power  $C_{M_\delta} = -\bar{V}_{HTP} C_{L_{\alpha T}} \epsilon_f$  3.24

The next relation gives the expression for the coefficient of moment at zero angle of attack.

$$\text{Coefficient of Moment at Zero Angle of Attack} \quad C_{M_0} = C_{M_{a.c.w}} + C_{D_0} \frac{z}{\bar{c}} + \frac{T_X (Z_T - Z_{cg})}{Q_\infty S_{ref} \bar{c}} - \frac{T_Z (X_T - X_{cg})}{Q_\infty S_{ref} \bar{c}} \quad 3.25$$

In the above expression, Equation 3.25, the additive coefficient (  $C_{D_0} \frac{z}{\bar{c}}$  ) accounts for the moment generated by the aircraft drag measured from about CG from the fuselage reference line. The expressions used in Equation 3.25 to capture the moment generated by the propulsion system are modeled using two different moment arms. The moment generated by the TVC system is a measurement of the moment generated by the thrust component in the Z direction. This moment arm is the measured distance from the engine CG to the aircraft CG. The moment generated by the x-axis thrust is a measurement of the moment generated by the thrust along the x-axis by the height above or below the CG. Combining Equations (3.23 - 3.25) and solving for the elevator effectiveness (  $\epsilon_f$  ) gives the following expression (equation 3.26).

$$\text{Control Deflection of the Elevator} \quad \epsilon_f = \frac{C_{M_{a.c.w}} + C_{D_0} \frac{z}{\bar{c}} + \frac{T_X (Z_T - Z_{cg})}{Q_\infty S_{ref} \bar{c}} - \frac{T_Z (X_T - X_{cg})}{Q_\infty S_{ref} \bar{c}} + (SM) C_L}{-\bar{V}_H C_{L_{\alpha_e}} \delta_e} \quad 3.26$$

The following relations are applicable to the take-off rotation maneuver and are extracted from references [32] and [31]. These relations are the representation of the required horizontal tail plane (HTP) area to insure takeoff rotation about the main gear contact point. To begin the following three equations that govern the aircraft equilibrium at the instant of rotation are modified to include the thrust vectoring component (equations 3.13 and 3.14).

$$\text{X-Axis Force} \quad T_x - D_g - \mu_g R_g = \frac{W}{g} \dot{U} \quad 3.27$$

$$\text{Z-Axis Force} \quad L_{wf_g} + L_{H_g} + R_g + T_z = W \quad 3.28$$

$$\text{Moment About Y-Axis} \quad -W (X_{mg_g} - X_{cg_g}) + D_g (Z_{D_g} - Z_{mg_g}) - T_x (Z_{T_g} - Z_{mg_g}) + T_z (X_{T_g} - X_{mg_g}) + L_{wf_g} (X_{mg_g} - X_{ac_{wf}}) + M_{ac_{wf}} + L_H (X_{ac_H} - X_{mg}) + \frac{W}{g} \dot{U} (Z_{cg} - Z_{mg}) = I_{yy_{mg}} \ddot{\theta}_{mg} \quad 3.29$$

In order to derive the required surface area for the HTP control effector, one must solve equation 3.28 for normal force (  $R_g$  ) and substitute this relation into equation 3.27. Plugging the

now modified equation 3.27 and equation 3.30 into equation 3.29 and rearranging the variables allows for the derivation of equation 3.31.

Force  
Generated by  
Horizontal Tail  
plane

$$L_{H_g} = C_{L_{max_{h_g}}} \eta_{h_g} S_h \bar{q}_{rotate} = C_{L_{\alpha_T}} \delta_e \epsilon_f S_h \bar{q}_{rotate} \quad 3.30$$

HTP  
Effectiveness

$$\epsilon_f = \frac{\begin{bmatrix} W(X_{cg_g} - X_{mg_g} - \mu_g Z_{cg_g} + \mu_g Z_{mg_g}) + D_g(Z_{D_g} - Z_{cg_g}) + T_x(Z_{cg_g} - Z_{T_g}) + \\ T_z(X_{T_g} - X_{mg_g} + \mu_g Z_{cg_g} - \mu_g Z_{mg_g}) + L_{wf_g}(X_{mg_g} - X_{ac_{wf_g}} + \mu_g Z_{cg_g} - \mu_g Z_{mg_g}) \\ + M_{ac_{wf_g}} - I_{yy_{mg}} \ddot{\theta}_{mg} \end{bmatrix}}{(C_{L_{\alpha_T}} S_h \delta_e \bar{q}_{rotate})(X_{ac_{h_g}} - X_{mg_g} + \mu_g Z_{cg_g} - \mu_g Z_{mg_g})} \quad 3.31$$

The subscript g refers to the respective value in ground effect during the take-off run. The follow equations (3.32 - 3.35) provide the derivations used in place of each respective variable of equation 3.31. The Inertia of equation 3.35 is calculated using a component weight estimation method provided by reference [12].

Drag Force

$$D_g = C_{D_{OTO}} + AKW (C_{L_{\alpha_w}} \alpha)^2 \quad 3.32$$

Wing-Fuselage  
Lift Force

$$L_{wf_g} = \bar{q}_{rot} C_{L_{\alpha_w}} \alpha S_W \quad 3.33$$

Wing-Fuselage  
Pitching Moment

$$M_{ac_{wf_g}} = \bar{q}_{rot} C_{M_{ac}} S \bar{c} \quad 3.34$$

Mass Moment of  
Inertia about Y-  
Axis

$$I_{yy_{mg}} = I_{yy_{cg}} + \frac{W}{g} \left\{ (Z_{mg_g} - Z_{cg_g})^2 + (X_{mg_g} - X_{cg_g})^2 \right\} \quad 3.35$$

Utilizing these methods allows for the assessment of the S&C feasibility of the selected design points. The next chapter section 3.3, Case Study, is discussed next.

### 3.3 Case Study

The TVC technology by itself, as a standalone ‘add-on’ technology, increases weight, system complexity, and total vehicle cost, while decreasing engine performance. [17] This research explores if the TVC enabled commercial aircraft, designed with TVC from the outset rather than as an ‘add-on’ technology, offers improved flight performance. Specifically this study examines the performance of a TVC enabled TAC commercial transport aircraft by applying a reduced empennage method. In particular, this study explores if the TVC technology in

combination with the reduced empennage method enables the TAC aircraft to synergistically evolve while complying with current stability and controllability regulation by examining specific DCFCs. The breakdown of the case study chapter section is outlined in Table 3.7.

Table 3.7 Case Study Breakdown

	<b>Chapter Title</b>	<b>Section</b>	<b>Major Discussion</b>
1	Case Study Mission Selection	3.3.1	AVDS Mission Inputs, Mission Identification Logic <b>Error! Reference source not found.</b>
2	Case Study Tasks	3.3.2	Reverse Engineering Study, Modify Case Study Model into TVC Receptive Configuration, Modify TVC Receptive Baseline into TVC Enabled Model

### 3.3.1 Case Study Mission Selection

When selecting a mission for the case study, its best to test TVC technology where it can create the biggest wave within the commercial transportation regime. This prompts the need to identify an appropriate mission profile that would best capture (understand, model, and assess) the first order multi-disciplinary effects of a TVC enabled commercial transportation aircraft.

#### 3.3.1.1 AVDS Mission Inputs

Before addressing the mission selection, one must identify what parameters of the MR make up the constant mission profile used within the AVDS code. The parameters used by the AVDS code to frame the MR are tabulated in Table 3.8. Of the parameters listed, the traditional mission definition parameters of range (D\_RANGE), velocity (D\_MACH), payload (WCARGO), and passengers (APAXD) are highlighted as they are instrumental in defining the appropriate mission of a commercial transportation aircraft.

Table 3.8 AVDS Mission Requirements

Variable	Description
APAXD	Number of passengers for the design mission
APAXMAX	Maximum number of passengers
CREW	Number of crew
WPAX	Weight of passengers
WCREW	Weight of crew
WCARGO	Weight of cargo
NCRUISE	Number of design cruise speeds/ranges [MAX 5]
D_RANGE	Design mission(s) range(s)
D_MACH	Mach number for design mission(s)
D_WR	Design weight ratio at cruise [NCRUISE] = 1 for typical fuel requirement calculation < 1 for specifying weight ratio for design mission
TOFL	Take-off field length
SLAND	Landing field length
ALT_SCEILING	Service Ceiling
NTTC	Time to climb constraint =0 yes, <i>DEFAULT</i> =1 No, max L/D and T/W available used for climb performance
TTC	Time to climb
RC_CEILING	Rate of climb at ceiling

The identification of the appropriate mission is approached in two parts. This first topic addressed is to identify the characteristics of the TVC plus reduced empennage method that would be best highlighted and influenced by the parameters of the MR. The second topic of mission identification is determining what AVDS parameter is best suited to capture the beneficial effects the TVC plus reduced empennage method to CD performance sizing.

### 3.3.1.2 Mission Identification Logic

One major responsibility of the empennage is to produce lift to provide moments to balance and control the aircraft. With respect to aerodynamics, "... *lift is very good, moment is useful, and drag is horrid. ...*" [11] The act of 'trimming' an aircraft, balancing the aircraft moments, produces a significant amount of drag-due-to-lift on the horizontal tail. [11] By

reducing the empennage, drag is reduced via reduced surface area. With less structure, weight is reduced. Additional drag savings can be gained by off-loading trim requirements (normally produced by aerodynamic control surfaces) to the TVC enabled propulsion systems; although this performance benefit is not explored by this research. The longer range the mission is the greater percentage of the flight profile is spent at cruise. Utilizing TVC for trim during the cruise segment can reduce the drag due to trim and the higher the PAX the greater the profit for each constant mission. Within the parametric sizing environment, these aspects snowball into an overall converged solution of lesser weight than the empennage savings alone. These beneficial aspects of a reduced empennage translate to reduced TOGW, OEW, and fuel burn.

When conceptually sizing aircraft in AVDS, the designer uses the objective function to obtain the best vehicle for a constant mission. The objective function is simply the function the designer wishes to maximize or minimize to filter the solution space to identify the desired vehicle. For commercial aircraft, there are many classical objective functions: TOGW, fuel burn, total DOC, etc. Of the mentioned objective functions, the total DOC function offers wide-ranging metrics that best embody the performance aspects of the total aircraft, e.g. fuel burn, TOGW, OEW, etc. The total DOC (Equations 3.36 - 3.40) provides the designer the capability to “... *control the weighting of fuel burn, systems complexity and acquisition cost through economic parameters (fuel cost, development cost, maintenance cost and depreciation). ...*” [15]

Total DOC	$DOC = DOC_{fly} + DOC_{maintenance} + DOC_{depreciation} + DOC_{LNTF}$	3.36
Flying DOC	$DOC_{fly} = f(\text{Fuel Burn, Fuel Cost, Crew Cost})$	3.37
Maintenance DOC	$DOC_{maintenance} = f(\text{TOGW, OEW, Thrust})$	3.38
Depreciation DOC	$DOC_{depreciation} = f(\text{Unit Cost})$	3.39
Landing, Navigation, Taxes and Fees DOC	$DOC_{LNTF} = f(\text{Empirical Fraction of DOC})$	3.40

As the cost to operate the aircraft is directly a function of weight, and the TVC plus reduced empennage method directly affects the weight of the converged aircraft, the total DOC metric is

a strong metric to measure the cost impact of TVC plus reduced empennage method. By normalizing total DOC versus the mission variables PAX and range, the objective function becomes relevant to mission specifics. The goal of the individual sizing study is to obtain a solution that minimizes the objective function, normalized total DOC (Equation 3.41).

$$\text{Normalized Total DOC} = \frac{DOC}{\text{Range} * PAX} \quad 3.41$$

The desired mission characteristics of long range and high PAX, identifies the mission profile of the Boeing 777-300ER as an appropriate candidate to model the MR around. The mission profile for the B777-300ER is available in Table 3.9.

Table 3.9 B777-300ER Mission Profile

Mission requirements	Data
<b>Crew weight</b>	
Crew (175 lbs crew + 27 lbs carry-on cargo) (1-Captin, 1-1st officer, 14 cabin attendants)	1474 kg (3,250 lbs)
<b>Payload weight</b>	
Passengers (175 lbs passenger + 40 lbs carry-on cargo)	
Maximum Passengers (370 PAX, 33,770 kg cargo)	69853 kg (154,000 lbs)
Design Passengers (325 PAX, 6,474 kg cargo)	38170 kg (84,146 lbs)
<b>Range</b>	
Design	14075 km (7,600 nm)
<b>Velocity</b>	
Design Cruise Speed	0.84 M
<b>Altitude</b>	
Max operating	12,200 m (40,000 ft)
Take-off field length (TOGW)	< 3,048 m (10,000 ft)
Landing field length (max landing weight)	< 1,767 m (5,797 ft)
Fuel reserves	926 km (500 nm)

Refer to the input file available in the appendix for more information regarding the exact values of constants used this MR and in the total DOC function.

### 3.3.2 Case Study Tasks

The following chapter sections address the tasks involved in evaluating the hypothesis. The evaluation process addresses the significance and feasibility of TVC technology by modeling and assessing the first order multi-disciplinary effects using the AVDS tool and the

TVC-TAC aircraft S&C tool. The performance sizing study results in the identification of the solution space that consists of converged vehicles that are capable of performing the MR. The S&C assessment evaluates the solution space to identify if the converged vehicles have adequately sized aerodynamic control effectors. The systematic process of the solution concept methodology shown in Figure 3.2, is applied to a case study that is segmented into three sequential steps: 1) Reverse Engineered Baseline Model, 2) TVC Receptive Baseline Model, and 3) TVC Plus Reduced Empennage Model. Figure 3.10 represents an overview of the case study. The images in Figure 3.10 are generated by the software Tecplot 10, using data generated by AVDS. The images shown are for illustrative and educational purposes only, representing the design point's relative size, shape, and position of hardware.

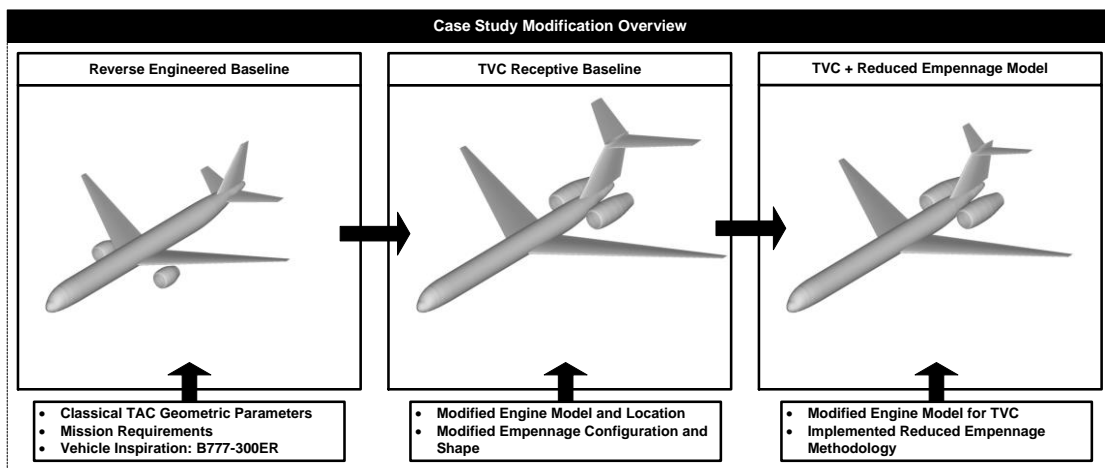


Figure 3.10 Case Study Modification Overview

### 3.3.2.1 Reverse Engineering Study

Before one can apply the new methodologies to evaluate TVC technology on a commercial airframe, it is first necessary to insure proper implementation of and competence in the AVDS code. This is illustrated by using the AVDS code to reverse engineer the B777-300ER, which compares the parametric model (selected methods, convergence, sizing logic, etc.) against public domain data on an existing airframe. Additionally this step establishes the

baseline model to utilize as a starting point and reference point for modifications and comparative purposes respectively.

In the B777-300ER reverse engineering baseline activity, the total configuration arrangement (geometric shaping parameters, hardware location, empennage configuration, etc.) is fixed. The design solution space is generated by iterating the dependent design variable ( $S_{pln}$ ) until convergence of the weight and volume budgets is achieved. The model is then iterated against a range of  $\tau$ . This iteration variable ( $\tau$ ) as discussed in Chapter 3.2.1, captures the classical W/S and T/W trades, reducing what was once a collection of constraints, into a single curve. [15] Additional iterations are performed using the independent design variable; **wing Aspect Ratio (ARw)**. The ARw trades generate separate solution space curves, representing the primary trade study utilized to determine the design point of the performance sizing study. The results of the AVDS tool output into a database file. For the purposes of rapid data visualization, this research activity utilizes the programming script language of MATLAB to acquire the data and perform the requisite data reduction analysis. Figure 3.11 below represents the meaningful results of this activity performed by the AVDS code using the assembled input file available in the appendix. The figure in the top left of Figure 3.11 represents the primary AVDS sizing figure. All three figures in Figure 3.11 work together to pinpoint the design point of the sizing study.

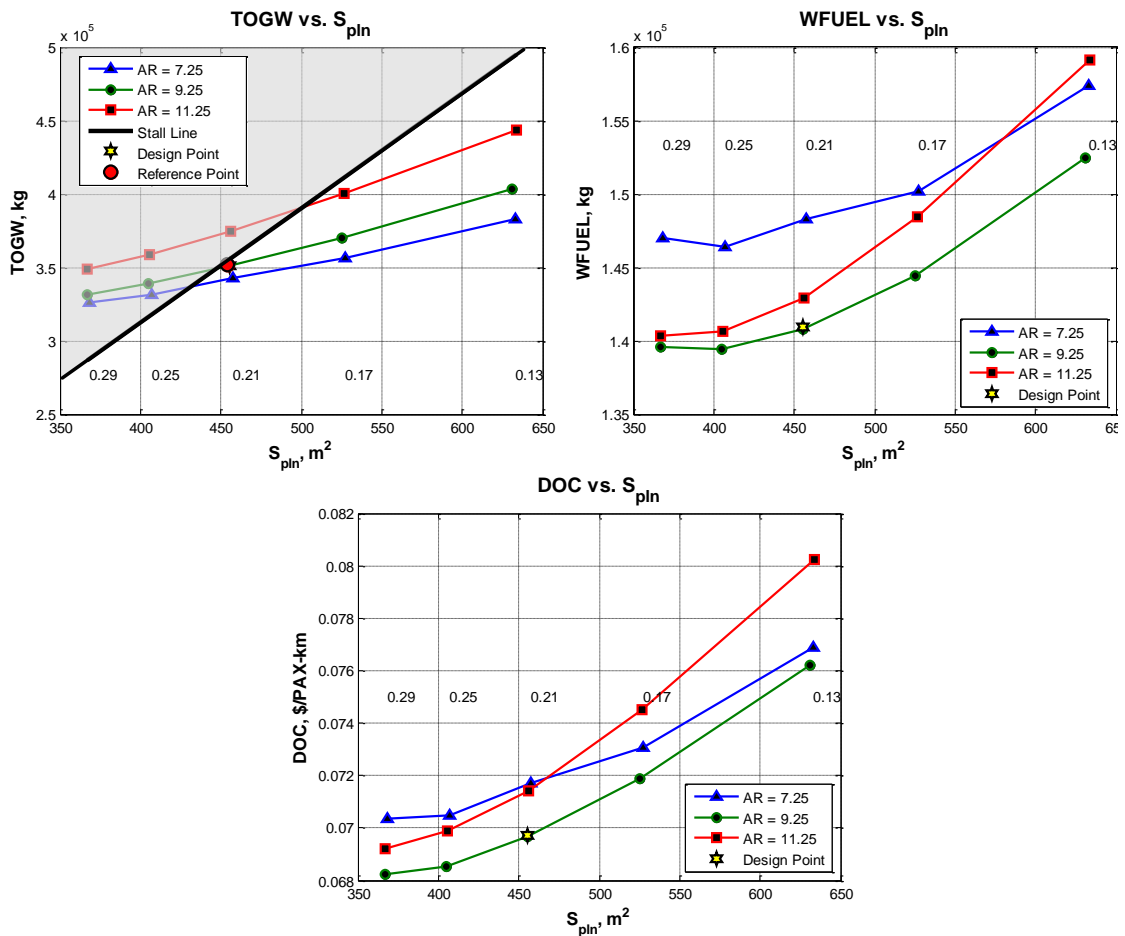


Figure 3.11 Solution Space Visualization of TOGW vs.  $S_{pln}$  (Top Left), Fuel Weight vs.  $S_{pln}$  (Top Right), Total DOC vs.  $S_{pln}$  (Bottom Center)

As shown in Figure 3.11, TOGW vs.  $S_{pln}$ , the W/S constraint (gray area) represents an area of infeasible converged vehicles. These points are not omitted by AVDS convergence logic (thus plotted) because the performance requirement of landing/stall is not explicitly a function of the T/W constraint. As seen in Figure 3.11, TOGW vs.  $S_{pln}$ , the trade of ARw from 7.25 to 11.25 is performed over a range of  $\tau$  from 0.13 to 0.29. This leads to three curves representing possible solutions to the reverse engineering study.

The goal of the ARw trade study is to identify the balance between the aerodynamic and structural weight benefits. Higher AR wings tend to have higher aerodynamic efficiency, thus

lower fuel burn, but are also associated with higher wing structural weight. For example, looking at Figure 3.11, Total DOC vs.  $S_{pln}$ , as  $\tau$  increases, one can see that the 7.25 ARw curve's slope begins to increase at a higher rate than the other two ARw trades. The ARw 7.25 wing represents a lower TOGW design but the increase in fuel burn, shown in Figure 3.11 Fuel Weight vs.  $S_{pln}$ , drives the total DOC up. This trade study (ARw versus  $\tau$ ), for the TAC commercial aircraft using the B777-300ER MR, demonstrates that the balance between aerodynamic efficiency and structural weight is around an ARw of 9.25.

As stated by Coleman, "... *the focus of early design studies is not on accuracy but correctness. ...*" [15] As such, the intention of selecting and minimizing the objective function (Normalized total DOC: Equation 3.41) is an attempt to filter the solution space for the cost optimal vehicle (correct), not to predict the final cost (accuracy). This approach identifies a design point, which represents the vehicle of the solution space that best satisfies the objective of the cost optimal vehicle. As seen in Figure 3.11, TOGW vs.  $S_{pln}$ , the design point occurs at the intersection of the AR 9.25 curve with the region of infeasible solutions. Table 3.10 represents the comparison of the reverse engineered baseline against the reference aircraft (Public domain data of the B777-300ER).

Table 3.10 Comparison of B777-300ER Reference vs. Reverse Engineered Baseline

<b>Geometry</b>	<b>Reference</b>	<b>Baseline</b>	<b>% Error</b>
<b>Input</b>			
$\tau$		0.21	
AR	9.25	9.25	
<b>Calculated</b>			
$S_{pln}$ (m <sup>2</sup> )	454.00	455.58	0.35%
b (m <sup>2</sup> )	64.8	64.92	0.18%
$l_{fus}$ (m)	73.08	74.46	1.89%
$D_{fus}$ (m)	6.20	6.2	0.00%
<b>Weight</b>			
TOGW (kg)	351535	351388	-0.04%
$W_{fuel}$ (kg)	145538	140982	-3.13%
MLW (kg)	251290	251172	-0.05%
$(W_{PAV})_{design}$ (kg)	38168	38168	0.00%
OEW (kg)	167829	172238	2.63%
<b>Aero-Propulsion</b>			
Fuel Fraction	0.414	0.401	-3.09%
Thrust (kN/engine)	514	500.9	-2.55%
SFC <sub>cruise</sub> (/hour)	0.56	0.56	-0.38%
<b>Cost</b>			
Total DOC (\$/PAX-km)		0.070	
Unit price (\$ Million)	202	201.1	-0.44%

As seen in Table 3.10, the reverse engineered aircraft is in good agreement with publically available reference data for the B777-300ER MR. This approach to parametric sizing provides insight into the minds of the original designers, revealing the first order multi-disciplinary effects that drove the design of this reference aircraft to meet the mission. The selected design point, represents the baseline model utilized by the next step of the case study.

The reverse engineering activity demonstrates proper implementation of and competence in the AVDS tool. Additionally, this activity demonstrates the overall validity of the parametric model (reversed engineered baseline) with public domain data, and explains the logic behind the design point identification. The next step is to modify the parametric model to be receptive of TVC technology. This step is required so that the benefits of the TVC plus reduced empennage method can be measured appropriately. This step isolates the benefits to the methodology alone, as if the specific configuration were to be redesigned with TVC from the outset. As such, this activity produces a 'baseline' for TVC modification and comparison, which serves to reveal if TVC plus reduced empennage method can synergistically evolve the classical TAC commercial aircraft.

### 3.3.2.2 Modify Case Study Model into TVC Receptive Configuration

This chapter section discusses the activity of modifying the reverse engineered baseline (B777-300ER parametric model) into a TVC technology receptive configuration. The modifications include changing specific geometric, propulsive, and weight parameters. This chapter section presents a modification summary of the AVDS input file used for the TVC receptive baseline. The modifications do not alter or exceed the validity of any disciplinary method used to model the reverse engineered B777-300ER baseline, nor are any disciplinary methods changed or added. The TVC receptive configuration is used as a comparative baseline for the TVC plus reduced empennage model.

As mentioned in the Chapter 2.2.3, aft-fuselage mounted engines are necessary to provide the greatest directional and longitudinal moment arm for the TVC system. Additionally, the aft-fuselage engine position significantly diminishes the adverse destabilizing yawing moment created in the OEI scenario. Also stated in Chapter 2.2.3, is the need for mixed flow turbofan jet engines to maximize the usefulness of the TVC technology. With aft-fuselage mounted engines, it is essential to select an empennage arrangement that places the horizontal tail plane out of the hot exhaust of the engines. The T-tail empennage configuration satisfies this condition.

The designer should note that additional attention must be paid to the new constraints that accompany the selected empennage configuration. For example, not normally associated with fuselage mounted HTP's is the deep stall phenomenon. This phenomenon describes the failure scenario typically experienced by aircraft of T-tail empennage configurations. As the aircraft increases angle of attack ( $\alpha$ ), highly turbulent air immediately behind the fuselage and main wing will eventually engulf the HTP. This causes the HTP to stall which proceeds to increase aircraft  $\alpha$  even more. This typically causes an undesirable uncontrollable spin with "...a very fast descent at low forward speed... and recovery from it is very doubtful. ..." [10] Many techniques can be utilized to prevent deep stall. Examples range from digital methods (flight

control systems) that limit  $\alpha$  to mechanical devices (stall doors) which deploy on the leading edge to create a pitch down moment at angles of attack approaching conditions for stall. There are many aerodynamic advantages and structural disadvantages to T-tails. For example, an advantage to T-tails are that they see clean air at low  $\alpha$  due to its geometric position. As stated by Torenbeek, *“placing one tail surface at the tip of another leads to an increase of about 50% in the aerodynamic aspect ratio... increasing the lift curve slope of the fin by roughly 15%. ...”* [10] Additionally, this empennage configuration allows the engines to be mounted on the rear fuselage, allowing for smaller landing gear (reduced weight). One significant disadvantage to T-tail empennage configurations is that designers must pay additional attention to preventing tail plane flutter. This leads to increased structural stiffness of the empennage that can lead to additional structural complexity and often time’s increased structural weight of the empennage. A more in-depth discussion of the advantages and disadvantages of the empennage configuration selection is discussed in many classical aircraft design texts, most notably, Nicolai [11], Torenbeek [10], and Roskam [12].

Table 3.11 contains an overview of the effected disciplines and modifications applied to alter the reverse engineered B777-300ER baseline input file into the TVC receptive baseline input file.

Table 3.11 TVC Receptive Baseline Modification Summary

TVC Receptive Baseline Modifications	
Discipline	Modification
Propulsion	Mixed flow turbofan engine deck*
Geometry	Empennage configuration receptive to aft-fuselage mounted engines
Weights	Fuselage weight increase for aft-fuselage mounted engines
	Wing inertial relief reduced with no Wing Mounted Engines
	Empennage Weight Increase due to T-tail
	Engine T/W correction ( -11% : Mixed Flow Turbofan )

\* Engine Deck provided by Coleman [15]

Now that the modification summary has been identified, the next step is to follow the procedure outlined in the reverse engineering of the B777-300ER model. This procedure preforms the same (but not numerically identical) AR versus  $\tau$  trade study logic to identify the design point. The determined design point of this study is used as a reference point for comparative analysis with the TVC plus reduced empennage model. The last step in this case study setup addresses the modification of the TVC receptive configuration to be representative of an airframe utilizing TVC technology.

### 3.3.2.3 Modify TVC Receptive Baseline into TVC Enabled Model

The TVC model input file is modified to be representative of TVC technology integrated into the propulsion system. This chapter section presents a modification summary of the AVDS input file. This modification does not alter or exceed the validity of any disciplinary method used to model the TVC receptive baseline, nor are any disciplinary methods changed or added. The

TVC enabled model is thus compared to the TVC receptive baseline. Table 3.12 represents an overview of the modification summary of the TVC enabled model.

Table 3.12 TVC Enabled Aircraft Modification Summary

<b>TVC + Reduced Empennage Model Modifications</b>	
<b>Discipline</b>	<b>Modification</b>
Propulsion	Thrust at sea level correction factor ( -8% : Additional thrust for control ) ( -4% : TVC Nozzle )
Weights	Engine T/W correction ( -4% : TVC Nozzle )
Cost	RDT&E + Flyaway Cost ( +100% )
	Materials ( +20% )
	Time Between Engine Overhauls ( -25% )

Now that the modification summary has been identified, the next step is to conduct the trade study similarly outlined in the reverse engineering of the B777-300ER model. This procedure performs the same (but not numerically identical) AR versus  $\tau$  trade study logic to identify the design point. This trade study is performed over a range of ERFs, starting with 1.0 down to 0.2 at an iteration interval of 0.1. The next chapter will present and discuss the results of the case study.

## Chapter 4

### RESULTS AND DISCUSSION

This chapter presents and discusses the results of the TVC plus reduced empennage case study and serves to evaluate the research hypothesis. The format of this chapter follows the roadmap outlined in Figure 3.2. Thus, the analysis begins with the AVDS analysis method of Figure 3.2 and is applied as outlined in Chapter 3.3.2. The AVDS analysis method is used to evaluate if the TVC plus reduced empennage method has the ability to improve performance and cost through reduced weight and drag, and therefore reduced aircraft fuel consumption.

After the satisfactory performance and cost is established, the next step of the methodology is to perform a S&C assessment to insure that the designs are capable of performing across the most demanding, design constraining flight conditions (DCFCs). This S&C analysis evaluates the critical corners related to the classical TAC aircraft and TVC critical corners not typically associated with purely aerodynamically controlled aircraft. Figure 3.6 visualizes the critical corners and DCFCs evaluated by this research. The conclusion of this S&C analysis yields an assessment of the control power available, sizing the LoCE (elevator) and DiCE (rudder) of the empennage. The completion of the solution concept methodology serves to evaluate the research hypothesis, determining the feasibility of TVC technology applied to traditional TAC commercial transports to show improved performance and cost whilst remaining controllable across the critical corners of the flight envelope.

For the remainder of this chapter, within the body of the text, the AVDS analysis to the first decision block of the Methodology is identified as step 1, and the S&C analysis to the last decision block as step 2.

#### 4.1 Results of Solution Concept Methodology

The method of step 1's design point selection used to identify the reverse engineered B777-300ER design point, outlined in Chapter 3.3.2, is similarly applied to perform the TVC plus

reduced empennage design study. The results of step 1 are collected and organized into figures of the format expressed in Table 4.1.

Table 4.1 Data Presentation Format

Left Vertical Axis	Right Vertical Axis	Horizontal Axis
Dependent Variable Data*	Percent Change Comparison	Empennage-Reduction Factor

\* Dependent Variable Data Types: Fuel Weight, Normalized Total DOC, Thrust, and Unit Cost

#### 4.1.1 Performance and Cost Study Results

The performance data presented are the results of the AR versus  $\tau$  trade studies, yielding converged solutions under the application of the objective function, minimum total DOC. Step 1 is repeated for range of empennage reduction factors ( 0.7 to 0.2 ). All step 1 figures of the dependent variable data type follow the same format visualized in Figure 4.1 below.

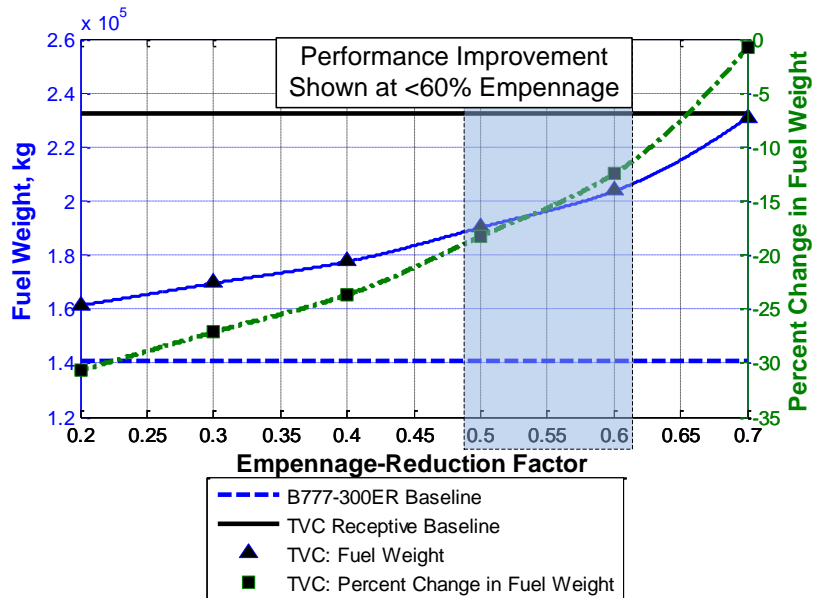


Figure 4.1 Fuel Weight vs. Empennage-Reduction Factor

As discussed in chapter 3.2.2.1, the ERF value is simply the percentage reduction dictated within the AVDS software. As seen in Figure 4.1, data regarding ERF above 0.7 and below 0.2

are not visualized. This is because all converged solutions above 0.7 and below 0.2 are within the infeasible design solution space (thus not plotted). Above 0.7, the converged aircraft are still capable of performing all the requirements of the MR—established in Table 3.9—but are unable to satisfy the FAR wing loading requirements for landing field length and stall. Below 0.2, the converged aircraft are unable to satisfy the static margin balancing criterion within AVDS.

As seen in Figure 4.1, the results are presented across two vertical axes: fuel weight and Percent Change in fuel weight. The right vertical axis of Figure 4.1 is the percent change in fuel weight of the reduced empennage TVC study against the TVC Receptive Baseline. This gives a measurement of the change in magnitude of fuel weight from the TVC receptive baseline. The relation of dependent variables—Normalized Total DOC, Thrust, and Unit Cost—versus ERF, are plotted in the same format described above and presented below in sequential order in Figure 4.2, Figure 4.3, and Figure 4.4 respectively.

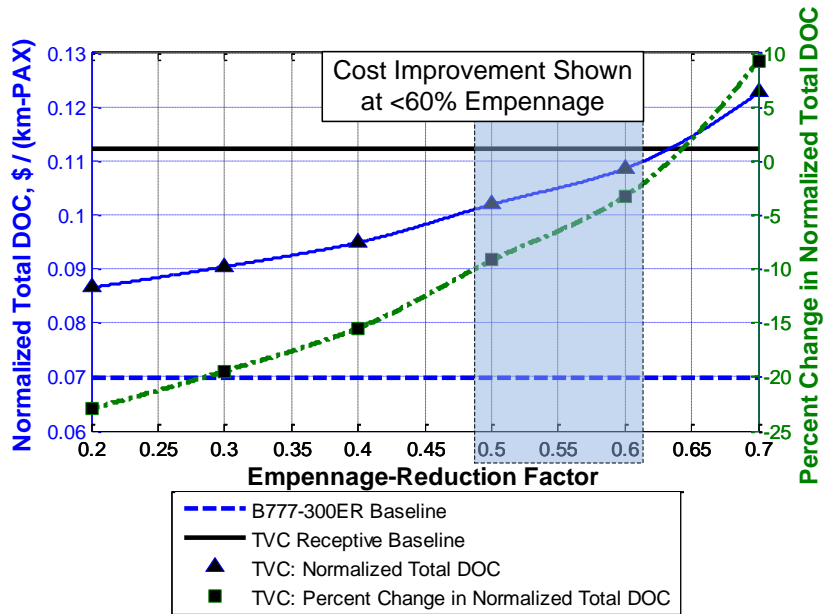


Figure 4.2 Normalized Total DOC vs. Empennage-Reduction Factor

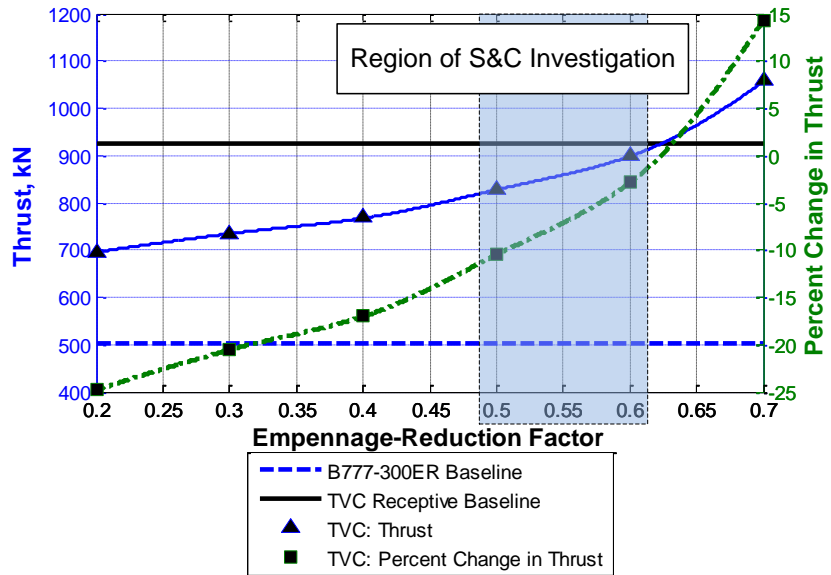


Figure 4.3 Thrust vs. Empennage-Reduction Factor

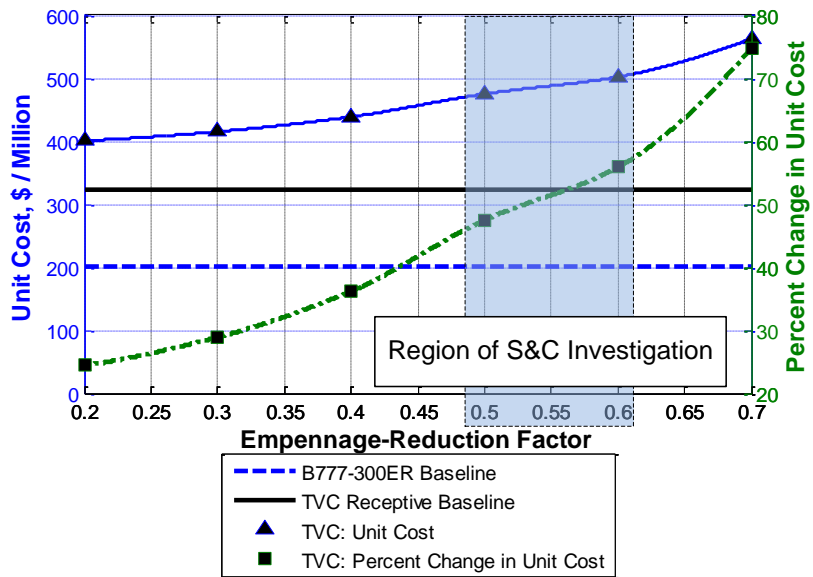


Figure 4.4 Unit Cost vs. Empennage-Reduction Factor

Due to the ERF being entrenched deep within the convergence logic of the AVDS code, a one to one reduction is not always the result. As the **Horizontal Tail Plane (HTP)**  $S_{pln}$  is reduced by the ERF, the **Vertical Tail Plane (VTP)**  $S_{pln}$  is resized according to the new aircraft parameters by the tail volume quotient method. This resizing takes place at the core of the AVDS tool as shown in Figure 3.5. Figure 4.5 represents the percent change in HTP  $S_{pln}$  and VTP  $S_{pln}$  as the ERF is traded. The percent change in HTP  $S_{pln}$  and VTP  $S_{pln}$  is measured against the TVC receptive baseline.

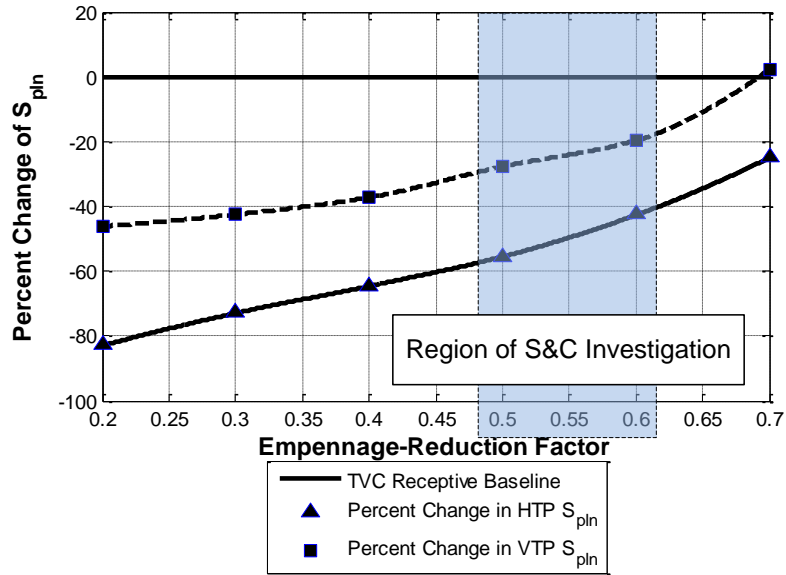


Figure 4.5 Percent Change of Empennage  $S_{pln}$

#### 4.1.1.1 Discussion of AVDS Analysis Results

This section discusses the results, assessing the first order multi-disciplinary effects the TVC plus reduced empennage method has related to the total system. In particular, this section discusses at what point the TVC technology can enable the TAC aircraft to synergistically

evolve, showing marked improvements in performance (reduced fuel consumption) and cost (reduced normalized total DOC).

The case study shows that the TVC plus reduced empennage method applied to the TAC aircraft does not synergistically evolve to show marked improvements in cost (reduced normalized total DOC) at ERF values above 0.6. This is shown in Figure 4.2. As shown in Figure 4.5, the maximum ERF value for marked cost improvements, translates to a minimum percent change of the HTP  $S_{pln}$  and the VTP  $S_{pln}$  of approximately 42% and 20% respectively. The reason for the higher normalized total DOC at an ERF above 0.7 can be deduced by reviewing, in conjunction, the results presented in Figure 4.1 and Figure 4.3. In Figure 4.1, at the ERF of 0.7, the reduced empennage design's fuel weight estimation shows minimal improvement from the TVC receptive baseline. Additionally, in Figure 4.3 the required thrust is around 14% above the TVC receptive baseline at the same ERF. At this ERF, the beneficial effects of reducing the empennage size have not balanced the negative effects the TVC technology has on the total system. This demonstrates that the snowball effect culminating in reduced aircraft fuel consumption—reduced surface area translating to reduced weight, reduced drag, and thus reduced aircraft fuel consumption—begins to balance out the performance maladies of the TVC enhanced propulsion system at and below a 0.6 ERF. Also related to fuel consumption is the unit cost, shown in Figure 4.4. At 0.2 ERF, the unit cost of each aircraft is around 24% more expensive than the TVC receptive baseline model, while the normalized total DOC, shown in Figure 4.1, shows a 23% improvement. As discussed in Chapter 3.3.1.2, the reason for these estimated savings is tied to the influence the fuel weight, thrust, and TOGW parameters have on the Total DOC function.

Lastly, a synergistic evolution of TAC aircraft by TVC technology is characterized by marked improvement in fuel consumption. Figure 1.1 classifies an evolution of TAC aircraft as the demonstration of marked reduced fuel consumption of 33% within 10 years. The TVC plus reduced empennage method demonstrates a marked improvement in fuel consumption of 33%

is nearly achievable with an ERF of 0.2, as shown in Figure 4.1. The value of 60% improvement in fuel consumption within 30 years, is not possible with the current methodology. It should be noted that, excluding reduced empennage, no TVC derived performance improvement options (Table 2.6) are implemented in the execution of the sizing study. As such, this study demonstrates the minimal-maximal improvement TVC technology can have applied to the TAC aircraft.

The region highlighted, dash-line, and labeled in Figure 4.1 through Figure 4.5 meet the minimum performance and cost requirements of the research objective. This region is from 0.6 ERF to 0.5 ERF. As such, the AVDS outputs this collected disciplinary data (Geometry, Aerodynamics, Propulsion, Performance, and Weight & Balance) to step 2 of the methodology.

#### *4.1.2 Controllability Assessment Results*

This section presents the controllability assessment of ERF trade-study design points identified in chapter 4.1.1.1. This controllability assessment determines if design points satisfy the DCFCs with regards to the LoCEs and DiCEs. As visualized in Figure 3.6, the viability of the each design point is analyzed at the mission critical corners of the flight envelope. The exact scenarios investigated are described in the test matrix of Table 3.6. For each design point of the ERF trade study, the output data from step 1, the AVDS analysis, is taken into step 2, the S&C analysis.

The output data of the S&C tool is segmented into two controllability assessment figures types. One figure type presents the results pertaining to the LoCE (elevator), and the other to the DiCE (rudder). The independent data is the percentage of CE surface area,  $S_{CE}$ , by the respective tail-plane surface area,  $S_{TP}$ . The dependent data is the required degree deflection of the CE at each respective CE surface area percentage. Knowing that CE deflection is simply a change to the airfoil section camber, excessive camber will lead to localized stall. As indicated by references [31], [11], and [32], the designer must remember that aerodynamic CE

deflections above 35 degrees may exhibit effector stall. This places an aerodynamic limit on the amount of CE deflection. Also indicated by references [31] and [11], CEs percentages above 45 percent are typically switched to all moving CEs. This places a limit on the independent axis. These limits are labeled as Aerodynamic CE Limit and Flap Effectiveness Limit respectively. The TVC System is limited to a maximum effective deflection of 15 degrees.

As indicated in Figure 3.2, the set CE sizing figures are created to identify the DCFC that sizes the CE. The scenarios investigated are detailed in Figure 4.6, which is an extract from Figure 3.2.

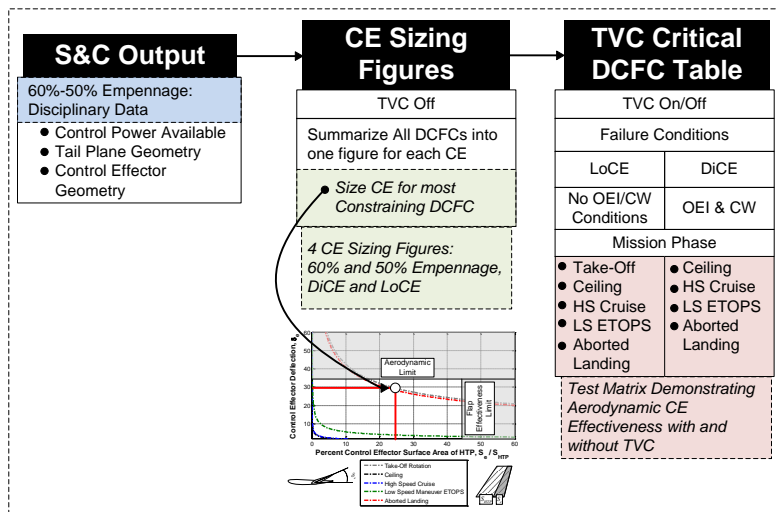


Figure 4.6 S&C Output Visualization of Solution Concept Methodology

The S&C analysis assesses the LoCE’s and DiCE’s effectiveness to trim over the four mission flight segments: 1) Ceiling, 2) High Speed (HS) Cruise, 3) Low Speed Maneuver – Extended range Twin engine Operation Performance Standards (LS-ETOPS), and 4) Aborted Landing. Additionally, the S&C analysis assesses the LoCE’s effectiveness at the take-off rotation maneuver. The S&C analysis assesses the DiCE’s effectiveness to maintain directional control during the two failure conditions: 1) asymmetric flight – Crosswind, and 2) One Engine Inoperative (OEI).

#### 4.1.2.1 Sizing the Control Effectors

To aid in determining the appropriate size of LoCE and DiCR, all DCFCs are plotted together on one figure that is unique for each trade study and CE. As indicated in Figure 4.6, four figures are produced, sizing the LoCE and DiCE for each trade study. The sizing logic is simply to select the most demanding DCFC to size the CE. This assessment determines the size of the Aerodynamic CE in the most critical portions of the flight profile. As such, the TVC system is not actuated to provide controlling moments. The following four figures (Figure 4.7, Figure 4.8, Figure 4.9, and Figure 4.10), make up the results of the controllability assessment.

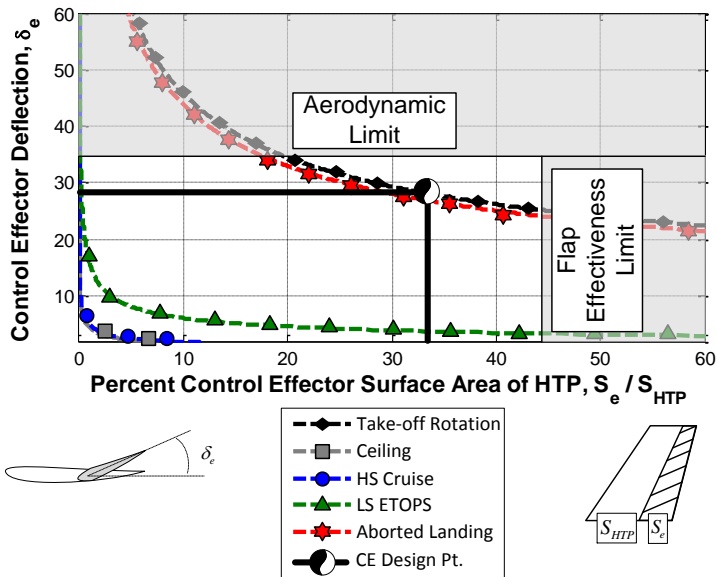


Figure 4.7 LoCE Sizing with TVC off on the 60% Reduced Empennage Trade Study

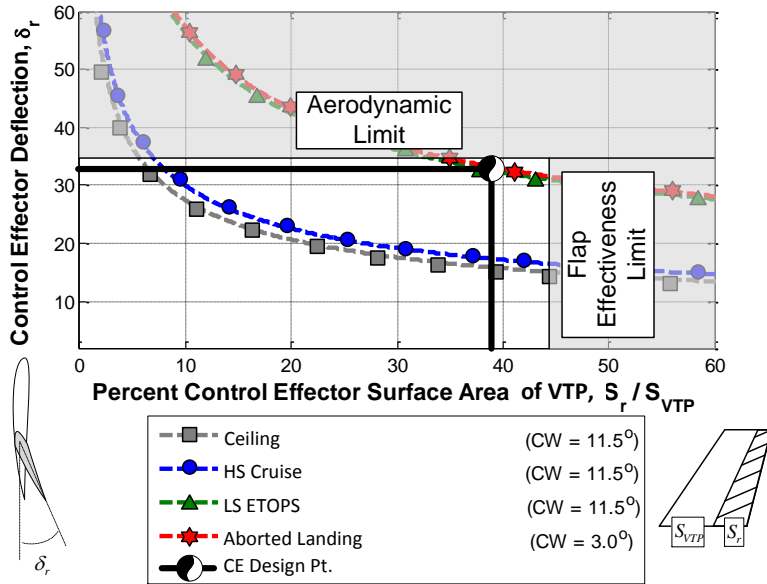


Figure 4.8 DiCE Sizing with TVC off, OEI, and indicated CW on the 60% Reduced Empennage Trade Study

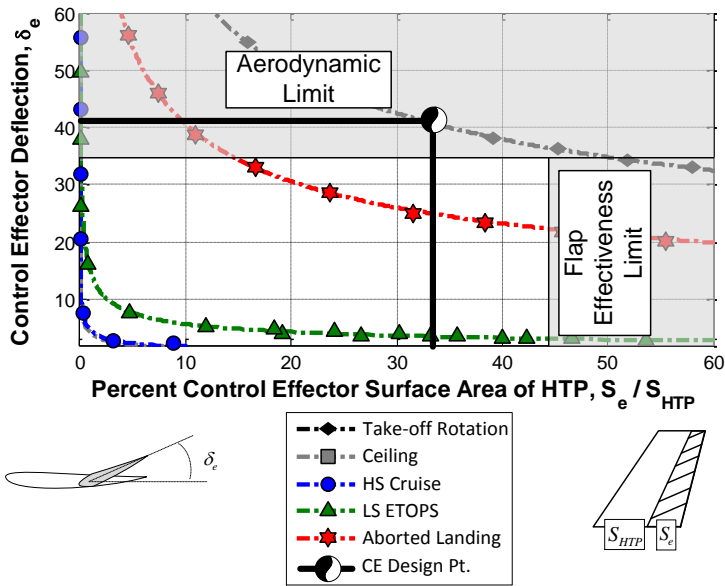


Figure 4.9 LoCE Sizing with TVC off on the 50% Reduced Empennage Trade Study

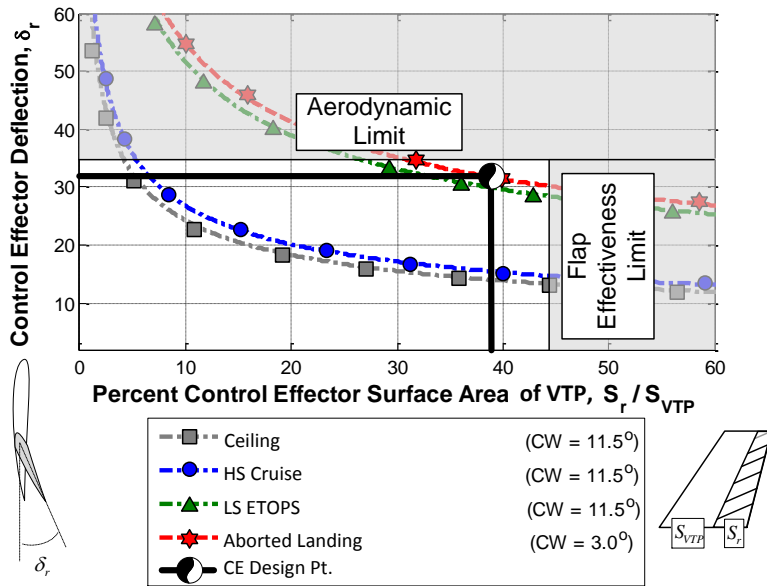


Figure 4.10 DiCE Sizing with TVC off, OEI, and indicated CW on the 50% Reduced Empennage Trade Study

From reference [32], a typical CE percentage for a B777 class aircraft is around a 33% - 40%.

The results of this study determine what amount of deflection is required to perform the most constraining DCFCs of the flight profile. Table 4.2 takes the design points of the above four figures and extracts the CE deflection and investigates the benefit to TVC actuation on the required deflection angle. This data reduction activity identifies the most critical DCFCs affected by TVC.

Table 4.2 DCFC Test Matrix of 60% and 50% Reduced Empennage

Aircraft:		Aircraft Data:																	
B777-TVC		Configuration Settings, Flight Condition Variables, Failure Condition																	
DCFC Scenario		L.G.	Air Speed	Altitude	Performance Segment	Weight	SM	TW	Engine Status	Crosswind Angle	TVC Moment	Max TVC Deflection	S <sub>CE</sub> /S	Tail Plane S <sub>pln</sub>	S <sub>CE</sub>	CE Deflection With TVC	CE Deflection Without TVC	Percent Difference in CE Deflection	
Mission Phase	Control Effector	(-)	(m/s)	(m)	(-)	(-)	(-)	(-)	(-)	(deg)	NM	(deg)	(%)	(m <sup>2</sup> )	(m <sup>2</sup> )	(deg)	(deg)	(%)	
60% Reduced Empennage	2	DICE	Up	247.9	12000.0	Ceiling	WR	0.020	0.170	OEI	11.5	44287.7	15	39.0	145.2	56.6	15.66	15.88	1%
	3	DICE	Up	255.5	8924.0	Design Cruise	WR	0.020	0.205	OEI	11.5	85966.7	15	39.0	145.2	56.6	17.11	17.33	1%
	4	DICE	Up	128.6	3000.0	ETOPS LS Cruise	WR	0.039	0.232	OEI	11.5	191610.4	15	39.0	145.2	56.6	31.31	32.60	4%
	5	DICE	Down	71.5	0.0	Aborted Landing	MLW	0.191	0.345	OEI	11.5	476263.6	15	39.0	145.2	56.6	N/A	N/A	N/A
	5	DICE	Down	71.5	0.0	Aborted Landing	MLW	0.191	0.345	OEI	3	476263.6	15	39.0	145.2	56.6	25.67	33.15	25%
	1	LoCE	Down	66.0	0.0	Take-Off	TOGW	0.191	0.241	AEO	0	290892.4	15	33.0	135.4	44.7	26.26	28.28	7%
	2	LoCE	Up	247.9	12000.0	Ceiling	WR	0.020	0.170	AEO	0	44287.7	15	33.0	135.4	44.7	1.00	1.05	5%
	3	LoCE	Up	255.5	8924.0	Design Cruise	WR	0.020	0.205	AEO	0	85966.7	15	33.0	135.4	44.7	1.10	1.15	4%
	4	LoCE	Up	128.6	3000.0	ETOPS LS Cruise	WR	0.039	0.232	AEO	0	191610.4	15	33.0	135.4	44.7	3.47	3.76	8%
	5	LoCE	Down	71.5	0.0	Aborted Landing	MLW	0.191	0.345	AEO	0	476263.6	15	33.0	135.4	44.7	25.25	27.00	7%
50% Reduced Empennage	2	DICE	Up	247.9	12000.0	Ceiling	WR	0.020	0.170	OEI	11.5	44287.7	15	39.0	131.6	51.3	13.85	14.06	2%
	3	DICE	Up	255.5	8924.0	Design Cruise	WR	0.020	0.206	OEI	11.5	85966.7	15	39.0	131.6	51.3	15.26	15.5	2%
	4	DICE	Up	128.6	3000.0	ETOPS LS Cruise	WR	0.039	0.232	OEI	11.5	191610.4	15	39.0	131.6	51.3	28.56	29.92	5%
	5	DICE	Down	71.5	0.0	Aborted Landing	MLW	0.188	0.339	OEI	11.5	476263.6	15	39.0	131.6	51.3	N/A	N/A	N/A
	5	DICE	Down	71.5	0.0	Aborted Landing	MLW	0.188	0.339	OEI	3	476263.6	15	39.0	131.6	51.3	23.99	31.68	28%
	1	LoCE	Down	66.0	0.0	Take-Off	TOGW	0.188	0.240	AEO	0	290892.4	15	33.0	106.1	35.1	38.45	40.89	6%
	2	LoCE	Up	247.9	12000.0	Ceiling	WR	0.020	0.170	AEO	0	44287.7	15	33.0	106.1	35.1	0.94	0.98	4%
	3	LoCE	Up	255.5	8924.0	Design Cruise	WR	0.020	0.206	AEO	0	85966.7	15	33.0	106.1	35.1	1.03	1.08	5%
	4	LoCE	Up	128.6	3000.0	ETOPS LS Cruise	WR	0.039	0.232	AEO	0	191610.4	15	33.0	106.1	35.1	3.22	3.52	9%
	5	LoCE	Down	71.5	0.0	Aborted Landing	MLW	0.188	0.339	AEO	0	476263.6	15	33.0	106.1	35.1	23.24	25.04	7%

Looking at the right most column in Table 4.2, the percent difference in CE deflection, it becomes clear what DCFC scenario is the most influenced by TVC actuation. For example, looking at the 60% reduced empennage trade study; the DiCE for the aborted landing performance segment under the OEI, **Crosswind (CW)** scenarios are most constrained by TVC actuation. This is due to the lesser CW angle that must be selected to allow for a controllable condition. At the regulation amount of 11.5 degrees from reference [11], the DiCE is unable to balance the moments experienced during this DCFC. The CW amount of 3 degrees must be selected to remain controllable during this DCFC. During this segment, if TVC actuation were to fail, contributing no correcting moment, the deflection must be changed from a maximum of 27 degrees to 35 degrees. That is a percent difference of 25%. During the 3 degree CW, the amount of moment generated due to the CW angle is to a greater extent, decreased, allowing the TVC system to impart a greater percentage of controlling moment. For the LoCE, take-off rotation, aborted landing, and ETOPS share the most critical DCFC for TVC.

One reason for such low moment contribution from the TVC system is due to the relative low T/W ratios associated with large commercial transportation aircraft. These systems are significantly different in comparison to classical TVC airframes, military fighter aircraft. The commercial airframes have much greater levels of inertia and much lower T/W ratios.

The low LoCE deflection required during HS cruise, ETOPS and ceiling is due to the sizing logic of the AVDS analysis tool. Embedded in its sizing routine is a convergence constraint to be longitudinally trimmed and balanced at a selected point in the flight profile. Due to the long-range nature of the mission, the HS cruise portion is selected for the trim point. Additionally, the converged aircraft are balanced to a static margin of 2% at HS cruise. This translates to low CE deflections during the aforementioned flight profile sections.

As indicated in Table 4.2 and Figure 4.9, the 50% reduced empennage case is unable to satisfy the DCFC of take-off rotation. This indicates the lower limit of empennage reduction and specifically the lower limit of reducing the tail plane of the LoCE.

With the knowledge gained from the controllability assessment, one can conclude that a minimal-maximal performance improvement (fuel weight) of approximately 16% can be seen. Also, as seen in Figure 4.2, the minimal-maximal improvement in normalized total DOC is approximately 8%. The next chapter concludes the research by addressing the research objective and providing derived recommendations related to this research for further study.

## Chapter 5

### CONCLUSIONS AND RECOMMENDATIONS

The goal of this research study was to evaluate this research's hypothesis. The hypothesis of this research is that TVC technology applied to the traditional TAC commercial transport is able to, 1) improve performance and cost by synergistically reducing the traditional empennage size, and 2) comply with current safety and certification regulation. As such, one must demonstrate the capacity to perform a feasibility assessment of an innovative technology (TVC) within commercial transportation. This feasibility assessment encompasses two primary activities, 1) a literature research activity, and 2) the development and implementation of a solution concept architecture.

The first activity requires the development of a supportive foundation based on the review of literature related to the topic. The TVC supportive foundation consist of: 1) the fundamentals (chapter section 2.2.1), 2) the historic application (chapter section 2.2.2), 3) the commercial aviation opportunities (chapter section 2.2.3), and 4) the synthesis of a commercial TVC system (chapter section 2.2.4). The supportive foundation enables the researcher to ask the correct questions and properly address the research objective.

The second activity requires one to capture (understand, model and assess) the first order multi-disciplinary effects using a multi-disciplinary parametric sizing tool, AVDS (chapter section 3.2.2), during the CD phase. Due to the lack of adequate S&C capability of AVDS tool, this necessitates the development and utilization of a unique TVC-TAC conceptual design S&C tool (chapter section 3.2.3). The developed S&C tool takes in over 220 unique inputs from the traditional aircraft disciplines to assess the controllability of the designs. These tools identify the solution space that results from a combination of data, knowledge, and parametric sizing, revealing the feasibility of the TVC enhanced TAC commercial aircraft.

The constructed methodology shown in Figure 3.2 of this research determines the minimal maximal improvement that TVC technology plus a reduced empennage can impart

when incorporated into the design at the earliest design phase. Addressing the research hypothesis, the implemented methodology indicates that the TVC plus reduced empennage method demonstrates the following:

- 1) Possible improvements in performance and cost (chapter section 4.1.1.1)
- 2) The operational advantages of this highly evolved aircraft configuration such as cabin evacuation, ground operation, safety, and certification are retained (chapter section 4.1.2.1)
- 3) Increased safety and capacity to handle adverse DCFs (chapter section 4.1.2.1)
- 4) Increased CE redundancies (chapter section 4.1.2.1)

This research studies the feasibility of applying an innovative technology to a commercial transport aircraft. As such, Table 5.1 serves as a comparative example to bring into proper perspective the approximate performance and cost benefits. Table 5.1 compares an existing innovative technology (Raked Wing Tips) and this research's innovative technology (TVC technology plus reduced empennage method).

Table 5.1 Innovative Technology Savings Comparison

	<b>Raked Wing Tips *</b>	<b>TVC plus Reduced Empennage</b>
Fuel Weight	~ 2 %	~ 13 %
Lbs/Year/Aircraft	~ 1.3 million	~ 12.3 million
Year/Aircraft	~ \$140,000	~ \$996,000

\* Constant Mission Analysis: B777-300ER [82]

In conclusion, TVC technology plus a reduced empennage, applied during the early conceptual design phase, enables the TAC commercial transport aircraft the capacity to improve performance and reduce cost while maintaining and improving the controllability of the design.

## Recommendations for Future Work

The following section contains derived recommendations related to this research for further study. The recommendations are:

- 1) The way the AVDS code is setup, a singular sizing study is limited to one independent design variable trade study at a time. The solution space is thus restricted by the independent design variable chosen for the trade study. This has the capacity to present an incomplete view of the possible solution space to the designer. For example, this study was limited to ARw trades; an additional propulsion system trade study may yield a different converged aircraft solution space. This leads to the development and implementation of an multi-point optimization routine. As a reminder, the goal of early conceptual design is not accuracy but correctness.
- 2) Develop a control allocation methodology to integrate the TVC systems with the aerodynamic control systems. This analysis would allow for accurate measurements of control authority available from a TVC system throughout the flight profile. Applying this methodology would allow for the exploration of additional potential performance benefits of the TVC system. For example, off-loading trim requirements (normally produced by aerodynamic control effectors) to the TVC enabled propulsion systems. This methodology would in turn likely see snowballing savings even greater than the results of the TVC plus reduced empennage research alone.
- 3) Additional improvements to performance might come from incorporating a method of accounting for the increased mass flow rate due to the entrainment of flow by the TVC system augmenting the exhaust angle. This would require the investigation of conceptual design methods that can estimate the interaction

between ambient flow and vectored exhaust. Depending on configuration, this interaction could augment the lift significantly.

APPENDIX A

AVDS INPUT FILE: B777-300ER BASELINE MODEL



!\*\*\*\*\*

<- APAXD  
325.0  
<- APAXMAX  
370.0  
<- CREW  
16.0  
<- WPAX [KG]  
97.52  
<- WCREW [KG]  
92.0  
<- WCARGO [KG]  
6474.0  
<- WCARGO\_MAX [KG]  
69853.0  
<- NCRUISE  
1.0  
<- D\_RANGE (KM)  
14075.2 5000.0  
<- D\_MACH  
0.84 0.84  
<- D\_WR  
1.0 0.5  
<- TOFL [m]  
3048.0  
<- ALT\_TO  
0.0  
<- ALT\_LAND  
0.0  
<- SLAND [m]  
1767.84  
<- ALT\_ICLIMB [m]1  
3048.0  
<- ALT\_SCEILING [m]  
12000.0  
<- NTTC  
0  
<- TTC [hr]  
1.2  
<- RC\_CEILING [m/s]  
0.5

\*\*\*\*\*

Fuel Selection input

\*\*\*\*\*

!Variable description\*\*\*\*\*

!FUEL\_DEN Fuel density (kg/m^3)

!\*\*\*\*\*

<- FUEL\_DEN (kg/m^3)

780.0

\*\*\*\*\*  
Regulation input  
\*\*\*\*\*

!Variable description\*\*\*\*\*  
!TO\_CGR           Take-off climb gradient  
!TO\_OEI           Take-off with OEI (1=yes, 2=no) NOT IN USE  
!ALAND\_CGR        Landing climb gradient  
!ALAND\_OEI        Landing with OEI (1=yes, 2=no) NOT IN USE  
!ALAND\_WR         Maximum Landing weight ratio  
!ALTRES           Cruise altitude for reserve fuel/divert  
!R\_MACH           velocity for reserve fuel/divert  
!TIMERES          loiter time for reserve fuel/divert  
!N\_ETOPS          ETOPS switch  
!                 =0 ETOPS not required  
!                 =1 ETOPS required  
!\*\*\*\*\*

<- TO\_CGR [RAD]  
  0.024  
<- TO\_OEI [RAD]  
  1  
<- ALAND\_CGR [RAD]  
  0.021  
<- ALAND\_OEI [RAD]  
  1  
<- ALAND\_WR  
  0.714  
<- ALTRES [KM]   \*\*\*\*double check\*\*\*\*  
  3048.0  
<- TIMERES [MIN]  
  60.0  
<- N\_ETOPS  
  1

\*\*\*\*\*  
Convergece input  
\*\*\*\*\*

!Variable description\*\*\*\*\*  
!NPM              Performance matching method switch  
!                 =1 Cruise Climb (Altitude Free)  
!                 =2 Cruise Climb (Altitude Fixed)  
!\*\*\*\*\*  
<- NPM  
  1  
!LOFTIN metod \*\*\*\*\*  
!SREF            Inital wing area guess  
!ALT(5)          Initial cruise altitude guess

```

!D_MVIHN           Location on drag polar for cruise (1 = L/D max)[NCRUISE]
!CLCRUISE         Inital cruise lift coefficient guess (for trim solution)
!TAU              Kuchemann's tau slenderness parameter
!*****

```

```

<- SREF(m^2)
500.0
<- ALTC (m)
8229.6 8229.6
<- D_MVIHN
1.0 0.2
<- CLCRUISE
0.52
<- TAU
0.21
<- AISTR
32.7

```

```

*****
Sizing input
*****

```

```

!Variable description*****
!WSINITIAL       Inital wing loading
!WSFINAL         Final wing loading
!WSSTEP          Wing loading step
!*****

```

```

<- WSINITIAL
450
<- WSFINAL
700
<- WSSTEP
25

```

```

*****
Configuration input
*****

```

```

!Variable description*****
!NFUSE           Number of fuselages or external bodies
!FUSAPEX         Fuselage Nose location (1-X, 2-Y, 3-Z)
!FUUSE_FILE      Fuselage file name (NFUSE)
!NFP            Number of fuselage polar coordinates
!AFTC_DF        Ratio of tail length to max fuselage diameter
!AFNC_DF        Ratio of nose length to max fuselage diameter
!ENGINES        Number of propulsion systems
!NPROPELLER     Number of Propellers (total)
!NNAC           Number of Nacelles
!NAC_REF        Refernce location indicator
!              =1 Fuselage Noise
!              =2 Wing apex

```

```

!ANAPEX          Nacelle apex location repeat (NNAC times) (1-X, 2-Y-, 3-Z)
!
!               IF NAC_REF =1 THEN
!                   X - percent fuselage length(positive aft)
!                   Y - percent fuselage width (positive righth from top view)
!                   Z - Percent fuselage height (positive up)
!               IF NAC_REF =2 THEN
!                   X - percent local chord location (positive aft)
!                   Y - percent span (positive out the right wing)
!                   Z - Percent nacelle height (positive down, zero corresponds to
center of nacelle at wing LE)
! NAC_FILE       Nacelle file
! NWING         Number of wings
! NAFW         Airfoil file index
!               1-39 AIRFOILS FROM FILES (NOT RECOMMEND FOR BWB
visualization)
!               40 - NACA 4 digit
!               41 - NACA 4 Digit modified
!               63 - NACA 63 SERIES (Thickness and camber from sizing results)
!               64 - NACA 64 SERIES          "
!               65 - NACA 65 SERIES          "
!               :
!               67 - NACA 67 SERIES          "
! WINGAPEX      Wing apex(1-X, 2-Y, 3-Z) (1-X/ALFUS, 2-Y/DMAX, 3-Z/DMAX)
! NHT          Number of Horizontal tails (canard, H-T, etc.)
! NAFH         Airfoil file index
!               1-39 AIRFOILS FROM FILES (NOT RECOMMEND FOR BWB
visualization)
!               40 - NACA 4 digit
!               41 - NACA 4 Digit modified
!               63 - NACA 63 SERIES (Thickness and camber from sizing results)
!               64 - NACA 64 SERIES          "
!               65 - NACA 65 SERIES          "
!               :
!               67 - NACA 67 SERIES          "
! HTAPEX       Horizontal tail apex (1-X/ALFUS, 2-Y/DMAX, 3-Z/DMAX) (reference to
fuselage nose)
! NVT          Number of vertical tails
! NAFV         Airfoil file index
!               1-39 AIRFOILS FROM FILES (NOT RECOMMEND FOR BWB
visualization)
!               40 - NACA 4 digit
!               41 - NACA 4 Digit modified
!               63 - NACA 63 SERIES (Thickness and camber from sizing results)
!               64 - NACA 64 SERIES          "
!               65 - NACA 65 SERIES          "
!               :
!               67 - NACA 67 SERIES          "
! VTAPEX       Vertical tail apex(1-X/ALFUS, 2-Y/DMAX, 3-Z/DMAX)
! NAFDD        Number of airfoils in database (MAX 10)
! AIRFOIL_FILE Airfoil ordinates file names
! MLG_REF      main landing gear reference location
!               =1 Wing mounted

```

```

!                                     =2 Fuselage mounted
!*****

!*****
!** FUSELAGE
!*****
<- NFUSE
  1
<- FUSAPEX
  0.000 0.000 0.000
<- FUSE_FILE
  RF-A320A.DAT
<- NFP
  48
<- AFTC_DF
  3.46
<- AFNC_DF
  1.6

!*****
!** PROLUSION
!*****
<- NENGINES
  2
<- NPROPELLER
  0
<- NNAC
  2
<- NAC_REF
  2
<- ANAPEX
  -0.5 0.3 0.55
  -0.5 -0.3 0.55
<- NAC_FILE
  GONDEL1.DAT
<- NNP
  48
!*****
!** WING SECTIONS
!*****
<- NWING
  1
<- NAFW
  63
<- WINGAPEX
  0.335 0.0 -0.35
<- NHT
  1
<- NAFH
  2
<- HTAPEX
  0.85 0.0 0.15

```

```

<- NVT
  1
<- NAFV
  1
<- VTAPEX
  0.85 0.0 0.40
!*****
!** AIRFOIL DATABASE
!*****
<- NAFDD
  2
<- AIRFOIL_FILE
  N64012.DAT
  N64008A.DAT

!*****
!** LANDING GEAR
!*****
<- MLG_REF
  1
<- ANG
  0.08 0.0 -0.5
<- AMG
  0.85 0.10 0.0

*****
Geometry input
*****

!METHOD SELECTION *****
!MGE0      Geometric sizing method
!          = 1 manual input of required geometry
!          = 2 wing thickness computed from cruise lift coefficient
!          Mach number and sweep angle to yield a wing critical
!          Mach number of 0.04 above the cruise Mach Number (Howe). The
!          emenage sweep is computed as inputted increment above the
!          wing sweep (Shaufele) and the emenage thickness is compute to
yield
!          a critical mach number 0.05 above the wing critical mach
!          number (Roskam)
!          = 3 vehicle sized with tau, using constant fuselage l/d and wing AR
!          = 4 vehicle sized with tau, using constant fuselage l/d and wing s/l
!*****

<- MGE0
  3

!WING *****
!wing span and AR, specify one and leave the other as 0.0
! ARW(5)      Wing Aspect ratio [max 5]
! BW(5)      Wing Span [max 5]
!S_LWING     ratio of wing semi-span to fuselage length

```

```

!TRW(5)          Wing Taper ratio [max 5]
!ALW(5)          Wing sweep
!AXCW(5)         chord location of wing sweep (x/c)
!***TCW(5)       Wing airfoil thickness (/c) [max 5]      (NOT REQUIRED FOR
MGEO=2)
!TWISTW(5)       Wing twist (deg) [max 5]
!DIHEDW          Wing dihedral
!*****

```

```

<- ARW
  9.25
<- BW [M] (NO LONGER IN USE Initial guess)
  0.0
<- S_LWING
  0.50
<- TRW
  0.15
<- ALW
  35.0
<- AXCW
  0.0
<- TCW
  0.11
<- TWISTW (deg)
  -3.0
<- TCT_MAX
  0.05
<- DIHEDW
  6.0

```

```

!Horizontal tail*****
!HT span and AR, specify one and leave the other as 0.0
!ARH(5)          HT Aspect ratio
!TRH(5)_TRW      HT Tapper ratio per wing TRW
!DALH           increment of H-T sweep from wing sweep
!Volume quotient, specify two and leave one blank
! VH(5)          HT volume quotient
! SHSREF(5)      HT area ratio(Sh/Sref)
! ALCH(5)        Lever arm from HT ac to Wing ac (l/c)
!VTTYPE         configuration correction factor
!               =1.0000, fuselage mounted tail
!               =0.8440, T-tail low wing
!               =1.3500, T-tail high wing
!DIHEDH         HT dihedral
!*****

```

```

<- ARH
  4.5
<- TRH_TRW
  2.33
<- DALH
  0.0

```

```

<- VH
0.93581
<- VTTYPE
1.000
<- SHSREF
0.2256
<- ALCH
0.0
<- DIHEDH
1.0

```

!Vertical tail\*\*\*\*\*

```

!VT span and AR, specify one and leave the other as 0.0
! ARV(5)          VT Aspect ratio
! BV(5)          VT Span
!TRV(5)_TRW      VT Tapper ratio per wing TR
!DALV           increment of V-T sweep from wing sweep
!Volume quotient, specify two and leave one blank
! VV(5)          VT volume quotient
! SVSref(5)      VT area ratio(Sh/Sref)
! ALCV(5)        Lever arm from VT ac to Wing ac (l/c)
!**SWETV(5)      VT wetted area
!**SEXPV(5)      VT exposed area
!**SFV(5)        VT frontal area
!*****

```

```

<- ARV
1.75
<- TRV_TRW
2.0
<- DALV
0.0
<- VV
0.067478
<- SVSREF
0.1220
<- ALCV
0.0
<- DIHEDV
90.0

```

!FUSELAGE\*\*\*\*\*

```

!NFUSE_FINE      Fuselage finess ratio used
                  = 0 constant Finess ratio
                  = 1 Constant cabin cross-section
!ALFUS_DFUS(5)   Fuselage length to max diameter
!HFUS_WFUS(5)    Fuselage hight to width
!CHFUS           Fuselage cross-sectional hight (required if ALFUS_DFUS=0)
!CWFUS           Fuselage cross-sectional width (required if ALFUS_DFUS=0.0)
!B2L(5)          Ratio of wing half span to fuselage length (Kuchemann's s/L)
!**DMAX(5)       Fuselage maximum diameter
!**FRFUS(5)      Fuselage finess ratio

```

```

!ALCAB(5)          Length of cabin
!WCAB(5)           Width of cabin
!HCAB(5)           Hight of cabin
!**VCAB(5)         Volume of cabin
!**SWETfuse(5)    Fuselage wetted area
!**SFfuse(5)      Fuselage frontal area
!*****

```

```

<- NFUSE_FINE
1
<- ALFUS_DFUS [-]
11.787
<- HFUS_WFUS [-]
1.0
<- CHFUS
6.20
<- CWFUS
6.20
<- B2L
0.0
<- ALCAB [m]
10.94
<- HCAB [m]
2.0
<- WCAB [m]
5.47

```

```

!Nacelles (INTIAL GUESS IF MSPROP = 1) *****
!ALNAC(10)         Nacelle length
!HNAC(10)         Nacelle hight
!WNAC(10)         Nacelle width
!DLNAC(10)        Inner Nacelle diamter
!ALNAC_CORR       Nacelle length correction factor
!                 =1.0 for non-mixed turbofan
!                 =1.8 for mixed flow turbofan (AE 3007)
!*****

```

```

<- ALNAC (m)
7.212 7.212
<- HNAC (m)
3.960 3.960
<- WNAC (m)
3.960 3.960
<- DLNAC(m)
3.960 3.960
<- ALNAC_CORR
1.0

```

```

*****
AERODYNAMICS input
*****

```

```

!Method Selection *****
!MCDFRIC      Skin friction method
!              =1 General Dynamics method (additional input required)
!              =2 General Dynamics method (additional input required)
!MCDI         Induced drag method
!              =1 VAC/DATCOM symetric drag polar method
!MCDTWAVE     Transonic Wave drag method
!              =1 McDonald Douglas method (MD, additional input required)
!              =2 Grassmeyer method via Mason Configuration Aerodynamcis
!MCDTRIM      Trim drag method
!              =1 Torenbeek/Coleman (additional input required)
!MCD_LG       Landing gear drag method
!              =1 Roskam (additional input required)
!MCD_Flaps    Flaps drag Method
!              =1 Roskam (additional input required)
!MCL_MAX      Maximum lift coefficient
!              =1 Roskam (additional input required)
!MCLA         Lift curive slope method
!              =1 DATCOM (additional input required)
!*****

```

```

<- MCDFRIC
2
<- MCDI
1
<- MCDTWAVE
2
<- MCDTRIM
1
<- MCD_LG
1
<- MCD_FLAP
1
<- MCL_MAX
1
<- MCLA
1

```

```

!CDfric GD Method *****
!ALGD         airfoil thickness location paramter
!              =1.2 x >= 0.30c
!              =2.0 x < 0.30c
!RFUS         Fuselage Correction factor, Fig III B.2-2a GD handbook
!QNAC         Nacelle interference factor
!*****

```

```

<- ALGD
1.2
<- APDF
100.0
<- RFUS
1.1

```

```

<- QNAC
  1.0
<- NF14
  0
<- RXTW
  2.65E6
<- RXTF
  0.25E6
<- AMAX_LFC
  0.60
<- TURB_LAM_LS
  1.0
<- TURB_LAM_FUS
  1.0
<- WIF
  1.0

```

```

!CLA DATCOM Method *****
!CLAFW(5)           Wing Airfoil lift curve slope
!CLAFH(5)           HT Airfoil lift curve slope
!*****

```

```

<- CLAFW
  6.30
<- CLAFH
  6.13

```

```

!CDI VAC/DATCOM Method *****
!ALERW(5)           Wing Airfoil leading edge radius over chord length, rle/c
!ALERH(5)           Wing Airfoil leading edge radius over chord length, rle/c
!IROUNW(5)          Wing airfoil leading edge shape
!                   =1 round
!                   =0 sharp
!IROUNH(5)          Wing airfoil leading edge shape
!                   =1 round
!                   =0 sharp
!DECORRECT          OSWALDS EFFICIENCY FACTOR CORRECTION FOR
SUPERCRITICAL WINGS
!                   LEADING EDGE CAMBER, VORTEX ATTENUATION, ETC.
!*****

```

```

<- ALERW
  0.007
<- ALERH
  0.007
<- IROUNW
  1
<- IROUNH
  1
<- DECORRECT
  1.05

```

```

!CDTWAVE MD Method *****
!MCRIT_H          Critical Mach number switch
!                = 0 manual input of critical Mach Number
!                = 1 Computation of Critical Mach number (Howe)
!AMACHCR          CRITICAL MACH NUMBER (See Corning/GD hand-book) (Not
required for MCRIT_H=1
!AK0              Approximation to the Sears-Haak Body, See methods library
!*****

```

```

<- MCRIT_H
0
<- AMACHCR
0.80
<- AK0
1.5

```

```

!CD_LG ROSKAM Method *****
!CD_LG            Drag increment due to landing gear (See Table ?? in Drag Methods)
!CD_DE            Oswald efficiency factor increment due to landing gear
!*****

```

```

<- CD_LG
0.015
<- DE_LG
0.0

```

```

!CD_flap ROSKAM Method *****
!CD_FLAP_TO      Drag increment due to Flaps in take-off position
!DE_FLAPTO       Oswald efficiency factor increment due to T-O flaps
!CD_FLAP_TO      Drag increment due to Flaps in take-off position
!DE_FLAPLAND     Oswald efficiency factor increment due to Landing flaps
!*****

```

```

<- CD_FLAP_TO
0.02
<- DE_FLAPTO
-0.010
<- CD_FLAP_LAND
0.075
<- DE_FLAPLAND
-0.015

```

```

!CL_Max ROSKAM Method *****
!CL_MAXMAXR      Maximum Lift Coefficient (See Figure 3.1 in ROSKAM)
!CL_LANDR        MAXIMUM Lift Coefficient during LANDING
!CL_MAXNCLEANR   MAXIMUM NEGATIVE Lift Coefficient (FOR VN DIAGRAM)
!*****

```

```

<- CL_MAXLANDR
2.95
<- CL_MAXCLEANR
1.5

```

<- CL\_MAXNCLEANR  
-1.0

!APPROXIMATE TRIM DRAG Coleman Method \*\*\*\*\*  
!CM0AF Approximate wing airfoil zero lift pitching moment  
!ANH Dynamic pressure ratio compared to free-stream at HT  
!AMH Hight of the HT from wing normalized to half span  
AMH=H/(B/2)  
(SEE METHODS LIBRARY FOR SUGGESTED VALUES)  
!\*\*\*\*\*

<- CM0AF  
-0.0175  
<- ANH  
0.85  
<- AMH  
0.0

\*\*\*\*\*  
PROPULSION input  
\*\*\*\*\*

!Method Selection \*\*\*\*\*  
!MTSFC Thrust specific fuel consumption  
! =1 Turbojet/Turbofan, Howe PROP\_MD1  
! =2 Turboprop, Howe Howe PROP\_MD2  
! =3 Turbojet,fan, or prop, Matthing PROP\_MD3  
! =4 GASTURB ENGINE DECK  
!MTSL\_TALT Ratio of thrust at altitude to thrust at sea-level  
! =1 Turbojet/Turbofan, Howe PROP\_MD4  
! =2 Turboprop, Howe PROP\_MD5  
! =3 Turbofan, Turbojet or turboprop Matthing PROP\_MD6  
! =4 GASTURB ENGINE DECK  
!MSPROP Method of sizing propulsion system  
! =0 Fixed  
! =1 Svoboda statistics  
!\*\*\*\*\*

<- MTSFC  
3  
<- MTSL\_TALT  
3  
<- MSPROP  
1  
<- SFCC  
1.00  
<- TTSLC  
1.00

!PROP\_MD3 MATTINGLY SFC for Turbojets, Turbofans and Turboprops\*\*\*\*\*  
!NMSOP Propulsion system option  
=1 High bypass turbofan

```

=2 Low bypass turbofan at mil power (max non-afterburning)
=3 Low bypass turbofan at max power (max afterburning)
=4 Turbojet at mil power (max non-afterburning)
=5 Turbojet at max power (max afterburning)
=6 Turboprop
=7 Manual input of statistical constants
!AK1M      1st constant (ONLY REQUIRED FOR NMSOP=7)
!AK2M      2nd constant (ONLY REQUIRED FOR NMSOP=7)
!          (AK1M+AK1M*MACH)*SQRT(THETA0)
!*****

```

```

<- NMSOP
7
<- AK1M
0.23
<- AK2M
0.48

```

```

!PROP_MD6 MATTINGLY T/Tsl for Turbojets, Turbofans and Turboprops*****
!NMTOP      Propulsion system option
=1 High bypass turbofan
=2 Low bypass turbofan at mil power (max non-afterburning)
=3 Low bypass turbofan at max power (max afterburning)
=4 Turbojet at mil power (max non-afterburning)
=5 Turbojet at max power (max afterburning)
=6 Turboprop
!TRM        Throttle ratio
!AK2M      2nd constant (ONLY REQUIRED FOR NMSOP=7)
!          (AK1M+AK1M*MACH)*SQRT(THETA0)
!*****

```

```

<- NMTOP
1
<- TRM
1.0

```

```

*****
Structural Load Estimation input
*****

```

```

!Method Selection *****
!MVN        Velocity-Load factor diagram (V-N)
!          =0 none
!          =1 FAR25 STRUCT_MD1
!NGLA       Gust load alleviation swith (using max maneuvering as limit)
!          =0 no gust load alleviation
!          =1 gust load alleviation
!*****

```

```

<- MVN
1
<- NGLA

```

0

\*\*\*\*\*  
Weigh Estimation input  
\*\*\*\*\*

!Method Selection \*\*\*\*\*  
!MFF Fuel fraction estimation (SWITCH INACTIVE, ROSKAM DEFAULT)  
! =0 VDK  
! =1 Roskam WB\_MD1 (additional input required)  
!MWING\_STRUC Wing weight method (IF MWING\_STRUC = 0 ISTR INPUT IS USED)  
! =0 VDK  
! =1 Howe WB\_MD2(additiona input required)  
! =2 Howe Physical WB\_MD7 (additiona input required)  
! =3 General Dynamics Method WB\_MD9 (additiona input required)  
!MFUSE\_STRUC Fuselage weight method  
! =0 VDK  
! =1 Howe WB\_MD 3 (additiona input required)  
! =2 Torenbeek (additiona input required)  
!MHT\_STRUC Horizontal tail/empenage weight method  
! =0 VDK  
! =1 Howe WB\_MD 8(additiona input required)  
! =2 Torenbeek (additiona input required)  
!MVT\_STRUC Vertical tail weight method  
! =0 VDK  
! =1 Howe WB\_MD 8(no additional input required, must use Howe for  
HT)  
! =2 Torenbeek (additiona input required)  
!MNAC\_STRUC Nacelle/Pylon strucutre  
! =0 VDK  
!MOPER Operational items  
! =0 VDK  
! =1 Howe WB\_MD6  
!MEQP Equipmment weight  
! =0 VDK  
! =1 Howe WB\_MD6  
!MLG\_STUC Landing Gear  
! =0 VDK  
! =1 Torenbeek (additional input required)  
!MSYS Fixed systems weight  
! =0 VDK  
! =1 Torenbeek (VDK is still active, set systems values to zero)  
!MBALANCE c.g. estimation method  
! =0 no balance computed, constant SM assumed  
! =1 Roskam (ADDITIONAL INPUT REQUIRED)  
!\*\*\*\*\*

<- MFF  
1  
<- MWING\_STRUC  
3  
<- MFUSE\_STRUC

```

1
<- MHT_STRUC
2
<- MVT_STRUC
2
<- MPROP
2
<- MOPER
0
<- MEQP
0
<- MLG_STRUC
1
<- MSYS
1
<- MBALANCE
1

```

```

!WEIGHT_MD1 ROSKAM FUEL FRACTION*****
!WR_ST          start up weight ratio
!WR_TAX         Taxi weight ratio
!WR_TO         Take-off weight ratio
!WR_DE         Descent weight ratio
!WR_L          Landing weight ratio
!climb, cruise and reserve weight ratios are computed internally
!*****

```

```

<- WR_ST
0.990
<- WR_TAX
0.995
<- WR_TO
0.995
<- WR_L
0.992

```

```

!WEIGHT_MD9 GENERAL DYNAMICS EMPRICAL WING WEIGHT *****
!REFERENCE FOR AMCORRECT IS AN ALUMINUM AIRFRAME WITH THE FOLLOWING TE
AND LE BOXS
!LE BOX        SLAT
!TE BOX        FOWLER/DOUBLE SLOTTED FLAPS
!              SPOILERS
!              AILERONS
!AMCORRECT_GD  Statistical correction to the wing weight fraction (SEE HOWE TABLE
AD4.1A)
!ENGMT         Inertial relief factor for wing mounted engines
!              =0.12 no wing-mounted engines
!              =0.2 2 wing-mounted engines
!              =0.22 4 wing mounted engines
!WING_MAT_GD   Material correction factor (multiplication)
!*****

```

```
<- AMCORRECT_GD
0.007
<- ENGMT_GD
0.2
<- WINGMAT_GD
1.0
```

```
!WEIGHT_MD12 TORENBEEK EMPRICAL HT WEIGHT *****
```

```
!AKHT          Statistical constant (see methods library)
!              =1.0, fixed HT
!              =1.1, variable incidence
!HTCORR        Horizontal tail correction factor
!*****
```

```
<- AKHT
1.1
<- HTCORR
1.0
```

```
!WEIGHT_MD13 TORENBEEK EMPRICAL VT WEIGHT *****
```

```
!ZH_BV         Vertial height of horizontal tail / span of vertical
!              =0.0 for fuselage mounted HT
!VTCORR        Horizontal tail correction factor
!*****
```

```
<- ZH_BV
0.0
<- VTCORR
1.0
```

```
!WEIGHT_MD3 HOWE FUSELAGE WEIGHT *****
```

```
!NPRES         PRESSURIZED FUSELAGE SWITCH
!              =0, NON PRESSURIZED FUSELAGE
!              =1, PRESSURIZED FUSELAGE
!C2            Statistical constant (see methods library)
!ALTCP         CABIN PRESSURE EQUIVLENT ALTITUDE (REQUIRED FOR NPRES=1
ONLY)
!*****
```

```
<- NPRES
1.0
<- C2
0.79
<- ALTCP (m)
3000.0
```

```
!WEIGHT_MD5 HOWE SYSTEMS, EQUIPMENT AND LG WEIGHT *****
```

```
!C4            Statistical constant (see methods library)
!*****
```

```
<- C4
0.16
```

```

!WEIGHT_MD14 Torenbeek Landing gear WEIGHT *****
!AGNG          Statistical constants for noise gear (see methods library)
!BGNG
!CGNG
!DGNG
!AKNR
!AGMG          Statistical constant for main gear(see methods library)
!BGMG
!CGMG
!DGMG
!AKMR
!*****

```

```

<- AGNG
  20.0
<- BGNG
  0.10
<- CGNG
  0.00
<- DGNG
  2.0e-6
<- AKNR
  1.0
<- AGMG
  40.0
<- BGMG
  0.16
<- CGMG
  0.019
<- DGMG
  1.5e-5
<- AKMR
  1.0

```

```

!WEIGHT_MD6 HOWE OPERATIONAL ITEMS WEIGHT *****
!NPAX_CARGO    PASSENGER OR CARGO SWITCH
!              =1 PASSENGER
!              =2 CARGO
!FOP           Statistical constant (see methods library)
!*****

```

```

<- NPAX_CARGO
  1
<- FOP
  16.0

```

```

!WEIGHT_MD15 TORENBECK FIXED SYSTEMS WEIGHT*****
!AKFCS        Statistical constant for flight control system
!AKHPS        Statistical constant for Hydraulic and pneumatic system
!AKFUR        Statistical constant for furnishings
!AOX          Statistical constant for oxygen system

```

!BOX Statistical constant for oxygen system  
!AKAPU Statistical constant for APU  
!AKBC Statistical constant for baggage handling equipment  
!AKAUX Statistical constant for auxiliary systems  
!\*\*\*\*\*

<- AKFCS  
0.44  
<- AKHPS  
0.006  
<- AKFUR  
0.211  
<- AOX  
40.0  
<- BOX  
2.4  
<- AKAPU  
0.013  
<- AKBC  
0.0  
<- AKAUX  
0.01

!WEIGHT DP2 VDK METHOD FOR COMMERCIAL TRANSPORTS\*\*\*\*\*

!FPRV passenger provisions (kg/person)  
!ETW Engine thrust to weight ratio (kg thrust/kg)  
!ETW\_SC Scramjet thrust to weight ratio (kg thrust/kg)  
!AKVE\_TJ Turbojet specific volume (m<sup>3</sup>/kg thrust)  
!AKVE\_SC Scramjet specific volume (m<sup>3</sup>/kg thrust)  
!AMU Mimimum OWE weight margine  
!FSYS variable system weight coefficient (kg/kg)  
!CUN Unmanned system weight (kg)  
!VUN Unmanned fixed system volume (m<sup>3</sup>)  
!FMND crew system specific weight (kg/person)  
!AKVV void volume coefficient (m<sup>3</sup>/m<sup>3</sup>)  
!AKVS system volume coefficient (m<sup>3</sup>/m<sup>3</sup>)  
!FCRW Fixed crew member specific volume(m<sup>3</sup>/person)  
!VPCRW crew provisions volume (m<sup>3</sup>/person)  
!AKCRW crew member volume (m<sup>3</sup>/person)  
!V\_PAX Passenger volume (m<sup>3</sup>/pax)  
!RHO\_CARGO Cargo density (kg/m<sup>3</sup>)  
!EBAND Error band around the strucutral fraction EBAND (+/- 0.049)  
!\*\*\*\*\*

<- FPRV  
16.0  
<- ETW  
5.98  
<- AKVE  
0.000  
<- AMU

```

0.00
<- FSYS
0.0
<- CUN
0.0
<- VUN (5 cu m VOID)
0.0
<- FMND
0.0
<- AKVV
0.20
<- AKVS
0.05
<- FCRW !ACCOUNTED FOR IN PAYLAOD AND CREW VOLUME
1.0
<- VPCRW
1.5
<- AKCRW
2.0
<- V_PAX
2.0
<- RHO_CARGO
326.72
<- EBAND
-0.049

```

```

*****
c.g estimation input
*****

```

```

!Roskam method *****
!!SM Target Static margin
!XCG_TOGW_D Initial TOGW c.g. location (% MAC)
!XCG_MLW Initial MLW c.g. location (% MAC)
!CRW_CG Crew c.g. (x, y, z)
! X - FRACTION OF NOISE
! Y - FRACTION OF WIDTH (FROM CENTERLINE)
! Z - FRACTION OF HEIGHT (FROM CENTERLINE)
!OP_CG Operating items c.g. (x, y, z)
! X - FRACTION OF FUSELAGE LENGTH
! Y - FRACTION OF FUSELAGE HEIGHT (FROM
CENTERLINE)
! Z - FRACTION OF FUSELAGE WIDTH (FROM CENTERLINE)
!APAY_D_CG Design Payload c.g. (x, y, z)
! X - FRACTION OF CABIN LENGTH
! Y - FRACTION OF WIDTH
! Z - FRACTION OF HEIGHT (FROM CENTERLINE)
!APAY_MAX_CG Max Payload c.g. (x, y, z)
! X - FRACTION OF CABIN LENGTH
! Y - FRACTION OF WIDTH (FROM CENTERLINE)
! Z - FRACTION OF HEIGHT (FROM CENTERLINE)

```

!FUEL.CG.W	Wing Fuel c.g. (x, y, z)
!	X - FRACTION OF CHORD LEGHTH
!	Y - FRACTION OF SPAN/2
!	Z - FRACTION OF THICNESS
!FUEL.CG.F	Fuselage fuel c.g. (x, y, z)
!	X - FRACTION OF FUSELAGE LENGTH
!	Y - FRACTION OF FUSELAGE HIGHT (FROM CENTERLINE)
!	Z - FRACTION OF FUSELAGE WIDTH (FROM CENTERLINE)
!WING.CG	Wing structure c.g. (x, y, z)
!	X - FRACTION OF CHORD LEGHTH
!	Y - FRACTION OF SPAN/2
!	Z - FRACTION OF THICKNESS
!HT.CG	Horizontal tail structure c.g. (x, y, z)
!	X - FRACTION OF CHORD LEGHTH
!	Y - FRACTION OF SPAN/2
!	Z - FRACTION OF THICKNESS
!VT.CG	Vertical tail structure c.g. (x, y, z)
!	X - FRACTION OF CHORD LEGHTH
!	Y - FRACTION OF THICKNESS
!	Z - FRACTION OF SPAN/2
!FUSE.CG	Fuselage structure c.g. (x, y, z)
!	X - FRACTION OF FUSELAGE LENGTH
!	Y - FRACTION OF FUSELAGE HEIGHT (FROM
CENTERLINE)	
!	Z - FRACTION OF FUSELAGE WIDTH (FROM CENTERLINE)
!NACC.CG	Nacelle strucutre c.g. (x, y, z)
!	X - FRACTION OF NAC LENGTH
!	Y - FRACTION OF NAC WIDTH (FROM CENTERLINE)
!	Z - FRACTION OF NAC HEIGHT (FROM CENTERLINE)
!ENG.CG	Engine c.g. (x, y, z)
!	X - FRACTION OF NAC LENGTH
!	Y - FRACTION OF NAC WIDTH (FROM CENTERLINE)
!	Z - FRACTION OF NAC HEIGHT (FROM CENTERLINE)
!ANG.CG	Noise gear c.g. (x, y, z)
!	X - FRACTION OF STRUT LENGTH
!	Y - FRACTION OF STRUT HEIGHT (FROM CENTERLINE)
!	Z - FRACTION OF STRUT WIDTH (FROM CENTERLINE)
!AMG.CG	Main gear c.g.(x, y, z)
!	X - FRACTION OF STRUT LENGTH
!	Y - FRACTION OF STRUT HEIGHT (FROM CENTERLINE)
!	Z - FRACTION OF STRUT WIDTH (FROM CENTERLINE)
!FC.CG	Flight control system c.g.(x, y, z)
!	X - FRACTION OF FUSELAGE LENGTH
!	Y - FRACTION OF FUSELAGE WIDTH (FROM CENTERLINE)
!	Z - FRACTION OF FUSELAGE HEIGHT (FROM
CENTERLINE)	
!HPS.CG	Hydraulic and pneumatic system c.g.(x, y, z)
!	X - FRACTION OF FUSELAGE LENGTH
!	Y - FRACTION OF FUSELAGE WIDTH (FROM CENTERLINE)
!	Z - FRACTION OF FUSELAGE HEIGHT(FROM
CENTERLINE)	
!ELS.CG	Electical system c.g.(x, y, z)

```

!
! X - FRACTION OF FUSELAGE LENGTH
! Y - FRACTION OF FUSELAGE WIDTH (FROM CENTERLINE)
! Z - FRACTION OF FUSELAGE HEIGHT (FROM
CENTERLINE)
!AIAE.CG Instrimentaion, Avionics and electronics system c.g.(x, y, z)
! X - FRACTION OF FUSELAGE LENGTH
! Y - FRACTION OF FUSELAGE WIDTH (FROM CENTERLINE)
! Z - FRACTION OF FUSELAGE HEIGHT (FROM
CENTERLINE)
!API.CG Air-conditioning, pressureization and anti/de-icing systemc c.g.(x, y, z)
!
! X - FRACTION OF FUSELAGE LENGTH
! Y - FRACTION OF FUSELAGE WIDTH (FROM CENTERLINE)
! Z - FRACTION OF FUSELAGE HEIGHT(FROM
CENTERLINE)
!APU.CG Aux power unit c.g.(x, y, z)
! X - FRACTION OF FUSELAGE LENGTH
! Y - FRACTION OF FUSELAGE WIDTH (FROM CENTERLINE)
! Z - FRACTION OF FUSELAGE HEIGHT (FROM
CENTERLINE)
!OX.CG Oxygen system c.g.(x, y, z)
! X - FRACTION OF FUSELAGE LENGTH
! Y - FRACTION OF FUSELAGE WIDTH (FROM CENTERLINE)
! Z - FRACTION OF FUSELAGE HEIGHT (FROM
CENTERLINE)
!FUR.CG Furnishings c.g.(x, y, z)
! X - FRACTION OF CABIN LENGTH
! Y - FRACTION OF FUSELAGE WIDTH (FROM CENTERLINE)
! Z - FRACTION OF FUSELAGE HEIGHT (FROM
CENTERLINE)
!BC.CG Baggage handling equipment c.g.(x, y, z)
! X - FRACTION OF FUSELAGE LENGTH
! Y - FRACTION OF FUSELAGE WIDTH (FROM CENTERLINE)
! Z - FRACTION OF FUSELAGE HEIGHT (FROM
CENTERLINE)
!AU.CG Auxiliary equipment c.g.(x, y, z)
! X - FRACTION OF FUSELAGE LENGTH
! Y - FRACTION OF FUSELAGE WIDTH (FROM CENTERLINE)
! Z - FRACTION OF FUSELAGE HEIGHT (FROM
CENTERLINE)
!PT.CG Paint c.g.(x, y, z)
! X - FRACTION OF FUSELAGE LENGTH
! Y - FRACTION OF FUSELAGE WIDTH (FROM CENTERLINE)
! Z - FRACTION OF FUSELAGE HEIGHT (FROM
CENTERLINE)
!*****
!General description*****
!*****

```

<- SM  
0.02

```
<- XCG_C_TOGW_D
0.285
<- XCG_C_MLW
0.15
<- CRW_CG
0.95 0.00 0.00
<- OP_CG
0.45 0.00 0.00
<- APAY_D_CG
0.65 0.00 0.00
<- APAY_MAX_CG
0.65 0.00 0.00
<- FUEL_CG_W
0.45 0.50 0.00
<- FUEL_CG_F
0.55 0.00 0.00
<- WING_CG
0.45 0.40 0.00
<- HT_CG
0.42 0.38 0.00
<- VT_CG
0.42 0.00 0.40
<- FUSE_CG
0.45 0.00 0.00
<- ANACC_CG
0.40 0.00 0.00
<- ENG_CG
0.50 0.00 0.00
<- ANG_CG
0.50 0.00 0.00
<- AMG_CG
0.50 0.00 0.00
<- FC_CG
0.61 0.00 0.00
<- HPS_CG
0.60 0.00 0.00
<- ELS_CG
0.60 0.00 0.00
<- AIAE_CG
0.60 0.00 0.00
<- API_CG
0.10 0.00 0.00
<- APU_CG
0.91 0.00 0.00
<- OX_CG
0.50 0.00 0.00
<- FUR_CG
0.65 0.00 0.00
<- BC_CG
0.65 0.00 0.00
<- AU_CG
0.41 0.00 0.00
```

<- PT\_CG  
0.50 0.00 0.00

\*\*\*\*\*

COST input

\*\*\*\*\*

!Method Selection \*\*\*\*\*

!MRDTE\_FA RDT&E and Fly away Costs  
! =1 Hess/Raymer (additional input required)  
! =2 levenson/Roskam (additional input required)  
! =3 Roskam (ballpark method, additional input required)  
!MBLOCK Block mission method  
! =1 Roskam (additional input required)  
!MFLYDOC Flying Direct operating cost  
! =1 Roskam (additional input required)  
!MMDOC MAINTAINENCE Direct operating cost  
! =1 Roskam (additional input required)  
!MDEPDOC Depreciation operating cost  
! =1 Roskam (additional input required)  
!MLNTFDOC LANDING, NAVIATION, TAXES AND FINANCING operating cost  
! =1 Roskam (additional input required)  
!\*\*\*\*\*

<- MRDTE\_FA  
1  
<- MBLOCK  
1  
<- MFLYDOC  
1  
<- MMDOC  
1  
<- MDEPDOC  
1  
<- MLNTFDOC  
1

!COST\_MD1\_DAPCA RDT&E+FLYAWAY COST \*\*\*\*\*

!QUANT Quantify of aircraf produced  
!FTA Number of flight test aircraft  
!TT4 Total temperature at turbine inlet (for engine cost)  
!RE Engineering costs per man hour (1999 dollars)  
!RT tooling costs per man hour (1999 dollars)  
!RM Manufacturing costs per man hour (1999 dollars)  
!CPAX Interior cost per passenger  
!IAVIONICS Aviations cost switch  
! =1 per OWE  
! =0 per RDT&E+Flyaway cost  
!CAVOWE Cost per OWE (required if IAVIONICS = 1)  
!CAVRD Cost per RDT&E+flyaway cost (required if IAVIONICS = 0)  
!AINFLAT Adjustment from 1999 dollars to then dollars  
!PRFMARG Required profit margin for the manufacturer

```

!ICARO      Cargo aircraft switch
!           = 0 no
!           = 1 yes
!CORMAT     Correction factor for materials (See Method Library)
!*****

```

```

<- QUANT
350.0
<- FTA
2
<- TT4
2500.0
<- RE
86.0
<- RT
88.0
<- RM
81.0
<- CPAX
2500.0
<- IAVIONICS
0
<- CAVOWE (NOT IN USE)
3000.0
<- CAVRD
0.25
<- AINFLAT
1.279
<- PRFMARG
0.20
<- ICARGO
0
<- CORMAT
1.0

```

```

!COST_MD10_RACUNIT A/C UNIT COST BALLPARK METHOD(ROSKAM) *****
!AUNITQ           CORRELATION COEFFICIENT
!BUNITQ           CORRELATION COEFFICIENT
! ACUNIT(1989)=10^(AUNITQ+BUNITQ*LOG(TOGW))
!AINFLATQ        INFLATION CORRECTION FROM 1989 TO THEN DOLLARS
!*****

```

```

<- AUNITQ
3.3191
<- BUNITQ
0.8043
<- AINFLATQ
1.7575

```

```

!COST_MD2_RBLOCK BLOCK MISSION (ROSKAM) *****
!R_BLOCK          block range

```

```

!IFLIGHT          Domestic or internation flight
!IAUTIL           Specification of Annual utilization
!                = 1 for commercial transport (based on block time)
!                = 0 manual input of annual flight hours
!UANNFLT          Annual flight hours (required if IAUTIL = 0)
!*****

<- R_BLOCK [KM]
  14075.2
<- IFLIGHT
  2
<- IAUTIL
  1
**<- UANNFLT [HRS/year]
  400.0

!COST_MD3_RFD0C Flying DOC (ROSKAM) *****
!ANCREW(4)        number of crew
!                ANCREW(1) = number of cabins
!                ANCREW(2) = number of copilots
!                ANCREW(3) = number of flight engineers
!                ANCREW(4) = number of flight attendents
!AVTIT(4)         Correction factor for vacation, training, insurance and taxes
!                AVTIT(1) = number of cabins
!                AVTIT(2) = number of copilots
!                AVTIT(3) = number of flight engineers
!                AVTIT(4) = number of flight attendents
!SAL(4)           Salery
!                SAL(1) = number of cabins
!                SAL(2) = number of copilots
!                SAL(3) = number of flight engineers
!                SAL(4) = number of flight attendents
!AH(4)            Number of flight hours per year
!                AH(1) = number of cabins
!                AH(2) = number of copilots
!                AH(3) = number of flight engineers
!                AH(4) = number of flight attendents
!TEF(4)           Travel expense for each flight crew member
!                TEF(1) = number of cabins
!                TEF(2) = number of copilots
!                TEF(3) = number of flight engineers
!                TEF(4) = number of flight attendents
!FUEL_P           Fuel price (per gallon)
!FUEL_D           Fuel density
!OLP              Oil price (per gallon)
!OD               Oil density
!FINSHULL         Annual hull insurance rate
!AINFDOC          Correct for flying DOC to then dollars
!*****

```

```

<- ANCREW (4)
  1.0 1.0 0.0 14.0

```

```

<- AVTIT (4)
  0.26 0.26 0.0 0.0
<- SAL (4) [$/year]
  85000.0 50000.0 0.0 32000.0
<- AH [HRS/year]
  750.0 750.0 0.0 750.0
<- TEF
  11.0 11.0 0.0 11.0
<- FUEL_P ($/liter) (approx $5.00/gallon, 1 U.S. $/ US gallon = 0.264172052 U.S. $/ liter)
  1.32086
<- FUEL_D_KGLIT (kg/liter)
  0.80763
<- OLP ($/liter)
  0.0
<- OD
  0.87063
<- FINSHULL
  0.05
<- AINFDOC
  1.0

```

```

!COST_MD4_RMDOC Maintenance DOC (ROSKAM) *****
!RAFM          Airframe maintence labor rate per man hour
!ICAFL         aiframe man hours switch
!              = 0 Compute from OWE
!              = 1 Compute from airframe maintenance man hrs / flt hr
!AMHRAF_FLT    Number of airframe and systems man hours per flight hour
!AMHRAF_BL     Number of airframe and systems man hours per block hour
!RENM          Engine maintence labor rate per man hour
!ICENG         Engine man hours switch
!              = 0 Manual input of engine maintenance man hrs / block hr
!              = 1 Compute from engine maintenance engine weight and TBO
!AMHREN_FLT    Number of engine maintenance man hours per flight hour
!TBO           Time between engine overhauls
!AINMDOC       Inflation rate between 1989 and then dollars
!ESPPF         Engine spare parts factor
!FAMLB         Overhead distribution factor for labor, building, etc.
!FAMMAT        Overhead distribution factor for labor, building, etc.
!*****

```

```

<- RAFM [$/hr]
  16.0
<- ICAFL
  0
<- AMHRAF_FLT (NOT USED)
  6.0
<- RENM [$/hr]
  16.0
<- ICENG
  1
<- AMHREN_FLT (NOT USED)
  0.45

```

```

<- TBO [HRS] (assumed!!!!)
16000.0
<- AINMDOC [THEN YEARS/1989]
1.27
<- ESPPF
1.5
<- FAMLB
1.10
<- FAMMAT
0.60

```

```

!COST_MD5_RDEPDOC Depreciation DOC (ROSKAM) *****
!FDAF           Airframe depreciation factor
!DPAF           Airframe depreciation period
!FDENG          Engine depreciation factor
!DPEN           Engine depreciation period
!FDPROP         Propeller depreciation factor
!DPPROP         Propeller depreciation period
!FDAV           Avionics depreciation factor
!DPAV           Avionics depreciation period
!FDAFSP         Airframe spare parts depreciation factor
!FAPSFAF        Airframe spare parts factor
!DPAFSP         Airframe spare parts depreciation period
!FDENSP         Engine spare parts depreciation factor
!FENSPAF        Engine spare parts factor
!ESPPF          Engine spare parts price factor
!DPENSP         Engine spare parts depreciation period
!*****

```

```

<- FDAF
0.85
<- DPAF [YRS]
20.0
<- FDEN
0.85
<- DPEN [YRS]
15.
<- FDPROP
0.85
<- DPPROP [YRS]
7.
<- FDAV
1.00
<- DPAV [YRS]
5.
<- FDAFSP
0.5
<- FAFSPAF
0.10
<- DPAFSP [YRS]
20.
<- FDENSP

```

```

0.85
<- FENSPAF
0.25
<- ESPPFD (part included in engine price, otherwise 1.5)
1.0
<- DPENSP [YRS]
7.

!COST_MD6_RLNTF LANDING,NAV,TAXES,FIN DOC (ROSKAM)
*****

!ICACLF          Landing fees switch
!                =0 manual input
!                =1 based on TOGW
!CACLF          airport landing fee per landing
!CACNF          aircraft landing fee per flight
!IFRT           tax rate switch
!              = 0 manual input
!              = 1 based on TOGW
!FRT            tax rate/DOC
!CFIN_DOC       fraction of finance fees per DOC
!*****

<- ICACLF
1
<- CACLF (NOT USED)
1.0
<- CACNF
10.0
<- IFRT
1
<- FRT (NOT USED)
1.0
<- CFIN_DOC
0.07

```

## BIBLIOGRAPHY

- [1] B. Chudoba, "Ch4 - aerospace transportation vehicles - flight vehicle synthesis and systems engineering," *Unpublished Class Notes - University of Texas at Arlington*, 2012.
- [2] F. Sterk and E. Torenbeek, "Unconventional aircraft concepts," *Delft University Press, Papers Presented at a Symposium, Organised by the Netherlands Association of Aeronautical Engineers*, 1987.
- [3] R. Rosario, R. Wahls and N. Madavan, "NASA subsonic fixed wing project overview," *NASA Fundamental Aeronautics Program, 2012 Technical Conference, Cleveland, OH; United States*, 2012.
- [4] B. Chudoba, "Ch3 - anatomy of aerospace forecasting - flight vehicle synthesis and systems engineering," *Unpublished Class Notes - University of Texas at Arlington*, 2012.
- [5] L. Nicolai and G. Carichner, "Fundamentals of aircraft and airship design: volume 2, airship design and case studies," *1st edition, AIAA Education Series, American Institute of Aeronautics and Astronautics*, 2013.
- [6] P. Birtles, "Boeing 777: jetliner for a new century," *1st edition, Zenith Press*, 1998.
- [7] N. Shute, "No highway," *1st edition, William Heinemann, United Kingdom*, 1948.
- [8] J. Anderson, "Aircraft performance and design," *1st edition, McGraw-Hill New York; United States*, vol. 1, 1999.
- [9] D. P. Raymer, "Aircraft design: a conceptual approach," *5th edition, American Institute of Aeronautics and Astronautics, Inc., Reston, VA; United States*, 1999.
- [10] E. Torenbeek, "Synthesis of subsonic airplane design," *1982 edition, Delft University Press, Kluwer Academic JournalNames; The Netherlands*, 1982.
- [11] L. Nicolai, G. Carichner and L. Malcolm, "Fundamentals of aircraft and airship design:

- volume 1, aircraft design," *1st edition, AIAA Education Series, American Institute of Aeronautics and Astronautics*, 2010.
- [12] J. Roskam, "Airplane design: part i-viii," *4th printing, DARcorporation, Lawrence, KS; United States*, 2006.
- [13] G. Corning, "Supersonic and subsonic airplane design," *3rd edition, Edwards Brothers, Inc, Ann Arbor, Mi; United States*, 1953.
- [14] B. Chudoba, "Stability and control of conventional and unconventional aircraft configurations," *Books on Demand*, 2002.
- [15] G. Coleman Jr, "Aircraft conceptual design-an adaptable parametric sizing methodology," *Dissertation, The University of Texas at Arlington*, 2010.
- [16] B. Chudoba and H. W, "Evolution of generic flight vehicle design and synthesis," *The Aeronautical Journal*, vol. 114, no. 1159, 2010.
- [17] E. Van Der Veen, "Civil applications of thrust vectoring - an exploration," *21st Congress of International Council of the Aeronautical Sciences, Melbourne; Australia, September 1998*.
- [18] R. Yin, "Case study research: design and methods," *5th edition, Applied Social Research Methods, SAGE Publications, Inc., 1984*.
- [19] G. Sutton and O. Biblarz, "Rocket propulsion elements," *6th edition, John Wiley & Sons*, 2010.
- [20] B. Gunston, *Tornado, Typhoon, F-35, Jane's Aero-Engines Issue Nineteen*, Jane's Information Group Inc., Alexandria, Virginia, 2006.
- [21] K. Deere, "Summary of fluidic thrust vectoring research conducted at nasa langley research," *21st AIAA Applied Aerodynamics Conference, Orlando, FL; United States*, 2003.

- [22] C. Anderson, V. Giuliano and D. Wing, "Investigation of hybrid fluidic/mechanical thrust vectoring for fixed-exit exhaust nozzles," *American Institute of Aeronautics and Astronautics, NASA Langley Research Center*, 1997.
- [23] F. Burcham Jr., J. Burken, T. Maine and C. Fullerton, "Development and Flight Test of an Emergency Flight Control System Using Only Engine Thrust on an MD-11 Transport Airplane," *NASA/TP-97-206217, Dryden Flight Research Center, Edwards, California*, 1997.
- [24] U. G. P. Office, "Electronic code of federal regulations: title 14: aeronautics and space, part 25-airworthiness standards: transport category airplanes," *United States*, October 15 2015.
- [25] F. Burcham, J. Burken, T. Maine and C. Fullerton, "Development and flight test of an emergency flight control system using only engine thrust on an md-11 transport airplane," *National Aeronautics and Space Administration, Dryden Flight Research Center*, 1997.
- [26] B. Gal-Or, "Civilizing military thrust vectoring flight control," *Aerospace America, American Institute of Aeronautics and Astronautics*, vol. 34, no. n4, 1996.
- [27] A. Omoragbon, "An integration of a modern flight control system design technique into a conceptual design stability and control tool, aeromech," *Thesis, University of Texas at Arlington*, August 2010.
- [28] H. Xiao, "A prototype computerized synthesis methodology for generic space access vehicle (sav) conceptual design," *1st Space Exploration Conference: Continuing the Voyage of Discovery, Orlando, FL; United States*, 2006.
- [29] P. Czysz, "Hypersonic convergence - volume 1," *AFRL-VA-WP-TR-2004-3114, Air Force Research Laboratory, Dayton, OH; United States*, 2004.
- [30] J. Morris and D. Ashford, "Fuselage configuration studies," *DOI:10.4271/670370, SAE*

*Technical Paper 670370, 1967.*

- [31] W. Phillips, "Mechanics of flight," *2nd edition, John Wiley & Sons, 2010.*
- [32] J. Roskam, "Airplane flight dynamic and automatic flight controls," *5th printing, Design, Analysis, and Research Corporation, 2007.*
- [33] B. Gal-Or, V. Sherbaum and M. Lichtsinder, "Fundamentals of catastrophic failure prevention by thrust vectoring," *Journal of aircraft*, vol. 32, no. 3, pp. 577-582, 1995.
- [34] A. Doyle, "Changing Directions," in *Flightglobal - Flight International, 2009.*
- [35] H. Ross and M. Robinson, "X-31: 20 years of successful international cooperation," *AIAA/ICAS International Air and Space Symposium and Exposition: The Next 100 Years, Dayton, OH; United States, 2003.*
- [36] J. Wilson, "X-31 finds a shorter path to success," *Aerospace America, 2003.*
- [37] W. Sears and C. Webster, "Wind tunnel test of a model utilizing vectored thrust for in-flight maneuverability.," *Defense Technical Information Center, 1972.*
- [38] B. Gal-Or, "Western vs eastern fighter technologies beyond 2000," *Freund Pub. House, London; England*, vol. 11, no. 2, pp. 113-118, 1994.
- [39] B. Gal-Or, "Vectored propulsion, supermaneuverability and robot aircraft," *1st edition, Springer-Verlag New York, 1990.*
- [40] F. Burcham, T. Maine, J. Burken and J. Bull, "Using engine thrust for emergency flight control: md-11 and b-747 results," *National Aeronautics and Space Administration, Dryden Flight Research Center, 1998.*
- [41] R. Coppinger, "Uk adds thrust to flapless vehicle," *London, Flightglobal, Aviation Connection, Aug 2005.*
- [42] T. Tucker, "Touchdown: The development of propulsion controlled aircraft at NASA Dryden," *NASA History Office, Office of Policy and Plans, NASA Headquarters, 1999.*

- [43] B. Gunston, "Tornado, typhoon, f-35, jane's aero-engines issue nineteen," *Jane's Information Group Inc., Alexandria, VA; United States*, 2006.
- [44] E. Wilson, D. Adler and P. Bar-Yoseph, "Thrust-vectoring nozzle performance modeling," *Journal of propulsion and power*, vol. 19, no. 1, pp. 39-47, 2003.
- [45] H. Visser, "Thrust-vectored windshear recovery," *Delft University of Technology, Aircraft Engineering and Aerospace Technology*, vol. 71, no. 4, pp. 329-337, 1998.
- [46] E. Cliff, H. Kelley and L. Lefton, "Thrust-vectored energy turns," *Automatica, Elsevier*, vol. 18, no. 5, pp. 559-564, 1982.
- [47] H. Kelley, E. Cliff and L. Lefton, "Thrust-vectored differential turns," *Automatica, Elsevier*, vol. 18, no. 5, pp. 565-568, 1982.
- [48] P. Quinto and J. Paulson, "Thrust-induced effects on subsonic longitudinal aerodynamic characteristics of a vectored-engine-over-wing configuration," *NASA TP 2228, Scientific and Technical Information Branch, Langley Research Center Hampton, VA; United States*, 1983.
- [49] B. Gal-Or and V. Sherbaum, "Thrust vectoring-theory, laboratory, and flight tests," *Journal of Propulsion and Power*, vol. 9, no. 1, pp. 51-58, 1993.
- [50] A. Doyle, "Thrust vectoring option for typhoon promises big gains," *Flight International*, 2009.
- [51] D. Ikaza, "Thrust vectoring nozzle for modern military aircraft," *Industria de Turbo Propulsores S.A., NATO R&T Organization Symposium on Active Control Technology Enhanced Performance Operational Capabilities of Military Aircraft Land Vehicles and Sea Vehicles*, 2000.
- [52] B. Gal-Or, "Thrust vectoring for flight control & safety: a review," *International Journal of Turbo and Jet Engines*, vol. 11, no. 2-3, pp. 119-138, 1994.

- [53] D. Ikaza and C. Rausch, "Thrust vectoring for eurofighter-the first steps," *Industria de Turbo Propulsores, S.A., ICAS 2000 CONGRESS*, vol. 2, no. 1, pp. 92-95, 2000.
- [54] B. Gal-Or, "Thrust vectoring flight control to maximize future jet transport flight safety," *International Journal of Turbo and Jet Engines*, vol. 18, no. 1, pp. 41-46, 2001.
- [55] S. Asbury and F. Capone, "Thrust vectoring characteristics of the f-18 high alpha research vehicle at angles of attack from 0 to 70 deg," *AIAA PAPER 92-3095, NASA Langley Research Center; Hampton, VA; United States*, 1992.
- [56] H. Friehmelt, "Thrust vectoring and tailless aircraft design - review and outlook," *AIAA Atmospheric Flight Mechanics Conf., San Diego, CA; United States*, pp. 96-3412, 1996.
- [57] H. Schograve, "Thrust vector control for (clustered modules) plug nozzles: Some considerations," *Journal of Propulsion and Power*, vol. 16, no. 2, pp. 196-201, 2000.
- [58] B. Gal-Or, "Thrust vector control eyed for passenger aircraft: A novel methodology to combine jet-engine tests with sub-scale proof-of-concept flight tests," *International Journal of Turbo and Jet Engines*, vol. 12, no. 4, pp. 241-251, 1995.
- [59] J. Petit and M. Scholey, "Thrust reverser and thrust vectoring literature review," *The Boeing Company, TR AFAPL-TR-72-11, Air Force Aero Propulsion laboratory, WP-AFB, OH; United States*, 1972.
- [60] M. Shandor and R. Walker, "Theoretical performance of selected fluid injectants for thrust vector control," *Defense Technical Information Center*, 1962.
- [61] J. T. Bosworth and P. Stoliker, "The x-31a quasi-tailless flight test results," *National Aeronautics and Space Administration, Office of Management, Scientific and Technical Information Program*, vol. 3624, 1996.
- [62] C. Alcorn, M. Croom, M. Francis and H. Ross, "The x-31 aircraft: advances in aircraft agility and performance," *Progress in Aerospace Sciences, Elsevier*, vol. 32, no. 4, pp.

- 377-413, 1996.
- [63] F. Capone, "The nonaxisymmetric nozzle-it is for real," *NASA, Langley Research Center, High-Speed Aerodynamics Div., Hampton, Va; United States*, vol. 79, p. 1810, 1979.
- [64] F. Capone, "The effects on propulsion-induced aerodynamic forces of vectoring a partial-span rectangular jet at mach numbers from 0.40 to 1.20," *NASA Langley Research Center; Hampton, VA; United States*, 1975.
- [65] N. A. F. S. P. C. Aircraft, "Technology opportunity: propulsion controlled aircraft," *Dryden Flight Research Center, NASA, Edwards, CA; United States*, August 2009.
- [66] L. A. C. Vought Aeronautics Division, "Technical proposal wind tunnel testing of vectored thrust for in-flight maneuverability," *LTV Aerospace Corporation, Vought Aeronautics Division*, 1970.
- [67] B. Gal-Or, "Tailless vectored fighters: theory, laboratory and flight tests," *The Jet Propulsion Laboratory, Technion-IIT*, 1991.
- [68] J. Petit and M. Scholey, "STOL transport thrust reverser/vectoring program, volume 1," *The Boeing Company, TR AFAPL-TR-72-109, Air Force Aero Propulsion laboratory, WP-AFB, OH; United States*, 1972.
- [69] M. Mason and B. Berrier, "Static performance of nonaxisymmetric nozzles with yaw thrust-vectoring vanes," *National Aeronautics and Space Administration, Scientific and Technical Information Division*, vol. 2813, 1988.
- [70] D. Wing, C. Mills and M. Mason, "Static investigation of a multiaxis thrust-vectoring nozzle with variable internal contouring ability," *NASA TP 3628, Langley Research Center, Hampton, VA; United States*, 1997.
- [71] B. Powers and D. Kier, "Simulator evaluation of the low-speed flying qualities of an experimental stol configuration with an externally blown flap wing or an augmentor wing,"

- NASA-TN-D-7454, H-780, NASA Flight Research Center; Edwards, CA; United States, vol. 7454, 1973.*
- [72] J. Pennington and A. Meintel Jr, "Simulation study of thrust vectoring for air combat maneuvering for a lightweight fighter-class aircraft," *NASA TM X-3270, NASA Langley Research Center, Hampton, VA; United States, 1975.*
- [73] J. Orme and R. Sims, "Selected performance measurements of the f-15 active axisymmetric thrust-vectoring nozzle," *ISABE Paper No. IS, Citeseer, vol. 166, p. 14, 1999.*
- [74] A. Komarov, "Russia names su-35 turbofan builder, but pak fa decision proves more elusive," *Aviation Week and Space Technology, 2009.*
- [75] J. Buffington, A. Sparks and S. Banda, "Robust longitudinal axis flight control for an aircraft with thrust vectoring," *Automatica, Elsevier Science Ltd; Great Britain, vol. 30, no. 10, pp. 1527-1540, 1994.*
- [76] B. Gal-Or, "Review of the debate and the development of thrust vectoring technology," *Journal of Thermal Science, Springer, vol. 7, no. 1, pp. 1-6, 1998.*
- [77] Y. Ochi and K. Kanai, "Propulsion control and trim adjustment for an impaired large transport aircraft," *Second International Conference on Nonlinear Problems in Aviation and Aerospace, Embry-Riddle Aeronautical University, Daytona Beach, FL; United States, vol. 2, pp. 563-570, 1998.*
- [78] Y. Li, H. Lu, S. Tian, Z. Jiao and J. Chen, "Posture control of electromechanical-actuator-based thrust vector system for aircraft engine," *IEEE Transactions on Industrial Electronics encompasses the applications of electronics, controls and communications, instrumentation and computational intelligence for the enhancement of industrial and manufacturing systems and processes., vol. 59, no. 9, pp. 3561-3571, 2012.*

- [79] J. McArdie and B. Esker, "Performance characteristics of a variable-area vane nozzle for vectoring an astovl exhaust jet up to 45°," *Lewis Research Center, National Aeronautics and Space Administration*, 1993.
- [80] E. Wilson, D. Adler, B. Gal-Or, V. Sherbaum and M. Lichtsinder, "Optimizing subcritical-flow thrust-vectoring of converging-diverging nozzles," *Journal Of Propulsion And Power*, vol. 16, no. 2, pp. 202-206, 2000.
- [81] G. Gilyard and A. Bolonkin, "Optimal pitch thrust-vector angle and benefits for all flight regimes," *National Aeronautics and Space Administration, Dryden Flight Research Center*, 2000.
- [82] Boeing and D. Heathers, "New boeing 777 raked wing tips improve fuel efficiency, good for the environment," *Boeing Media, News Release-Statement*, URL:<http://boeing.mediaroom.com/2002-10-01-New-Boeing-777-Raked-Wing-Tips-Improve-Fuel-Efficiency-Good-for-the-Environment>, 2002.
- [83] B. Dunbar and M. Curry, "Nasa dryden fact sheet -propulsion controlled aircraft," URL: <http://www.nasa.gov/centers/dryden/news/FactSheets/FS-041-DFRC.html>, August 2009.
- [84] A. Sobester and A. Keane, "Multi-objective optimal design of a fluidic thrust vectoring nozzle," *AIAA 2006-6916, 11th AIAA/ISSMO Multidisciplinary Analysis and Optimization Conference, Portsmouth, VA; United States*, vol. 6916, 2006.
- [85] A. Bowers, G. Noffz, S. Grafton, M. Mason and L. Peron, "Multiaxis thrust vectoring using axisymmetric nozzels and postexit vanes on an f/a-18 configuration vehicle," *NASA Dryden Flight Research Facility; Edwards, CA; United States*, 1991.
- [86] F. Alvi, P. Strykowski, D. Washington, A. Krothapalli, F. Alvi, P. Strykowski, D. Washington and A. Krothapalli, "Multi-axis fluidic thrust vectoring of supersonic jets via counterflow," *The First National Student Conference: NASA University Research Centers*

- at *Minority Institutions*, pp. 97-393, 1997.
- [87] D. Gu, K. Natesan and I. Postlethwaite, "Modelling and robust control of fluidic thrust vectoring and circulation control for unmanned air vehicles," *Proceedings of the Institution of Mechanical Engineers, Part I: Journal of Systems and Control Engineering*, SAGE Publications, vol. 222, no. 5, pp. 333-345, 2008.
- [88] B. Gal-Or, "Maximizing thrust-vectoring control power and agility metrics," *Journal of Aircraft*, vol. 29, no. 4, pp. 647-651, 1992.
- [89] B. Gal-Or and D. Baumann, "Mathematical phenomenology for thrust-vectoring-induced agility comparisons," *Journal of Aircraft*, vol. 30, no. 2, pp. 248-255, 1993.
- [90] P. Stoliker, J. Bosworth and J. Georgie, "Linearized poststall aerodynamic and control law models of the x-31a aircraft and comparison with flight data," *NASA/TM-97-206318*, NASA 1.15:206318, H-2194, NASA Dryden Flight Research Center; Edwards, CA; United States, 1997.
- [91] G. Schmid, P. Strykowski, M. Madruga, D. Das and A. Krothapalli, "Jet attachment behavior using counterflow thrust vectoring," *Proceedings of 13th ONR Propulsion Conference, Minneapolis, MN; United States*, pp. 63-68, 2000.
- [92] F. Saghafi and A. Banazadeh, "Investigation on the flight characteristics of a conceptual fluidic thrust-vectorized aerial tail-sitter," *Proceedings of the Institution of Mechanical Engineers, Part G: Journal of Aerospace Engineering; SAGE Publications*, vol. 221, no. 5, pp. 741-755, 2007.
- [93] M. Zeutzius and S. Matsuo, "Investigation of a gas dynamic thrust vector control using a semi-empirical method," *Saga University Faculty of Science and Technology Collection Report 25*, 1996.
- [94] B. Berrier and J. Taylor, "Internal performance of two nozzles utilizing gimbal concepts for

- thrust vectoring," *National Aeronautics and Space Administration, Office of Management, Scientific and Technical Information Program*, vol. 2991, 1990.
- [95] D. Wing and R. Re, "Internal performance of a nonaxisymmetric nozzle with a rotating upper flap and a center-pivoted lower flap," *NASA-TP-3385, NASA Langley Research Center; Hampton, VA; United States*, vol. 3385, 1993.
- [96] J. McArdle, "Internal characteristics and performance of several jet deflectors at primary-nozzle pressure ratios up to 3.0," *Lewis Flight Propulsion Laboratory, Cleveland, OH; United States*, 1958.
- [97] C. Rausch and K. Lietzau, "Integrated thrust vectored engine control," *RTO AVT Symposium on Active Control Technology for Enhanced Performance Operational Capabilities of Military Aircraft, Land Vehicles and Sea Vehicles, Braunschweig, Germany*, vol. 12, pp. 1-12, 2000.
- [98] M. Harefors and D. Bates, "Integrated propulsion-based flight control system design for a civil transport aircraft," *Proceedings of the 2002 IEEE International Conference on Control Applications*, vol. 1, pp. 132-137, 2002.
- [99] A. Steer, "Integrated control of a second generation supersonic commercial transport aircraft using thrust vectoring," *Modeling, Control and Simulation Science Group, Flight Management and Control Department, DERA Bedford*, 2000.
- [100] K. Hammett, W. Reigelsperger and S. Banda, "High angle of attack short period flight control design with thrust vectoring," *American Control Conference*, vol. 6, pp. 170-174, June 21-23 1995.
- [101] T. Tucker, "Harnessing the brute: the development of propulsion controlled aircraft at nasa dryden," *NASA Ames Research Center; Dryden Flight Research Center*, no. 19990021055, 1998.

- [102] R. Coppinger, "Ground trials start for uk vectored thrust prototype uav," *London, Flightglobal, Aviation Connection*, Oct 2009.
- [103] E. Wilson, D. Adler and P. Bar-Yoseph, "Geometric evaluation of axisymmetric thrust-vectoring nozzles for aerodynamic performance predictions," *Journal of propulsion and power*, vol. 18, no. 3, pp. 712-716, 2002.
- [104] B. Gal-Or, "Fundamentals and similarity transformations of vectored aircraft," *Journal of Aircraft*, vol. 31, no. 1, pp. 181-187, 1994.
- [105] R. Joslin and D. Miller, "Fundamentals and applications of modern flow control," *1st edition, Progress in Astronautics and Aeronautics Series (Book 231). AIAA*, vol. 231, 2009.
- [106] B. Gal-Or, "Fundamental concepts of vectored propulsion," *Journal of Propulsion and Power*, vol. 6, no. 6, pp. 747-757, 1990.
- [107] A. DuPont, "Full scale test of a transport aircraft thrust vectoring system," *American Institute of Aeronautics and Astronautics, 1997 World Aviation Congress, DuPont Aerospace Co., Inc.*, 1997.
- [108] B. Gal-Or, "Flying scaled vectored f-22 to maximize post-stall agility: towards tailless, completely vectored, future designs," *Technion - Israel Inst. of Tech., Haifa. Faculty of Aerospace Engineering.*, 1993.
- [109] B. Gal-Or, "Flying jet powered models with thrust vectoring to maximize future jet transport flight safety," *Jet Laboratory, Technion - Israel Institute of Technology, CEO Vector Turbo Power B. V., EC-Funded Gas Turbine Consortium*, 1999.
- [110] D. Joyce, "Flying beyond the stall: the x-31 and the advent of supermaneuverability," *Library of Congress, National Aeronautics and Space Administration*, 2014.
- [111] M. Mason and W. Crowther, "Fluidic thrust vectoring of low observable aircraft," *CEAS*

- Aerospace Aerodynamic Research Conference, Cambridge; UK, pp. 1-7, 2002.*
- [112] R. Williams, "Fluidic thrust vectoring and throat control exhaust nozzle," *AADC and America, Rolls-Royce North and Baily Vittal, 2002.*
- [113] W. Lord, D. MacMartin and T. Tillman, "Flow control opportunities in gas turbine engines," *AIAA 2000-2234, Fluids, Denver, CO; United States, 2000.*
- [114] Y. Ochi, "Flight control system design for propulsion-controlled aircraft," *Proceedings of the Institution of Mechanical Engineers, Part G: Journal of Aerospace Engineering, SAGE Publications, vol. 219, no. 4, pp. 329-340, 2005.*
- [115] A. Omoragbon and G. Coleman Jr., "Feasibility study of a thrust vector control transport," *Proceedings of the 2013 ASEE Gulf-Southwest Annual Conference, American Society for Engineering Education, 2013.*
- [116] J. Smolka, L. Walker, G. Johnson, G. Schkolnik, C. Berger, T. Commers, J. Orme, K. Shy and C. Wood, "F-15 active flight research program," *The Aerospace Profession, NASA Dryden Flight Research Center, 1996.*
- [117] C. Hunter, "Experimental, theoretical, and computational investigation of separated nozzle flows," *AIAA-98-3107, NASA Langley Research Center, Hampton, VA; United States, vol. 3107, p. 1998, 1998.*
- [118] J. Flamm, K. Deere, M. Mason, B. Berrier and S. Johnson, "Experimental study of an axisymmetric dual throat fluidic thrust vectoring nozzle for supersonic aircraft application," *43rd AIAA/ASME/SAE/ASEE Joint Propulsion Conference & Exhibit, Cincinnati, OH; United States, vol. 5084, 2007.*
- [119] J. Jie, Z. Jingyun, Z. Mingheng and L. Chuanxin, "Experimental investigation of static internal performance for an axisymmetric vectoring exhaust nozzle," *Chinese Gas Turbine Establishment, ICAS 2000 Congress, 2005.*

- [120] K. Waithe and K. Deere, "Experimental and computational investigation of multiple injection ports in a convergent-divergent nozzle for fluidic thrust vectoring," *AIAA 2003-3802, 21st Applied Aerodynamics Conference, Orlando, FL; United States*, vol. 3802, p. 2003, 2003.
- [121] S. C. Asbury and others, "Effects of internal yaw-vectoring devices on the static performance of a pitch-vectoring nonaxisymmetric convergent-divergent nozzle," *National Aeronautics and Space Administration, Office of Management, Scientific and Technical Information Program*, 1993.
- [122] R. Colgren and R. Loschke, "Effective design of highly maneuverable tailless aircraft," *Journal of Aircraft*, vol. 45, no. 4, pp. 1441-1449, 2008.
- [123] Z. Wang, P. Jiang and I. Gursul, "Effect of thrust-vectoring jets on delta wing aerodynamics," *Journal of Aircraft*, vol. 44, no. 6, pp. 1877-1888, 2007.
- [124] A. Agrawal, J. Yang and H. Kosaka, "Effect of actuator dynamics and fixedtime-delay on the stability of actively controlled structures," *American Control Conference*, vol. 1, pp. 510-514, 1999.
- [125] B. Gai-Or, "Dynamic scaling of prototypes using radius of gyration method: theory, laboratory and flight tests," *Jet Propulsion Lab, Department of Aerospace Engineering, Technion - Israel Institute of Tech.*, 1991.
- [126] B. Dunbar and M. Curry, "Dryden history," *URL: <http://www.nasa.gov/centers/dryden/history/pastprojects/PCA/index.html>*, August 2009.
- [127] R. Sparks, S. Michie, K. Gill, W. Crowther and N. Wood, "Development of an integrated circulation control/fluidic thrust vectoring flight test demonstrator," *Northern Ireland; UK*, vol. 86, 2005.
- [128] J. Flamm, K. Deere, M. Mason, B. Berrier and S. Johnson, "Design enhancements of the

- two-dimensional, dual throat fluidic thrust vectoring nozzle concept," *3rd AIAA Flow Control Conference, NASA Lanley Research Center, Hampton, VA; United States*, vol. 3701, p. 2006, 2006.
- [129] R. Steinhauser, G. Looye and O. Brieger, "Design and evaluation of control laws for the x-31a with reduced vertical tail," *AIAA 2004-5031, AIAA Guidance, Navigation, and Control Conference and Exhibit, RI; United States*, 2004.
- [130] P. Yagle, D. Miller, K. Ginn and J. Hamstra, "Demonstration of fluidic throat skewing for thrust vectoring in structurally fixed nozzles," *Journal of Engineering for Gas Turbines and Power, American Society of Mechanical Engineers*, vol. 123, no. 3, pp. 502-507, 2001.
- [131] A. Jadbabaie and J. Hauser, "Control of a thrust-vectoring flying wing: a receding horizon—lpv approach," *International Journal of Robust and Nonlinear Control, Wiley Online Library*, vol. 12, no. 9, pp. 869-896, 2002.
- [132] N. Rademakers, "Control of a tailless fighter using gain-scheduling," *Traineeship report, Eindhoven University of Technology, Netherlands*, 2004.
- [133] K. Deere, "Computational investigation of the aerodynamic effects on fluidic thrust vectoring," *36th Joint Propulsion Conference and Exhibit; 36th, Huntsville, AL; United States*, no. 2000-3598, pp. 10-2514, 2000.
- [134] B. Gal-Or, V. Sherbaum, M. Lichtsinder and M. Turgemann, "Complete thrust vectoring flight control for future civil jets, f-22 superiority fighter and cruise missiles. part i: vectored f-22, f-16 and f-15," *International Journal of Turbo and Jet Engines*, vol. 10, no. 1, pp. 1-18, 1993.
- [135] J. Bowlus, D. Multhopp and S. Banda, "Challenges and opportunities in tailless aircraft stability and control," *Wright Laboratory, Wright-Patterson AFB, OH, 45433-7531; United States*, pp. 1713-1718, 1997.

- [136] P. Strykowski and A. Krothapalli, "An experimental investigation of active control of thrust vectoring nozzle flow fields," *Air Force Office of Scientific Research, Boiling Air Force Base, Washington DC; United States*, 1994.
- [137] R. Woodrey, P. Whitten, C. Smith and R. Bradley, "An experimental investigation of a vectored-engine-over-wing powered-lift concept. volume i-low speed and transonic tests," *AFFDL-TR-76-92*, 1976.
- [138] P. Whitten, "An experimental investigation of a vectored-engine-over-wing powered-lift concept," *US Air Force Flight Dynamics Laboratory Technical Report AFFDL-TR-76-92*, vol. 2, 1978.
- [139] M. Hreha, G. Schkolnik and J. Orme, "An approach to aircraft performance optimization using thrust vectoring," *AIAA 94-3361*, 1994.
- [140] S. Johnson, "Aircraft ground test and subscale model results of axial thrust loss caused by thrust vectoring using turning vanes," *National Aeronautics and Space Administration, Office of Management, Scientific and Technical Information Program*, vol. 4341, 1992.
- [141] P. Wilde, W. Crowther, A. Buonanno and A. Savvaris, "Aircraft control using fluidic maneuver effectors," *AIAA 2008-6406, 26th AIAA Applied Aerodynamics Conference, Honolulu, HI; United States*, vol. 6406, 2008.
- [142] W. Case, "Aerospike thrust vectoring slot-type compound nozzle," *Masters Thesis, Faculty of California Polytechnic State University, San Luis Obispo, CA; United States*, 2010.
- [143] M. Brenner, "Aeroservoelastic modeling and validation of a thrust-vectoring f/a-18 aircraft," *National Aeronautics and Space Administration, Office of Management, Scientific and Technical Information Program*, vol. 3647, 1996.
- [144] A. Matesanz, A. Velazquez and M. Rodriguez, "Aerodynamic performance prediction of thrust-vectoring nozzles," *Journal of Propulsion and Power*, vol. 14, no. 2, 1998.

- [145] H. Kowal, "Advances in thrust vectoring and the application of flow-control technology," *Canadian Aeronautics and Space Journal, NRC Research Press Ottawa; Canada*, vol. 48, no. 2, pp. 145-151, 2002.
- [146] B. Berrier and R. Re, "A review of thrust-vectoring schemes for fighter applications," *American Institute of Aeronautics and Astronautics and Society of Automotive Engineers, Joint Propulsion Conference, 14th, Las Vegas, NV; United States*, 1978.
- [147] A. Cain and P. Doane, "A methodology for the analysis and modeling of thrust vectoring usage," *McDonnell Aircraft Co., Saint Louis, MO; United States*, p. 389, 1992.
- [148] F. Lallman, J. Davidson and P. Murphy, "A method for integrating thrust-vectoring and actuated forebody strakes with conventional aerodynamic controls on a high-performance fighter airplane," *NASA/TP-1998-208464, Langley Research Center, Hampton, VA; United States*, 1998.
- [149] Y. Yang and T. Hsu, "A dynamic model for two-dimensional thrust-vectoring nozzles," *AIAA 2005-3505, 4th AIAA/ASME/SAE/ASEE Joint Propulsion Conference & Exhibit, Tucson, AZ; United States*, pp. 1-8, 2005.

## BIOGRAPHICAL INFORMATION

From the earliest memories, Vincent Ricketts has been intrigued and curious with the unknown and the technological progress of humanity. The perceived miracle that flight presented drove him to peruse a path that would open up the possibility of applying his mind to understanding the unknown. This path lead to him to graduate with a Degree in Aerospace Engineering from the University of Texas at Arlington in 2012. During his undergraduate studies, he joined the Universities student rocketry club—the Rocket Mavericks. This gave him the opportunity to apply his knowledge. The highly motivated qualities of this organization’s members, led Dr. Chudoba to recruit potential undergraduate researchers for the Aerospace Vehicle Design (AVD) Laboratory.

After joining the AVD team, he had had the opportunity to tease his thirst for knowledge by contributing to multiple design projects in the AVD laboratory. While volunteering in the AVD Lab, he contributed to multiple design projects. During the summer of 2010, he was tasked with the development of a comprehensive rocket motor database in parallel with the AVD Lab's solution space screening of the NASA/DARPA Hypersonic Endurance Demonstrator. Over the winter semester of 2010, he served as the orbital mechanics expert for the AVD lab team, working in parallel with NASA, on the Manned Geosynchronous Servicing study; the result of this contribution being the ability to coauthor a journal paper.